ALADIN-HIRLAM Newsletter

No. 15, June 23rd, 2020

Joint 30th ALADIN Wk & HIRLAM ASM 2020, 30 March - 3 April 2020

ALADIN Programme, c/o P. Termonia, IRM, Avenue Circulaire 3, 1180 Bruxelles, Belgium

HIRLAM-C Programme, c/o J. Onvlee, KNMI, P.O. Box 201, 3730 AE De Bilt, The Netherlands

CONTENT

Introduction: a Covid-19 proof Workshop/All Staff Meeting ?

Welcome to the combined 15th edition Newsletter of the ALADIN and HIRLAM consortia.

This early summer 2020 edition is mainly dedicated to the "***30th ALADIN Workshop & HIRLAM All Staff Meeting 2020***".

The Slovenian Environment Agency (ARSO) should have hosted the 2020 joint meeting in Ljubljana, from 30 March to 3 April 2020, a decision that was taken in quite period. Beginning of March the countries started to take measures to limit the spread of the Corona virus and the countries very rapidly closed their borders for international travel. **We decided on 9 March to switch the meeting to a video conference meeting.** We had no previous experience with organizing the Wk/ASM meeting via web conferencing. **Many problems had to be faced**: the stability of the connections, how to manage the discussions, how to organize side meetings. **The program was adapted** within the limits of technical and time constraints of the participants and **we decided to go for it. Our meeting (44 presentations in 9 sessions, 15 posters, 2 side-meetings) went well**, with very nice presentations and discussions. So did the LTM and the HMG-CSSI meetings. However, we did miss the informal discussions during the icebreaker, Ljubljana visit and the diner down-town. Hopefully, we will resume that part for the **All Staff Workshop 2021 in Ljubljana (15-19 March)**.

Thank to all of the participants who joined the meetings. More than 215 persons connected to the meeting and identified themselves, including 6 colleagues from ECMWF and the COSMO Scientific Project Manager (who also accepted to write his impressions in the editorial). Maximum simultaneous attendance was 125 people on big sessions (opening, DA, system, physics and even 135 for surface), 95 people for dynamics, EPS, verification, applications and closing and still about 80 for the posters introduction and the fog side-meeting.

We like to thank all those that contributed to this Newsletter with their articles, most of them based on the presentations or posters presented at the Wk/ASM.

Please contact authors directly for any needed additional information on their article.
Please be also reminded that a full overview and all presentations (videos and pdf files) can be viewed from the ALADIN website … although it would take more then 24 hours to watch them all !

Furthermore, we also introduce some articles recently published and a new Doctor from Bratislava.

Last but not least, a summary list of upcoming events, planned for the near future (as from second semester 2020 and after) is available.

We hope you enjoy reading the fifteenth ALADIN-HIRLAM Newsletter. Once again, thanks all authors for their contributions and hand it off first to the COSMO Scientific PM for the Edito that gives an external point of view on our Wk/ASM, points the challenges of the video meeting setting ... and illustrates the differences in the working practices/spirit between COSMO and ALADIN-HIRLAM consortia.

Patricia and Frank

Further consortia information needed?
Please visit the ALADIN and HIRLAM websites or contact us.

Edito : **Impressions of an External Participant**

by Dmitrii Mironov
Deutscher Wetterdienst, Offenbach am Main, Germany

The 2020 ALADIN Workshop -HIRLAM All Staff Meeting held as a web conference was informative and interesting, particularly for the COSMO Scientific Project Manager in which capacity I serve the COSMO Consortium at the time being. It is always very useful to know what the colleagues and friendly competitors are up to. Given the current difficult situation, the Wk-ASM went out smoothly. You did a very good job, congratulations and sincere thanks! However, there is surely room for improvement. I would mention two points which I feel can facilitate our future communication via the net (although I dare hope the situation changes for the better and we will not need to hold large-scale web meetings in the future, at least not too often).

During the Wk-ASM sessions, all questions were posed through the chat. Given a large number of the meeting participants, this was probably the only manageable way. A chat communication, however, imposes heavy demands on the questions and, most notably, on the session convening. Questions should be formulated in a concise and lucid way. The questions posed through the chat are read by a session convener, or (pretty often) formulated in convener’s own words. In doing so, caution must be exercised so that the essence of the question is conveyed as exactly as possible. This was not always the case during the sessions.

An important point concerns the closing session. The discussion that followed the summary presentations by the ALADIN and HIRLAM Program Managers was wrapped up far too quickly. The problem seems to be that the audience simply did not have enough time to digest the summary presentations and hence was unable to actively participate in the discussion. An in-depth discussion right after the summary talks would not have been easy, even though the meeting were held in a usual way. The web-based format further complicated the issue. Considering the paramount importance of the summary presentations (among other things, they crown the entire meeting and to a considerable extent specify the focal points of the Consortium activity over the coming year), an extensive and vivid final discussion is very desirable. To this end, a long break (two-three hours) can be made prior to the final discussion. This will give the meeting participants enough time to contemplate on the various issues outlined in the summary presentations. One more viable alternative is to hold a final discussion on the next day. This should pose no problem, considering that the time restrictions during the web conference are not severe (nobody must catch his/her airplane).

Events announced for 2020 (and later on)

The Newsletters presents a static overview (twice a year) with upcoming meetings for the (near) future time frame. For actual updates (year round) please check the ALADIN / HIRLAM websites and the LACE website.

1 ALADIN/HIRLAM related meetings in 2020

- 25th ALADIN GA, HIRLAM Council, LACE Council, 6th Joint ALADIN GA and HIRLAM Council, virtual meeting, 25-26 June 2020
- EWGLAM/SRNWP meeting, Brussels or virtual meeting, 28 September - 1st October 2020
- 29th ALADIN LTM meeting, Brussels or virtual meeting, 28 or 29 September 2020
- 11th Joint PAC-HAC meeting, virtual meeting, 19-20 October 2020
- 26th ALADIN GA, HIRLAM Council, LACE Council, 7th Joint ALADIN GA and HIRLAM Council, Toulouse, 26-27 November 2020

2 ALADIN/HIRLAM Working Weeks / Days

Following topics through working weeks/days will be addressed:

- 2020 Joint LACE Data Assimilation & DAsKIT Working Days, Vienna, date t.b.d.
- DA/UO, Madeira or Portugal, 26-30 Oct.
- EPS fall: t.b.d.
- SRNWP EPS 2: t.b.d.
- System: Norrkoping or virtual meeting; mid October
- General Harmonie training for newcomers: webinair?
- Machine learning workshop EUMETNET, Brussels, Febr 26-29, 2021
- MUSC-training: in 2021

3 Regular group video meetings

Regular group video meetings (via google hangouts) are organized for several topics (from both ALADIN and HIRLAM). Outcomes are noted as very valuable. If you like more details how to organize please contact Roger Randriamiampianina, Daniel Santos Munoz or Patrick Samuelsson.

Maria Monteiro (ALADIN DA coordinator) has established regular specific regular video-conferences with DAsKIT countries (ALADIN DA starter countries).

4 About the past joint events

During the first semester of 2020:

- the (virtual-)LTM met on 31st March 2020 ;
- the HAC and PAC met by virtual meeting in 14-15 May

The minutes of these meetings have been validated and are on-line (use the links below):

- joint ALADIN Workshops & HIRLAM All Staff Meetings,
- minutes of the HMG/CSSI meetings,
- minutes of HAC/PAC meetings,
- minutes and presentations : joint ALADIN General Assemblies and HIRLAM Councils

30th ALADIN Wk & HIRLAM ASM 2020

30 March – 3 April 2020
video-conference

The meeting had to be cancelled in-situ in Ljubljana, but was held by videoconference on the same dates. The agenda had been adapted to the video-conference format:

- **side-meetings**: verification and system side-meetings were postponed to dedicated visio-meetings after the Wk/ASM; HARMONIE-climate side-meeting took place on Thursday afternoon as planned, with a dedicated visio-conference between the members of the team; surface and fog side-meetings took place as planned, with part of the time dedicated to additional presentations;
- ***ALADIN LTM meeting*** **on Tuesday 31 at 11:00**
- Posters introduction session on Tuesday 31 at 16:00
- **Thursday 2 April afternoon and Friday 3 April until 15:30 : *HMG-CSSI meeting***
- **the Wk/ASM sessions were recorded** : you can watch or download the videos by speakers directly on bluejeans website (one link per half day meeting).
    - Monday morning : due to some bluejeans website issues, the mpeg files are not available there but mpeg files can be downloaded (see the links in the agenda of the opening and the DA sessions, one file per presentation)
    - Monday afternoon : **video of the surface session and surface side-meeting**
    - Tuesday morning : **video of the System session**
    - Tuesday afternoon : **video of the Dynamics and EPS sessions**
    - Wednesday morning : **video of the Physics session**
    - Wednesday afternoon : **video of the Verification session and fog side-meeting**
    - Thursday morning : **video of the Applications and Closing sessions**
- Consult the **chat discussions during the sessions and side-meetings**
- Consult the list of **registered Participants**

1 Agenda of the Wk/ASM, with link to the pdf of the presentations

In the Agenda below, click on the title of a presentation/poster to get access to the corresponding slides (pdf). In the agenda and the posters list, **the authors and titles are highlighted in yellow** when there is a dedicated article in this newsletter.

Opening session :

- Patricia POTTIER: Opening of the Meeting and practical information, **see the video**
- Piet TERMONIA: ALADIN status overview, **see the video**
- Jeanette ONVLEE: HIRLAM highlights of the past year, **see the video**
- Balazs SZINTAI: Status of the C-SRNWP project, **see the video**
- Plenary session: Data Assimilation. Chair : Jean-François Mahfouf
- Benedikt STRAJNAR: Data assimilation activities in RC LACE, **see the video, 20 first minutes**
- Claude FISCHER: Recent progress on DA at Météo-France, **see the video, from 20 minutes recording**
- Maria MONTEIRO: The DAsKIT programme: status and plans, **see the video**
- Roger RANDRIAMAMPIANINA: Progress in Hirlam upper-air data assimilation , **see the video**

Plenary session: Surface

- Camille BIRMAN: Land surface data assimilation for NWP at Météo-France
- Patrick SAMUELSSON: Overview of HIRLAM surface activities
- Yurii BATRAK: Pseudo-dynamic sea-ice cover in AROME-Arctic

- Mariken HOMLEID : Snow
- Kristian Pagh NIELSEN: Turbulent surface fluxes and wind, temperature and specific humidity ..
- Samuel VIANA: Experiments with roughness & ECOCLIMAP-SG

Side meeting on Surface : additional presentations and discussion

- Roger RANDRIAMAMPIANINA: Integrating citizen observations in operational weather forecasts
- Laura Rontu : Satellite snow extent for NWP

Plenary session: System Chair

- Daniel SANTOS MUÑOZ : HIRLAM System: Past, present and ... future?
- Ryad EL KHATIB: Porting AROME on AMD platform
- Claude FISCHER: Cycles and the likes
- Alexandre MARY: Of models code development and validation
- Roel STAPPERS : JSON schema validation of experiment configurations

Plenary session: Dynamics

- Petra SMOLIKOVA: Dynamics in RC LACE
- Daan DEGRAUWE: Progress in the SPDY package

Plenary session: E.P.S.

- Martin BELLUS: LAM-EPS activities in LACE
- Clemens WASTL: Application of convection permitting EPS C-LAEF at ZAMG

Plenary session : Physics

- Yann SEITY: On going work at Météo-France in ARPEGE and AROME physics
- Sander TIJM: HARMONIE-AROME physics developments
- Martina TUDOR: LACE physics developments
- Radmila BROZKOVA: Roughness length determination and tests
- Wim DE ROOY : Improved parametrization of the boundary layer in Harmonie-Arome (focusing on low clouds)
- Laura RONTU: About aerosol strategy and tactics
- Daniel MARTIN: Update of the Use of CAMS aerosols in HARMONIE-AROME
- Oskar LANDGREN : Impacts on Norwegian coastal precipitation by aerosol forcing
- Andre SIMON: Forecasting of wet snow and freezing rain accretion on power lines

Side meeting on Fog : additional presentations and discussion

- Salome ANTOINE: SoFog3D field campaign and improvement offog forecast at hectometric scale
- Sander TIJM: More results from Cabauw fog study

Plenary session: Verification

- Bent Hansen SASS: QA in HIRLAM-C 2019-2020
- Christoph ZINGERLE: Something about harp / verification

Plenary session: Applications

- Geert SMET: Probabilistic storm forecasts for wind farms in the North Sea
- Sylvie MALARDEL : Coupling AROME-Oversea with NEMO and WW3
- Danijel BELUSIC : HARMONIE-climate: recent achievements
- Bert VAN ULFT : HARMONIE-climate: system developments and plans

Plenary closing session.

2 Posters

- Martina TUDOR: Croatian Meteorological and Hydrological Service, main building, Grič 3, Zagreb, after 5.5 M Earthquake on 5:24 UTC 22nd March 2020
- Geoffrey BESSARDON : Physiography sensitivity testing over Ireland
- Bogdan BOCHENEK : Operational activities in Poland
- Katarína ČATLOŠOVÁ : Mode-S data assimilation at SHMU
- Rónán DARCY : Met Eireann operational poster
- Mustapha ELOUARDI : Validation of integrated water vapor derived from global positioning system over Morocco and from numerical weather prediction (NWP) AROME

- Pau ESCRIBÀ : AEMET-gSREPS: forecasting uncertainty in AEMET operational forecasts
- Mario HRASTINSKI : The NWP activities at Croatian Meteorological and Hydrological Service
- Martin IMRISEK : GNSS slant total delays in the ALADIN NWP system: Phasing of the source code from cy40h1 to cy43t2
- Heiner KÖRNICH : Modeling parameter uncertainty for atmospheric icing
- Kristian Pagh NIELSEN : Reference computations for solar and thermal radiation
- Patricia POTTIER : The NWP systems at Meteo-France
- Jana SANCHEZ-ARRIOLA : AEMET NWP activities
- Gabriella SZEPSZO : NWP activities at the Hungarian Meteorological Service
- Jozef VIVODA : Transition of the VFE scheme from LAM to the global model
- Eoin WHELAN & Rónán DARCY : SAPP Implementation at Met Eireann

3 HMG/CSSI meeting

More information (minutes) on the **HMG/CSSI dedicated page** on the ALADIN website.

RC LACE Data assimilation activities

Benedikt Strajnar & contributors from LACE DA

1 Introduction

This is a summary of recent DA assimilation activities within the RC LACE data assimilation teams and summarizes work of many contributors from the involved member countries. It includes an overview of operational status, algorithmic developments for upper-air and surface, and developments related to use of observations.

2 Operational status

RC LACE NWP centres are currently running a total of 10 data assimilation systems, among them two ensemble prediction systems (EPS). Four systems are based on AROME and the other six use ALARO model configuration. The systems typically include 3D-Var analysis in combination with surface OI (CANARI), and 3 systems additionally combine this with spectral blending techniques. Most centres are in transition between cy40 and cy43; ALARO-based systems in the Czech Republic and Slovenia already use cy43 for a while, while other members plan to switch to the recent export cycle in the near future. The operational situation is summarized in Fig. 1. The members apply either 3 or 6 hour assimilation interval, except the new Austrian AROME nowcasting setup which applies the analysis hourly.

The member countries generally use a large variety of different global and regional observations. Except for rather small extensions to existing observations sources, there was no major observational upgrade in 2019.

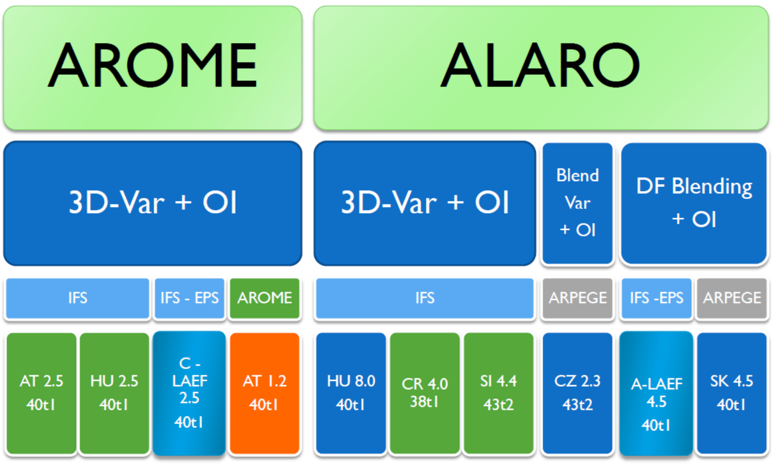

Figure 1: Operational data assimilation status in RC LACE countries. The suites (bottom row) are grouped according to model setup (first row), assimilation algorithm (second row) and LBCs (third row). Horizontal resolution is given by number next to the county code. The box colour indicate the cycle frequency (6-hourly in blue, 3-hourly in green and hourly in orange).

3 Algorithmic developments

AROME Nowcasting

The hourly assimilation system at 1.2 km resolution was put into operations in Austria in November 2019, after being evaluated over most of 2019 as an e-suite. The system uses 30 minute cut-off time, 120 minute observation window, and assimilates several high-resolution data sources (surface data, radar data from OPERA and bilateral exchange, Mode-S, ZTD). The final implementation consists of assimilation and production cycles. The assimilation cycle supresses spin up with a back-phased incremental analysis update (IAU) applied between -1h and -15 min. This is then extended to 1 hour to serve as first guess for the production cycle. The production run (12 h forecast) uses 1 h first guess trajectory plus an additional IAU (between initialization time and +7.5 min), latent heat nudging (LHN) of a rain rate product coming from the INCA nowcasting systems (during the first 35 min), and additional nudging of surface station data (during the first 30 min). The nudging further enhances the realism of analysis. The system uses an ensemble B matrix which is recalculated daily to incorporate the differences of the day (recent differences between assimilation and production cycles are added to the sampling statistics). The AROME Nowcasting setup is illustrated in Fig. 2. It can be observed how the realism of a forecast of a convective event enhances with decreasing forecast length. Some improvements can be demonstrated by AROME Nowcasting compared to 2.5 km operational AROME suite in terms of classical scores and specific situations (e.g., cases with low cloudiness).

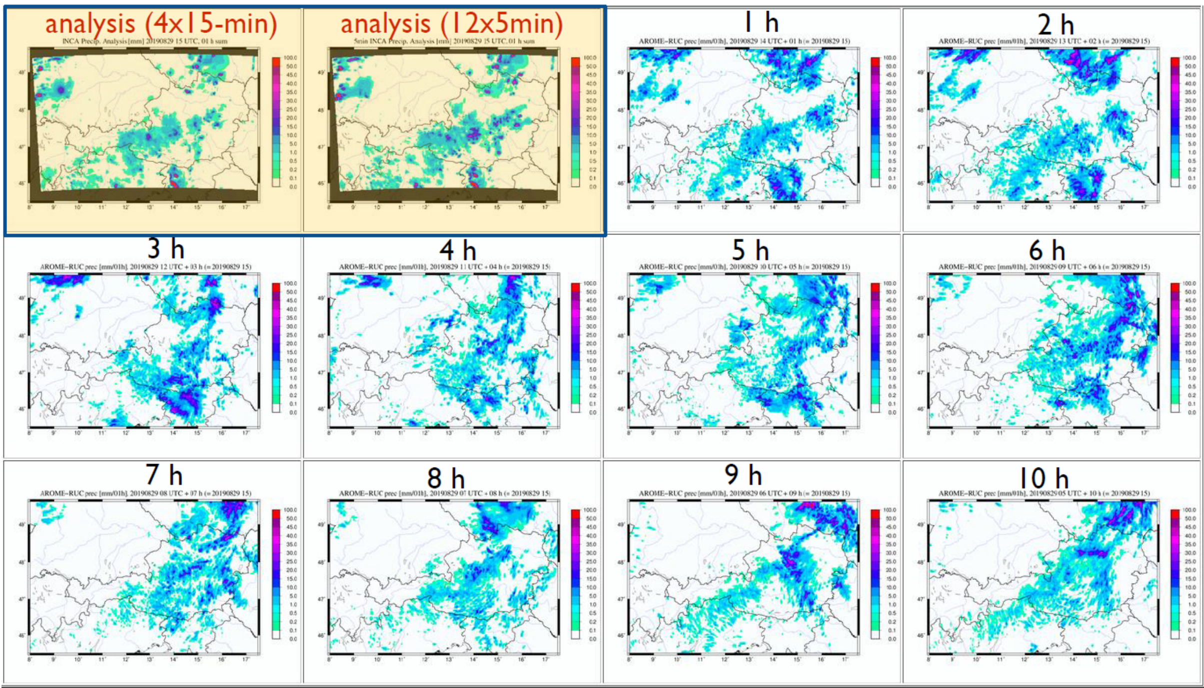

Figure 2: Illustration of setup and performance of AROME Nowcasting. Analysis of hourly precipitation (two upper-left frames) as reference and 1-10h forecast for the same period.

Advances of SEKF for surface analysis

Efforts to implement Simplified Extended Kalman Filter (SEKF) for soil assimilation continued in 2019 mainly at the Austrian meteorological service. In order to assimilate satellite-derived land surface temperature (LST), a set of input observations was prepared. The data from Meteosat Second Generation (MSG) were downscaled with high-resolution Sentinel-3 information. Bias correction using CDF-matching technique was also performed. The experimentations with this high spatial resolution LST indicated a small but positive impact of 2 m temperature, as compared against Austrian weather station data (Fig. 3).

Another project was devoted to assimilation of soil moisture, using SCATSAR-SWI. Tests using different horizontal resolutions (2.5 and 1.25 km), different observation errors (global and local) and dynamical settings were performed. AROME-SURFEX forecasts at 1.25 km were shown to be warmer and drier compared to station measurements due to moisture assimilation.

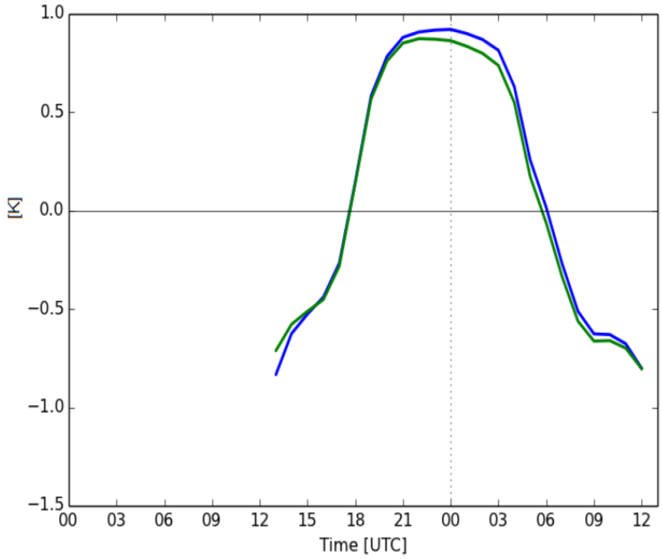

Figure 3: Improvement of 2 m temperature bias (green) by assimilation of LST within SEKF.

4 Improvements in use of observations for atmosphere

OPERA radar data

RC LACE invests more and more efforts into radar data assimilation. Reflectivity and Doppler winds are already operationally assimilated in Austria (setups with AROME). Other countries currently perform validation of reflectivity assimilation, the performance of reflectivity observation operator with ALARO physical parametrizations is being examined in particular. It was shown that using prognostic graupel (experimental setup in ALARO) can somewhat improve the first guess departures.

The radial winds in LACE area are often aliased because low Nyquist velocities (reflectivity-optimized scanning modes) are used. There is an ongoing effort to develop a common dealiasing procedure (example in Fig. 4). Three de-aliasing techniques are being investigated, including the one used operationally in Austria, with the aim to select the optimal one based on accuracy and robustness.

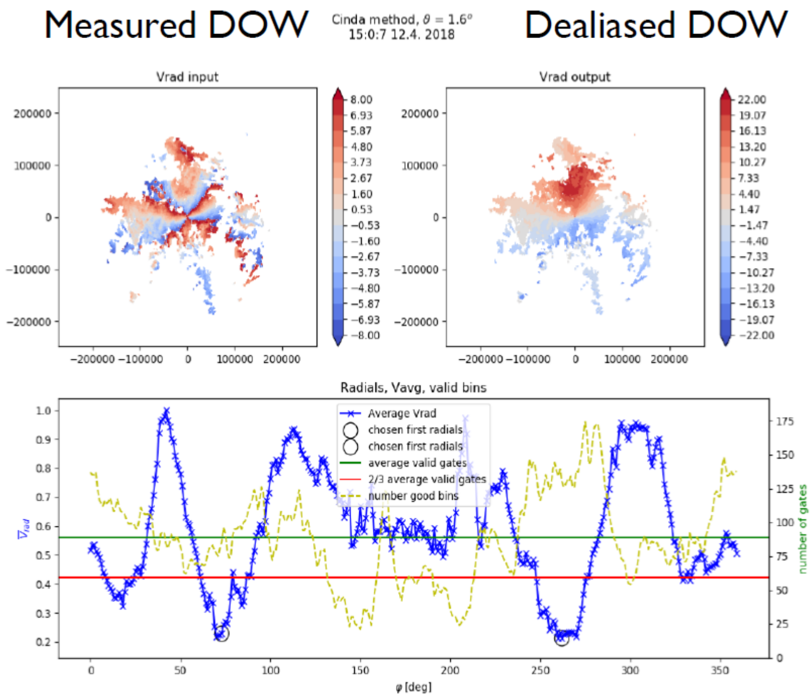

Figure 4: Raw and dealiased Doppler wind measurement (top) and demonstration of de-aliasing procedure (bottom).

Assimilation of GNSS slant total delays

GNSS-derived observations are seen as promising source of moisture information. In order to enable assimilation Slant Total Delay (STD) observations, the already existing code developed by HIRLAM was reviewed and phased to a recent model cycle cy43 (stay at KNMI). The currently ongoing validation includes tangent-linear and adjoint tests of the observation operator for STD. Figure 5 shows an experimental analysis increment where only STD data from Slovakia are assimilated.

Impact of STD was also verified in Austria, based on locally phased STD code in cy40t1. Evaluation of impact on precipitation was carried out for selected weather events and some improvements in terms of fractional skill score could be demonstrated.

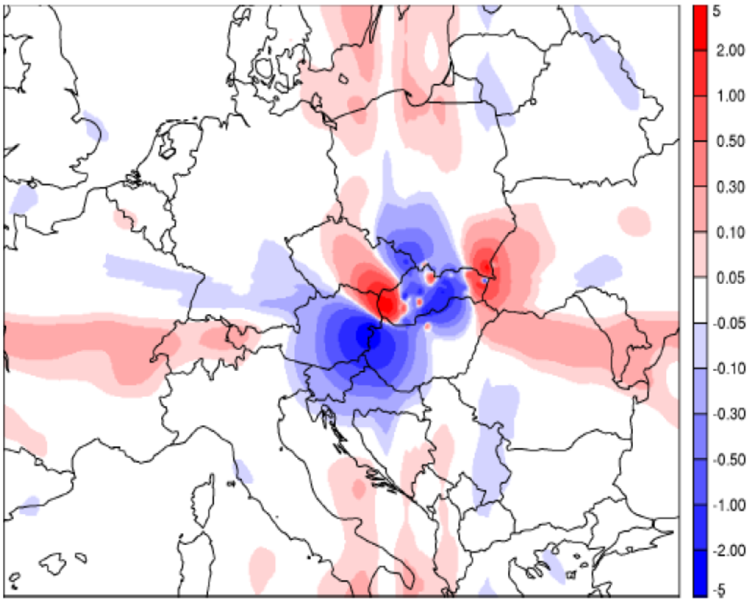

Figure 5: Specific humidity analysis increment at level 60/87 in ALARO-SK at 4.8km, where only STD data from Slovakia is assimilated.

Mode-S observations

Availability of Mode-S type of aircraft observations in LACE has been increased in 2019 by operational exchange of Mode-S MRAR from the Czech Republic. A coordination with EMADDC (KNMI) regarding real-time pre-processing of data from several countries is ongoing.

In Slovakia, impact of Mode-S impact was investigated by means of Degrees of Freedom for Signal (DFS, Fig. 6). It is once again confirmed that Mode-S has high impact on analysis (and also short term forecast as shown earlier).

Limited experimentation with AMDAR humidity was carried out in Hungary. Small and mostly neutral impact was detected, most probably due to limited data counts.

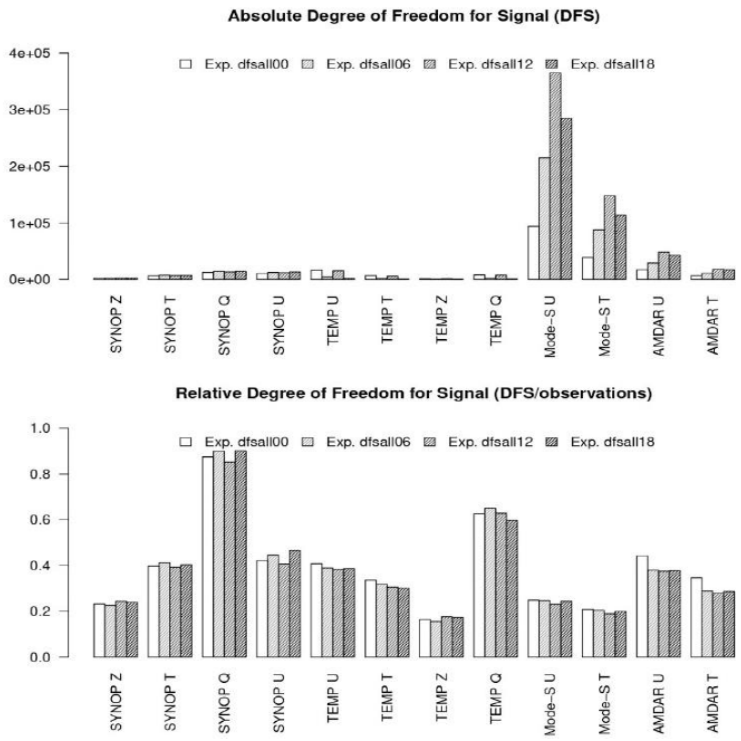

Figure 6: Impact (weight) of Mode-S in analysis as diagnosed by DFS (ALARO-SK).

Assimilation of microwave links

A feasibility study on a sample of 600 telecommunication data links in Slovenia was carried out in Slovenia. The first goal was to efficiently separate attenuation data in rainy and dry conditions. Wet/dry period and attenuation were dynamically modelled by a factor graph approach. Baseline attenuation, needed to separate dry from wet cases, was determined as a second-order linear state-space model. Finally, the relation between attenuation and rain modelled as a power law equation.

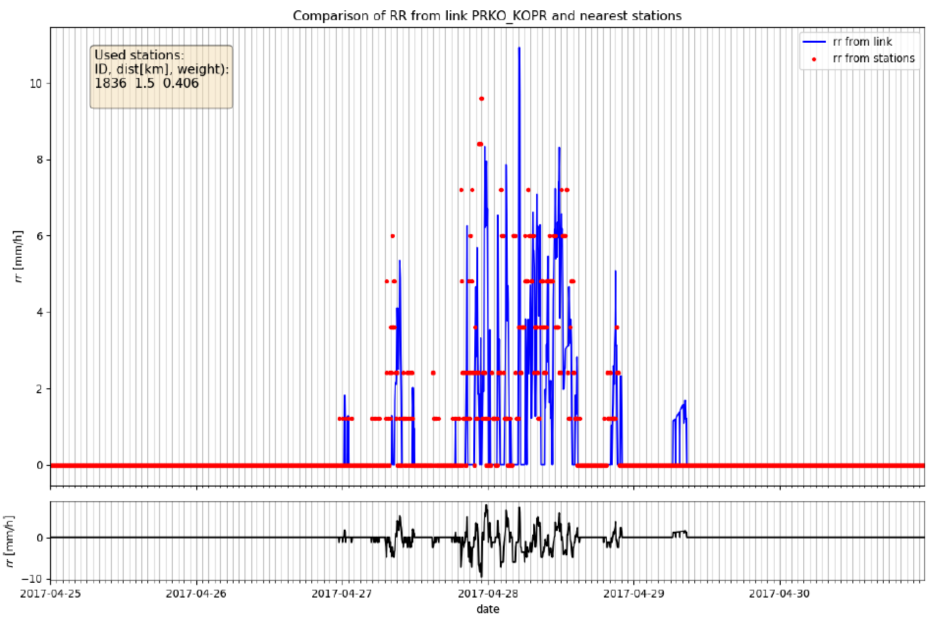

Figure 7: Intercomparison of rain estimates from a microwave link in Slovenia (blue) and nearby station measurements (red dots).

5 Summary and outlook

The activities of RC LACE assimilation group are focused on operational application of data assimilation of high-resolution LAMs, which includes refinements of existing upper-air assimilation algorithms, gradual introduction of improved surface assimilation schemes and additions of as many different observations as possible. The current focus in RC LACE is a rapid (hourly) assimilation system. Austrian AROME Nowcasting is the first operational system of this kind, and similar systems are under design and evaluation in the Czech Republic, Hungary and Slovenia. On observation side, the current priority is the assimilation of OEPRA radar data, especially reflectivity. Other non-conventional observations such as GNSS, Mode-S and microwave attenuations are also under continuous development.

6 Literature

Martin Imrišek, 2019: GNSS slant total delays in the ALADIN NWP system, RC LACE stay report, KNMI.

The DAsKIT programme: status and plans

Maria Monteiro, Ouali Aitmeziane, Haythem Belghrissi, Andrey Bogatchev, Yelis Cengiz, Alex Deckmyn, Idir Dehmous, Fatima Hdidou, Wafa Khalfaoui, Marcin Kolonko, João Rio, Zahra Sahlaoui, Meral Sezer, Malgorzata Szczęch-Gajewska, Boryana Tsenova

1 Introduction

The Data Assimilation starters Kit, hereby designated by 'DAsKIT', is an ALADIN Strategic Core Programme which promotes the coordination and synergy between the ALADIN countries which are starting their local activities in operational Data Assimilation (DA) taking advantage of the work previously done by ALADIN and HIRLAM countries experts along their progress track in this area of Numerical Weather Prediction (NWP).

The programme was first introduced at the annual all staff meeting during the "Joint 30th ALADIN Workshop & HIRLAM All Staff Meeting 2020", held by vision-conference at the end of March 2020. The work is being developed by the eight countries: Algeria, Belgium, Bulgaria, Morocco, Poland, Portugal, Tunisia and Turkey, with the collaboration of the remaining countries from both ALADIN and HIRLAM consortia.

This article summarises the main aspects of the programme and answers the three basic questions: "How did DAsKIT programme start ?", "In terms of milestones, what was achieved so far ?" and "What is the initial DAsKIT set ?". The article is splitted in the following way: in Section 2, its motivation and main goals are registered; in Section 3, the available tools and applied methodology are described; an overview on the progress done so far and on the actual status is given in Section 4; an illustration of the preliminary results is shown in Section 5; and, finally, some conclusions and outlook is given in Section 6.

2 Motivation and Goals

How did DAsKIT programme start ?

To answer this question, let us analyse the ALADIN-HIRLAM consortia situation on operational DA back to year 2016. It was then recognised that DA added value to our forecast's performance and that new observational systems were arriving which would require a convergence of efforts around the NWP community to tackle them .

The Figure 1A, presented by [1] during the ALADIN General Directors Assembly (GA) in 2016, illustrates the situation among ALADIN countries, what concerns operational DA and, Figure 1B, illustrates the situation over HIRLAM countries. By analysing these two figures we can distinguish four groups of countries, concerning capacities and progress in terms of DA: i) France (bottom line on the Table of Figure 1A), with fully established DA activities; ii) the consortium RC-LACE (remaining turquoise lines of Figure 1A), where most of the countries where cycling a DA solution related to the ALARO physics and whose progress had been boosted through the creation of the centralised

OPLACE pre-processing system [2], through a close cooperation and exchange of scientific and technical know-how and tools, and the commitment of a fixed man-power per team [3]; and iii) the HIRLAM consortium (Figure 1B), where most of the countries already had a combined solution of surface plus upper-air DA. However, in more than half of the ALADIN countries there were no visible operational DA activities. Therefore, during the Strategy Meeting held in Toulouse in 2016 [4], it was found beneficial and a common opportunity to all the consortia to support some coordination and synergy between those ALADIN countries.

Operational configurations	RUN OVER															
RUN BY	Algeria	Belgium	Bulgaria	Morocco	Poland	Portugal	Tunisia	Turkey	Austria	Croatia	Czech Rep	Hungary	Romania	Slovakia	Slovenia	France
Algeria	ALADIN 12					ALADIN 12	ALADIN 12			ALADIN 12					ALADIN 12	
Belgium		ALARO 4														
Bulgaria			ALADIN 7													
Morocco	ALADIN 18	ALADIN 18	ALADIN 18	AROME 2.5		ALADIN 10	ALADIN 18	ALADIN 18	ALADIN 18	ALADIN 18	ALADIN 18	ALADIN 18	ALADIN 18	ALADIN 18	ALADIN 18	ALADIN 18
Poland		ALARO 4	ALARO 4		AROME 2.5				AROME 2.5	ALARO 4	AROME 2.5	AROME 2.5	ALARO 4	AROME 2.5	AROME 2.5	
Portugal						AROME 2.5										
Tunisia							ALADIN 12									
Turkey			AROME 2.5					AROME 2.5		ALARO 4.5			ALARO 4.5		ALARO 4.5	
Austria		ALARO 5							AROME 2.5	AROME 2.5	AROME 2.5	AROME 2.5		AROME 2.5	AROME 2.5	
Croatia									ALARO 8	ALARO 2	ALARO 8	ALARO 8		ALARO 8	ALARO 2	
Czech Rep		ALARO 4.7	ALARO 4.7		ALARO 4.7				ALARO 4.7	ALARO 4.7	ALARO 4.7	ALARO 4.7	ALARO 4.7	ALARO 4.7	ALARO 4.7	
Hungary		ALARO 8	ALARO 8		ALARO 8				ALARO 8	ALARO 8	ALARO 8	AROME 2.5	ALARO 8	AROME 2.5	AROME 2.5	
Romania			ALARO 6.5									ALARO 6.5	ALARO 6.5	ALARO 6.5		
Slovakia		ALARO 9	ALARO 9		ALARO 9				ALARO 9	ALARO 9	ALARO 9	ALARO 9	ALARO 9	ALARO 9	ALARO 9	
Slovenia		ALARO 4.4							ALARO 4.4	ALARO 4.4	ALARO 4.4	ALARO 4.4		ALARO 4.4	ALARO 4.4	
France		AROME 1.3														AROME 1.3

ALADIN/ALARO/AROME configurations — horizontal resolution in km — with DA — without DA

Figure 1A: Distribution of DA expertise among ALADIN countries: in turquoise, countries with DA activities (France plus LACE countries); in brick, countries with no visible DA activities.

Domain	Cycle	Grid	DA	forecast length/ cycle
AEMET	38h1.2	2.5 km 65 lev	3DVar + surf ana	48h/4times
DMI	38h1.2	2 km 65 lev	blending + surf ana	54h/4 times
FMI	38h1.2	2.5 km 65 lev	3DVAR + Surf ana	54h/8times
KNMI	36h1.4.bf1	2.5 km 60 lev	3DVAR + Surf ana	48h/8 times
LHMS	37h1.2	2.5 km 60 lev	blending + Surf ana	54h/4 times
MetEireann	37h1.1	2.5 km 65 lev	blending + Surf ana	54h/4 times
MetCoOp	38h1.2	2.5 km 65 lev	3DVAR + Surf ana	66h at 00,06,12,18, 3h at
VI-Iceland	38h1.2	2.5 km 65 lev	blending + Surf ana	48h/4 times

Figure 1B: Distribution of DA expertise among HIRLAM countries.

The Strategic Core Programme on Data Assimilation was after approved in 2017, by the ALADIN GA with support of HIRLAM Council, with the goal '*to develop a cross-consortia coordination to set-up a basic 3D-Var data assimilation cycle with a limited set of observations*' that should be '*suitable for operational implementation*'. Moreover, a 20% DA coordinator position was created to easy the convergence of synergies. However, one should notice that this is not a simple task, because this basic set should be able to be maintained by lower man-power teams, with short High Performance Computing (HPC) resources and knowing that many of these countries were not ECMWF, EUMETNET or EUCOS members or cooperating members (for instance, at the date of writing this article and from this group of eight countries, only three countries are ECMWF members - Belgium, Portugal and Turkey; two are cooperating members - Bulgaria and Morocco; and the remaining three are not related to ECMWF - Algeria, Poland and Tunisia).

The DAsKIT programme started at the beginning of 2018, and it required the identification of the main steps, knowing that the code and its applications are always evolving as well as the available cross-countries DA tools, what made this a dynamical task: in fact, in order to optimise the efforts, the programme should take advantage of the progress previously done by the other three groups of countries inside ALADIN-HIRLAM consortia. Besides, good communication platforms had to be implemented, including training.

3 Tools and Methodology

At the start of the programme, in the beginning of 2018, the relationship between the tasks to implement inside DAsKIT countries in order to establish and boost local operational DA capacities, and the available cross-consortia tools was the one represented in Figure 2.

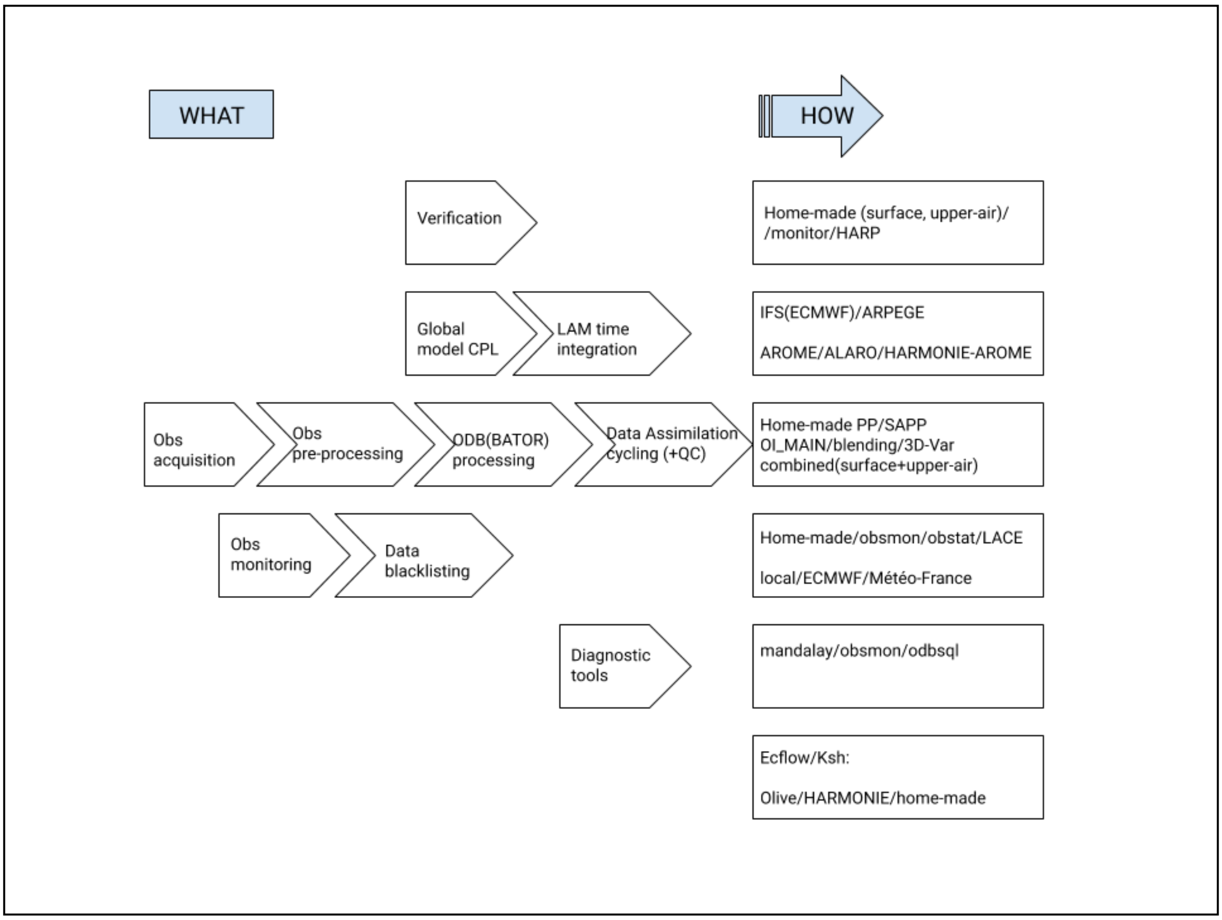

Figure 2: Relationship between DA tasks to implement in DAsKIT countries vs. available cross-consortia DA tools: WHAT-tasks to implement (left, represented by arrows); HOW-tools (right, represented in the boxes).

Some of the tools already existed in these countries, like the Limited Area Model (LAM) time integration and a home-made verification package (or other), but many other tools and related practices had to be locally implemented or established from scratch. In this way, balancing between what could be an opportunity to a common progress in the ALADIN-HIRLAM consortia and the real possibilities inside these countries, the following options were made *a priori*: to use HARP as a common verification tool; ARPEGE as the coupling (CPL) model; AROME as LAM; home-made pre-processing of GTS/WMO BUFR formatted data; the combined OI_MAIN plus 3D-VAR algorithm as DA solution; OBSMON to implement observations monitoring practices; and, finally, to use Korn shell scripts to establish the DA algorithm workflow, which could be easily implemented under Ecflow, the European Medium-range Weather Forecasts centre (ECMWF) scheduler.

4 Progress and Status

In terms of milestones, what was achieved so far ?

The Agenda of the dedicated DA Working Days (WD) [5] organized so far is illustrative of the main milestones of the programme in the last couple of years:

- in 2017, the preliminary WD held in Lisbon allowed the establishment of local BATOR processing activities (see Figure 2) with GTS BUFR SYNOP data in all countries. Taking advantage of this step; and
- after an extensive kick-off inquire done at the DAsKIT countries in 2018, an initial surface DA scripts set (from now on called 'DAsKIT' set) was created in a reference environment - Météo-France (using the 'T' version of the ALADIN system code [6] over 'beaufix' HPC platform);
- during the 2018 DAsKIT WD, the surface DAsKIT set was proposed to all the countries which tested it, discussed it and adapted it to their geographical domains, and started to implement it in their local operational environments under testing mode. All the countries did this last step, except Poland which entered the RC-LACE consortium meanwhile and is integrating the ALARO physics, initialised by a CANARI analysis.
- Already in 2019, during the latest '2019 Joint LACE DAWD & DAsKIT WD' the countries started to show and discuss their local results, work which is on-going in parallel with their developments towards 3D-Var under the reference environment. In this way, the common DAsKIT progress has been envisaged under a step-by-step assembly process of a combined solution of surface + 3D-Var algorithm.

Figures 3-5, show the progress done by DAsKIT countries in detail (further information can be found at the presentation [7]). These Figures were obtained by keeping up to date the kick-off inquiry to DAsKIT countries, done in 2018, and illustrate, for comparison, the actual situation (right panels) together with the situation registered at the start of the project (left panels) at the beginning of 2018.

In the first place, concerning 'Data Acquisition', it is registered that almost all the countries have now local access to GTS BUFR SYNOP, TEMP and AMDAR data. Besides, many countries have available conventional data which is only accessed locally and not through GTS.

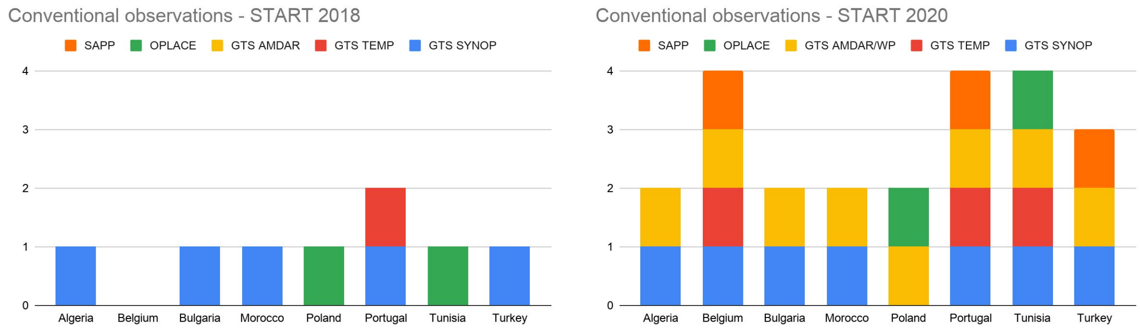

Figure 3: Conventional data types locally pre-processed (home-made or through SAPP) and available (through OPLACE), at the DAsKIT countries: at the beginning of 2018 (left panel); and at the beginning of 2020 (right panel).

Figure 3 illustrates the progress done on local 'Data pre-Processing', of conventional observations, due to the availability of BUFR formatted data. All the countries are now able to handle BUFR duplications due to corrections or amendments in some of these conventional data types, and are also able to filter different BUFR templates. Besides we can announce some universal home-made tools that can be used by other countries, in particular, created by Belgium and Bulgaria. Simultaneously, two of the DAsKIT countries (Poland and Tunisia) are still receiving OPLACE pre-processed data and in parallel, three of the countries (Belgium, Portugal and Turkey) have actions to implement locally the Scalable Acquisition and Pre-Processing (SAPP) system at ECMWF.

Concerning 'BATOR processing', the main effort was to make all the countries to converge to the same cycle version locally in order to optimise the issues resolution. All the countries are now locally working with the same cycle version - CY43T2_bf10 - and those who did not do it yet are having problems with their HPC infra-structures or are waiting for a new HPC. At the same time, more countries are now able to create ODB for the three conventional data types (SYNOP, TEMP and AMDAR), in particular all the countries are now able to create ODB from locally available SYNOP observations under BUFR format.

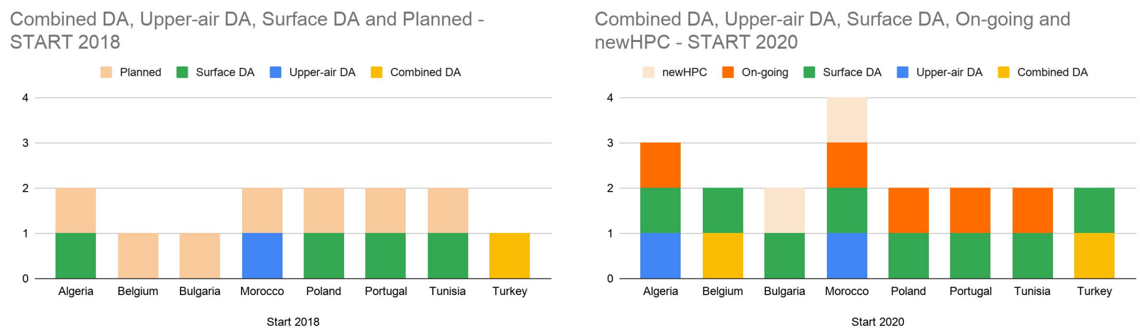

Figure 4: Local DA algorithms cycled for LAM initialization at the DAsKIT countries, at the beginning of 2018 (left panel) and at the beginning of 2020 (right panel): for surface, shadow in green; for upper-air, shadow in blue; for combined surface+upper-air, shadow in yellow; for on-going assembly of a combined, shadow in dark orange, or blocked, in light orange.

In Figure 4, the algorithms locally implemented and cycled are represented. From this figure it is possible to see that at this moment, all the countries are able to cycle, at least, a surface DA scheme and this is due to the creation of the initial surface DA set. At the same time, we can see, the trend for all these countries is to have a combined surface plus upper-air DA solution and in fact, two of the countries, Belgium and Turkey, already have in-doors a cycling scheme of this combined solution. Moreover, some countries, like Bulgaria and Morocco, are now blocked waiting for the new HPC structure to have this step done.

What concerns the 'complementary accessories' that we need to implement locally in order to have operational DA in-doors, some overview is registered in Figure 5, on five of these applications on data monitoring, diagnostics and verification, although for the ODBSQL (ECMWF) tool and for MONITOR (verification tool used by HIRLAM), there was not enough information available to take some conclusions. As mentioned before, concerning data monitoring, the target tool chosen *a priori* was OBSMON.

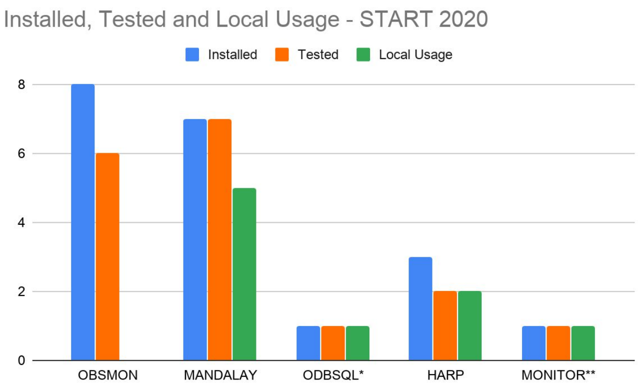

Figure 5: Number of DAsKIT countries with local use of cross-consortia DA tools required to establish full operational DA activities: installed, in blue; tested, in orange; and regular use, in green.

And, as confirmed by Figure 5, this tool was implemented in all the countries, but it is not being used locally; instead, MANDALAY is generally still in use. Similarly, the same is happening with the verification tool HARP: some countries have implemented it but only a very few are using it and instead, MONITOR is still in use.

5 Preliminary results

What is the initial DAsKIT set ?

The DAsKIT set solves, for one network, the so called OI_MAIN analysis, following the surface DA algorithm, proposed by [8] in 2000 for ARPEGE, having as input GTS BUFR SYNOP observations, using home-made pre-processing and preparing an AROME first-guess with some specific tasks: 'ADDSURF', 'CPLTS' and 'Blendsur', where the first task adds surface fields to the guess for technical reasons; the second task deals with the difference in tiles characterisation from SURFEX to CANARI; and the last task updates the Sea Surface Temperature (SST) of the guess with the fresh one provided by the coupling file from the global model ARPEGE. The kit was created under the reference environment of Météo-France at CY40T1_bf07 and written as a Korn shell script. The idea is now to assemble, step-by-step, 3D-Var tasks and to make a full scripting system of this combined solution at CY43T2_bf10.

In this Section, some examples of the preliminary validation results of the local surface DAsKIT set implementations are illustrated. They can be splitted in two parts: in the first part, the results obtained on the local cycling implementation with the initial surface DA settings (DAsKIT set) are shown; and, in the second part, some feasibility studies on a reference environment - Météo-France - towards a local 3D-Var implementation, are described.

Local implementations scores for surface DA

Starting with Algeria, Figure 6 shows the time series for bias at 00UTC of 2-metre temperature and 2-metre relative humidity, for the initial time step of AROME-Al integration. The model is initialised with and without DA (spin-up mode), and cycled along a 20-day period. For this experiment, AROME-Al was run with 2.5km resolution; besides, locally available GTS BUFR SYNOP data was assimilated on a 3-hour assimilation cycle.

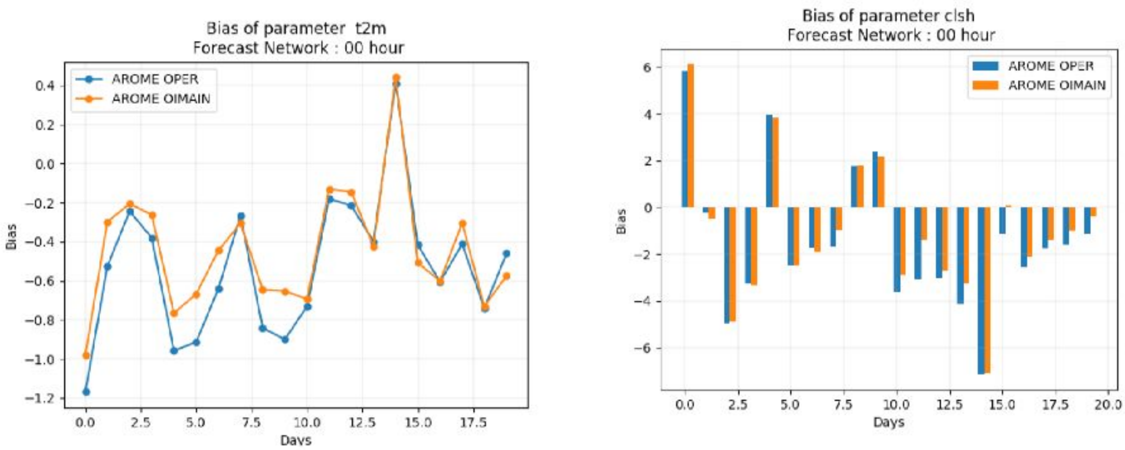

Figure 6: Time series of 00UTC initial model state bias of AROME-Al with (yellow line/shadow) and without (blue line/shadow) surface DA assimilation, along a 20-day period for: 2-metre temperature (left panel) and 2-metre relative humidity (right panel).

By comparing the two lines (blue and yellow) on each of the Figure 6 panels, it is possible to see that there is a general decrease of the bias values for these screen level parameters: generally, all over the 20-day cycling for 2-metre temperature and after a 9-10 day cycling for 2-metre relative humidity.

In the next example, the results from Belgium and Portugal are shown together. The root mean square error (RMSE) for 2-metre temperature as a function of the time step is shown when the AROME model is initialised with and without surface DA (DAsKIT set). In these countries' experiments, the CANOPY [9] scheme was switched off from the AROME physics and Geylen's diagnostic [10] is used to compute the screen level parameters; AROME-Be is run with 1.3 km horizontal resolution and its hourly output is extended up to 36-hour lead time; while AROME-PT is run with 2.5 km resolution and it is shown with a 3-hour output up to 48-hour lead time. Locally available GTS BUFR SYNOP data (more than 200 for AROME-Be and more than 300 for AROME-Pt domain) is assimilated at each 3-hour network. For the two models, the experiments are cycled over a period of more than 1-month time, overlapped for a while, during Fall for AROME-Be and Summer for AROME-Pt.

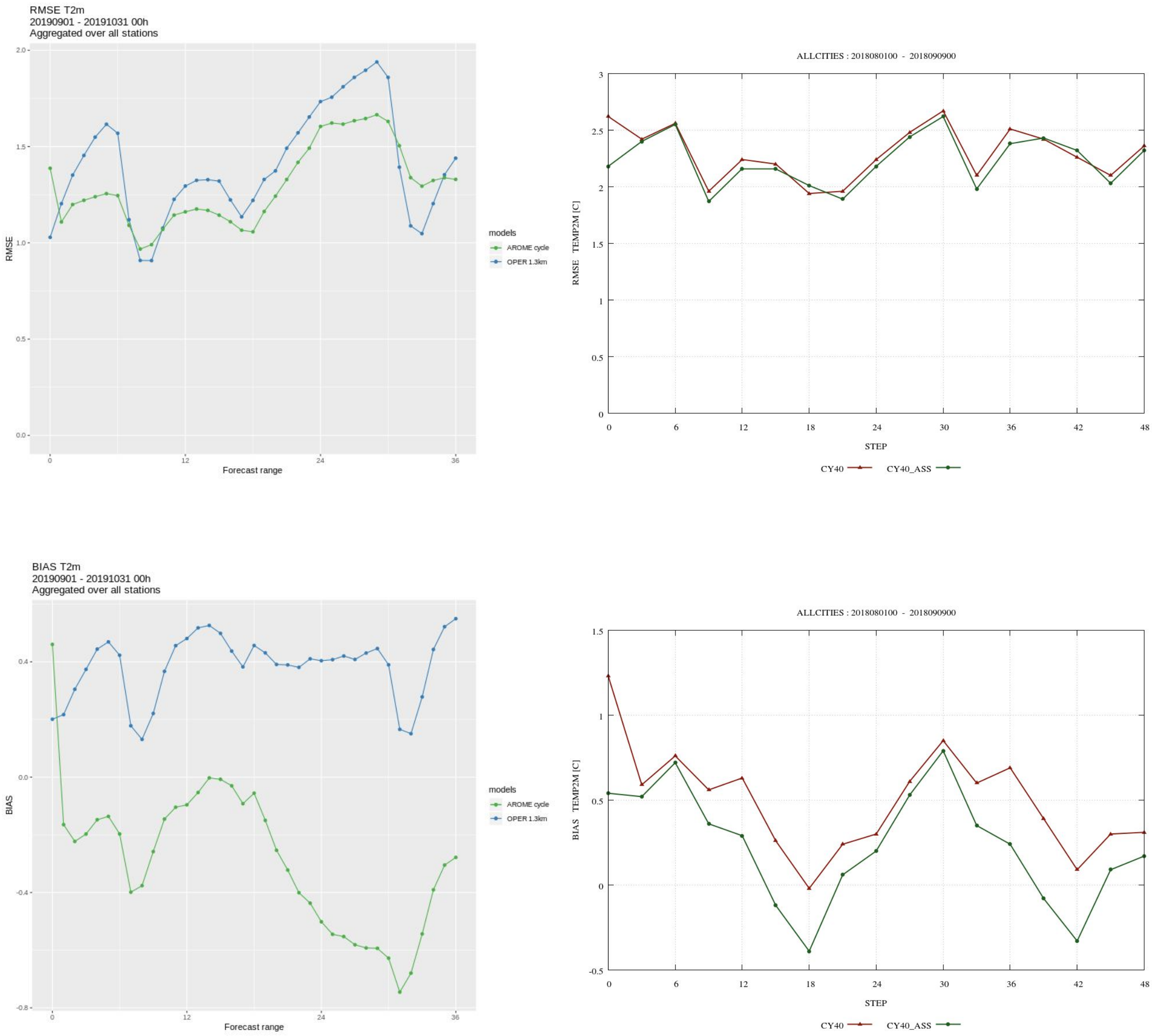

Figure 7: RMSE (top) and Bias (bottom) for 00UTC forecasts of AROME-Be (left panels with a lead time up to 36-hour) and AROME-Pt forecasts (right panels with a lead time up to 48-hour), with and without surface DA (green line) initialization.

For both models domains the RMSE is generally decreased when initialization is done through the DAsKIT set, except during a short period of the diurnal cycle which is early morning for AROME-Be and late afternoon for AROME-Pt. The detailed analysis of RMSE seems to point to a general good consistency of both models results, except at the initial time step, when post-processing may drive us to a misleading result.

The Figure 8 illustrates the example of Turkey (for details, see [11]). Once again, the AROME-Tk results are shown in parallel with those obtained for Portugal. In the same way and as on the previous example, the root mean square error (RMSE) as a function of the time step is shown when the AROME model is initialised with and without surface DA (DAsKIT set), although the chosen parameter is now 2-metre relative humidity. Both models have 2.5 km of horizontal resolution; CANOPY was switched off; the experiments are conducted over a Winter period of two weeks for

AROME-Tk and more than one month for AROME-Portugal. Locally available GTS BUFR SYNOP data is assimilated (around 100 observations for AROME-Tk and around 200 for AROME-Pt).

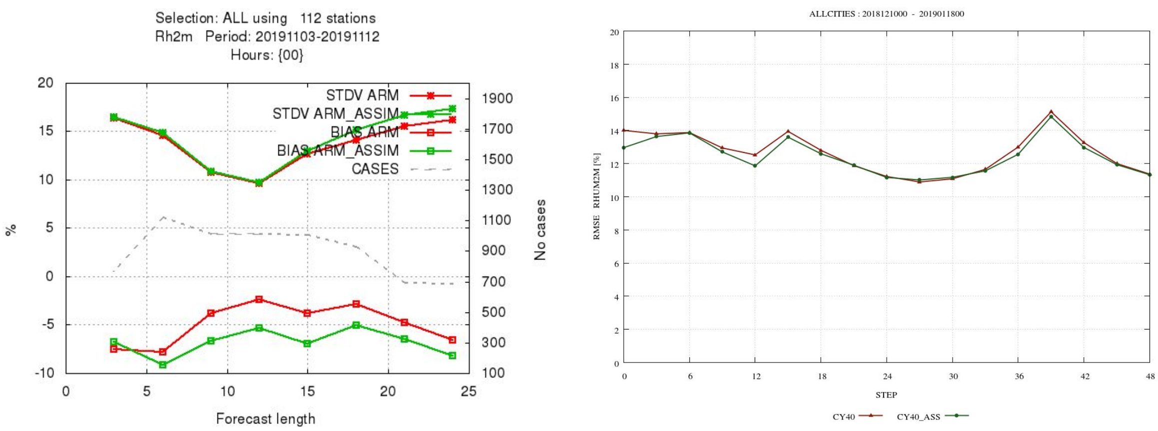

Figure 8: RMSE (top) and Bias (bottom) for 00UTC forecasts of AROME-Tk (left panels with a lead time up to 24-hour) and RMSE for AROME-Pt forecasts (right panels with a lead time up to 48-hour), with and without surface DA (green line) initialization.

As the last example of this series, the RMSE of 2-metre temperature is shown for ALARO-Pl (Poland). The model is run at 4km resolution with and without surface DA. Figure 9 shows the results for 1-week of accumulated scores, after a 20-day period of cycling. And we can see there is a decrease of RMSE values along the lead time, except during some periods of the diurnal cycle.

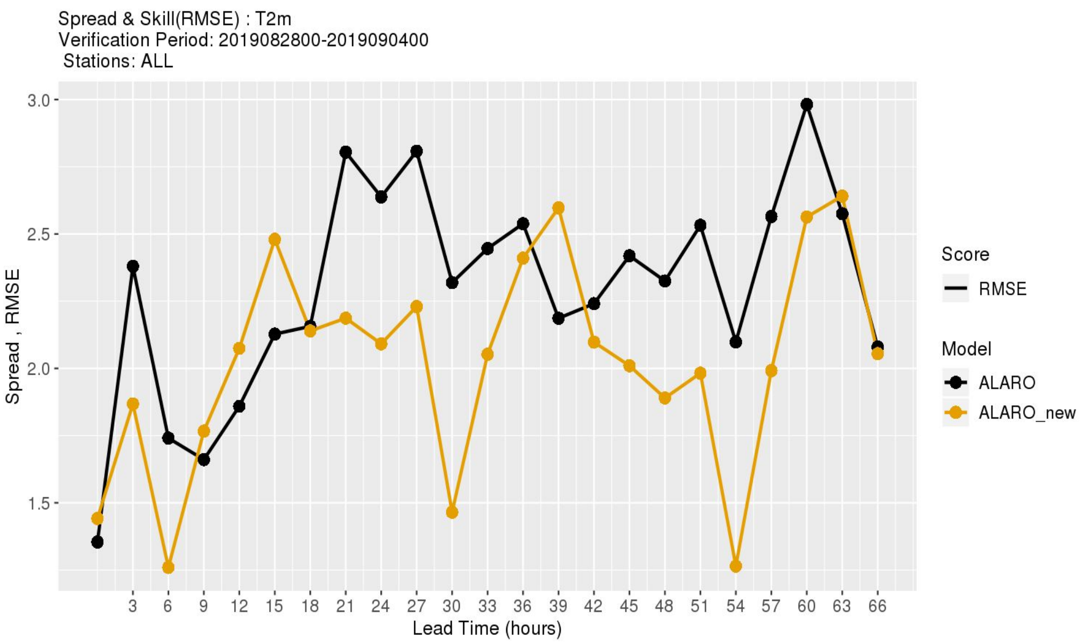

Figure 9: RMSE (top) for 00UTC forecasts of ALARO-Pl (left panels with a lead time up to 66-hour) with different initializations: after surface DA (CANARI), yellow line; and without DA, black line.

Feasibility studies on a reference environment at Météo-France

In the next sequence of examples the studies on ensemble B-matrix modelling from Algeria and Portugal, and also from Tunisia and Morocco, are illustrated. These studies have been performed during short scientific stays at Météo-France at the local HPC. The difference between the two first countries and the two second countries, is that for the first pair the study concerns a first B-matrix obtained from an ensemble where the model is run under spin-up mode, whereas for Tunisia and Morocco a second B-matrix has already been computed by Ensemble Data Assimilation (EDA) methodology, where the dispersion on an ensemble of DA cyclings is used to estimate the background errors.

Starting with Algeria and Portugal examples, the vertical profiles of the standard deviation of background errors of the model control variables for AROME-Al and AROME-Pt are illustrated in Figure 10, together with those obtained from different AROME-Fr error estimates. The analysis of these results is still on-going and is being done taking into account the prevailing weather conditions at play during the seasonal periods chosen to compute the background errors and the corresponding climatological B-matrix.

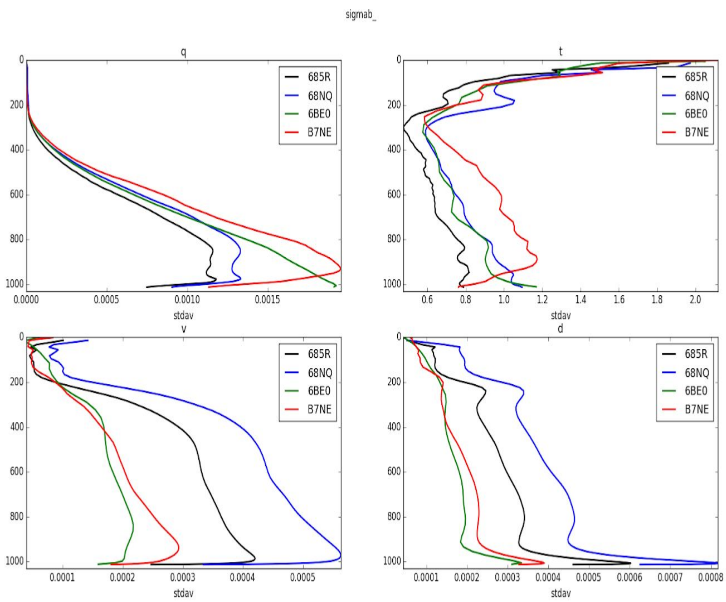

Figure 10: Vertical profiles background error standard deviations, for the different geographical domains of AROME-Al (green line), AROME-Pt (red line) and AROME-Fr (blue and black lines), for different control variables: specific humidity (top left panel); temperature (top right panel); vorticity (bottom left panel); and divergence (bottom right panel).

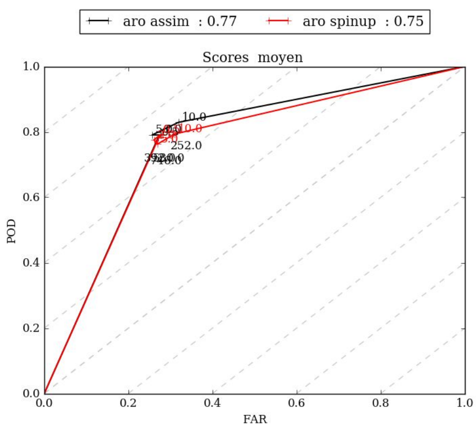

Studies on the validation of these first B-matrices have been started and at Figure 11 an illustration of the impact of 3D-Var initialization (using the computed B-matrix) over the dynamical adaptation AROME-Pt integration is accessible.

Figure 11: Averaged Probability of Detection vs. False Alarm Rate of 24-hour accumulated precipitation of AROME-Pt, over the period 20190122(03UTC) - 20190210(03UTC), initialized by dynamical adaptation (red line) and assimilation (black line) .

The impact is seen over the 24-hour accumulated precipitation, in terms of an improvement of Skill Scores (not shown) and Probability of Detection (PoD) keeping the False Alarm Rate (FAR). And to evaluate the impact of 3D-Var over the spin-up model configuration, the assimilation of ODIM HDF5 volumetric data for Portugal and Spain was successfully added.

In the next examples, we can see the same kind of profiles for Morocco and Tunisia, but now the background error estimates are obtained by EDA methodology, using the first B-matrix, in order to obtain a second B-matrix. For both the countries there is, in general and more clearly for vorticity and divergence, an increase on the vertical standard deviations, that will impact on the forecasts performance during high impact weather conditions.

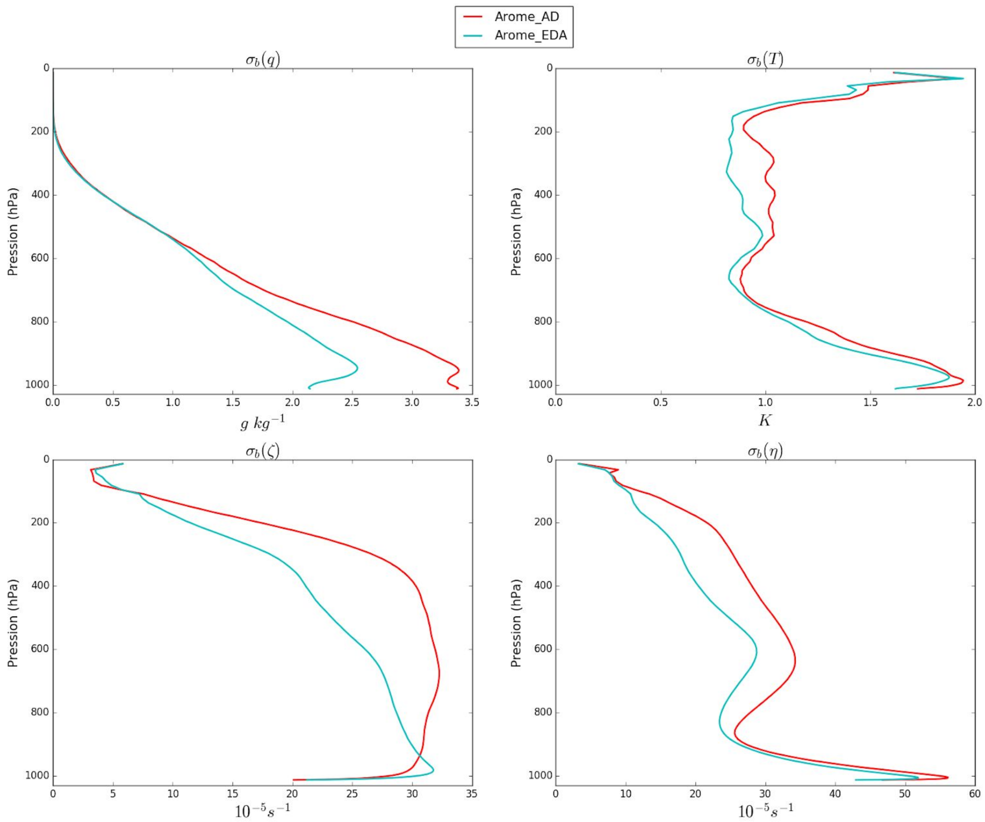

Figure 12: Vertical profiles background error standard deviations, for the AROME-Mo, estimated by ensemble technique with spin-up model (blue) and EDA (red), for different control variables: specific humidity (top left panel); temperature (top right panel); vorticity (bottom left panel); and divergence (bottom right panel).

Figure 12 illustrates de standard deviations for the background errors of AROME-Mo, when estimated by two different ensemble techniques, with the model at spin-up mode and by EDA. Figure 13 shows the same kind of information but for AROME-Tn.

Studies on the validation and impact of the second B-matrix are on-going on the two countries by evaluating the impact of these B-matrices in case-studies of heavy-rain weather conditions.

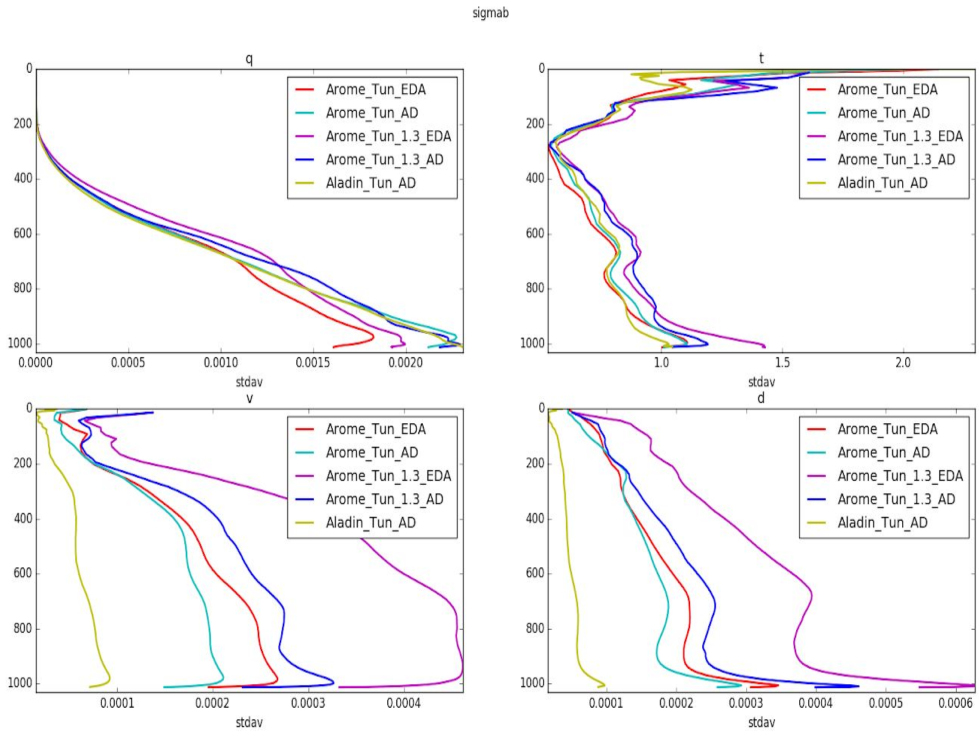

Figure 13: Vertical profiles background error standard deviations, for the AROME-Tu, estimated by ensemble technique with spin-up model (blue) and EDA (red), for different control variables: specific humidity (top left panel); temperature (top right panel); vorticity (bottom left panel); and divergence (bottom right panel).

6 Conclusions and Outlook

As main conclusions, we can deliver that: i) all the countries have now know-how to keep some DA cycle with conventional observations in-doors; ii) the efforts of these countries are now focused on combining OI_MAIN with 3D-Var at CY43 and these efforts are splitted between surface, what concerns validation and tuning of the local DAsKIT set and upper-air, setting 3D-Var still on a reference environment; besides, iii) all countries have now data monitoring in-doors but some effort still has to be done so that it can be used on a regular basis; finally, iv) the validation tools in-doors are still missing and, although this could be a good opportunity to implement HARP this was not yet the case.

Two remarks should be added here: i) although the ‘2019 Common ALADIN-HIRLAM DA Training Course’ was a good opportunity to get in touch with the actual available cross-country DA tools, many DAsKIT countries could not be present; and ii) DAsKIT have implemented several communication platforms therefore everyone is invited to join them or to use them whenever needed.

As short-term actions, two announcements are added here: i) the usual quarter’s video-conference which will take place this June; and ii) the ‘2020 Joint LACE DAWD & DAsKIT WD’ that will be held in Vienna, in September, this year.

Acknowledgements

To Piet Termonia, Martina Tudor and Jeanette Onvlee for promoting the synergy among the groups and teams; Piet, in particular, believed in the momentum of the ALADIN teams towards operational DA. To Alena Trojakova for her endless and efficient support to DAsKIT colleagues and her long-term commitment to the success of the programme; to Pierre Brousseau and Claude Fischer, for the scientific and technical guidance during DAsKIT colleagues scientific stays in Météo-France; to Roger Randriamampianina, for establishing the bridges between the HIRLAM and ALADIN DA experts (and tools); and to Máté Milé, for the original DA scripts on Météo-France's HPC platforms. Finally, to Patricia Pottier for keeping the DAsKIT web page alive.

7 References

[1] Termonia, P., 2016: *MoU5 & ALADIN-HIRLAM agreement*, ALADIN GA 2016, at http://www.umr-cnrm.fr/aladin/IMG/pdf/6_mou.pdf.

[2] Trojáková, A., Mile, M., and Tudor, M.: Observation Preprocessing System for RC LACE (OPLACE), Adv. Sci. Res., 16, 223–228, https://doi.org/10.5194/asr-16-223-2019, 2019.

[3] http://www.umr-cnrm.fr/aladin/IMG/pdf/oplace_aladin_strategy_meeing_mate_mile.pdf.

[4] http://www.umr-cnrm.fr/aladin/spip.php?article300.

[5] http://www.umr-cnrm.fr/aladin/spip.php?article348.

[6] Termonia, P., Fischer, C., Bazile, E., Bouyssel, F., Brožková, R., Bénard, P., Bochenek, B., Degrauwe, D., Derková, M., El Khatib, R., Hamdi, R., Mašek, J., Pottier, P., Pristov, N., Seity, Y., Smolíková, P., Španiel, O., Tudor, M., Wang, Y., Wittmann, C., and Joly, A.: The ALADIN System and its canonical model configurations AROME CY41T1 and ALARO CY40T1, Geosci. Model Dev., 11, 257–281, https://doi.org/10.5194/gmd-11-257-2018, 2018.

[7] http://www.umr-cnrm.fr/aladin/IMG/pdf/2020aladin_daskit_presentation.pdf.

[8] Giard, D and Bazile, E.: Implementation of a New Assimilation Scheme for Soil and Surface Variables in a Global NWP model, Monthly Weather Review, 128, 997-1015, 2000.

[9] Masson, V., and Seity Y.: Including Atmospheric Layers in Vegetation and Urban Offline Surface Schemes, Journal of Applied Meteorology and Climatology, 48(7), 1377-1397, DOI: 10.1175/2009JAMC1866.1, 2009.

[10] Geleyn J.-F., 1988: Interpolation of wind, temperature and humidity values from model levels to the height of measurement. Tellus, 40A, 347-351.

[11] Cengiz,Y. and Sezer, M.: Implementation of CANARI in AROME TURKEY, ALADDIN-HIRLAM Newsletter, nº 14, January 29th, 2020, https://www.umr-cnrm.fr/aladin/IMG/pdf/nl14.pdf.

Snow

Mariken Homleid

1 Introduction

How do the presence of snow affect near surface weather - in reality and in our Numerical Weather Prediction models? That is the underlying question and motivation here and in ongoing snow related developments. The physical properties of snow are briefly touched in sec. 2, followed by a short status on snow related issues in current cycle of HARMONIE-AROME. Finally some snow related improvements in Copernicus ARctic ReAnalysis are presented; improvements that affect the performance on the glaciers (permanent snow) and the use of satellite snow extent to better discriminate between snow free and snow covered ground.

2 Snow properties

Figure 1: "Winter night in Rondane" by Harald Solberg, 1914. (https://no.wikipedia.org/wiki/%C2%ABVinternatt_i_Rondane%C2%BB)

Snow has several properties that all help to lower the temperatures above the snow. Snow has low heat capacity, isolates and prevents heat transport between the ground and the atmosphere and emits as a black body. These are all properties that might contribute to rapid and strong cooling in stable conditions, particularly during night, including the arctic night. Furthermore, snow has high albedo and reflects most of the incoming radiation, so also in day time will the presence of snow strongly influence the near surface temperatures. The effect of the snow on the near surface temperatures depends on the fractional snow cover which is a key parameter in the snow modelling.

The snow also affects the wind speed and exchange of heat, effects that are parameterized through specific roughness lengths for snow.

3 Snow status in current cycle of HARMONIE-AROME

The current cycle of HARMONIE-AROME (Bengtsson et al. 2017) - cycle 40 - uses SURFEX (Surface externalisée) (Masson et al. 2013) - version 7.3. SURFEX has 3 optional snow schemes, of increasing complexity. The 1 layer snow scheme (D95, Douville et al. 1995), is still in use, with prognostic equations for Snow Water Equivalent (SWE), snow density and albedo. Fractional snow cover is diagnosed from SWE and fraction of vegetation. The scheme gives realistic snow aggregation, but a slight delay of the melting, given that the forcing is realistic. Precipitation amounts and face, and temperature are the most important forcing variables. Too much precipitation e.g. in mountainous areas in West Norway might lead to too much snow aggregated during the winter.

The SWE is adjusted to observed snow depths in the snow analysis to correct for deficiencies in the snow scheme or forcing (precipitation, temperature). The snow analysis is performed by CANARI (Taillefer, 2002) and is based on the Optimal Interpolation method. The background error correlation includes both a horizontal and a vertical term. Only conventional snow depth observations are used in the present operational HARMONIE-AROME versions. The snow analysis is performed once daily, at 06 UTC, when most snow depth observations are available. The performance is good in regions with representative observations. But we have learned that monitoring of the snow analysis in the operational NWP models is important. Currently the first guess to the snow analysis from observations at pure SEA or WATER points will, for technical reasons, be 0. Repeated observations of snow will give positive analysis increments in the surroundings of the station as long as snow is observed. One way to avoid the problem, is to blacklist all such stations. It is also important to make sure that the observations not are rejected in the First Guess check due to too narrow limits.

4 Snow related improvements in CARRA

Copernicus ARctic ReAnalysis (CARRA) will be the first European regional atmospheric reanalysis targeted for Arctic areas. It is performed with HARMONIE-AROME cycle 40 on two domains with 2.5 km grid, and will cover the time period from July 1997 to June 2021. For more information, see https://climate.copernicus.eu/copernicus-arctic-regional-reanalysis-service.

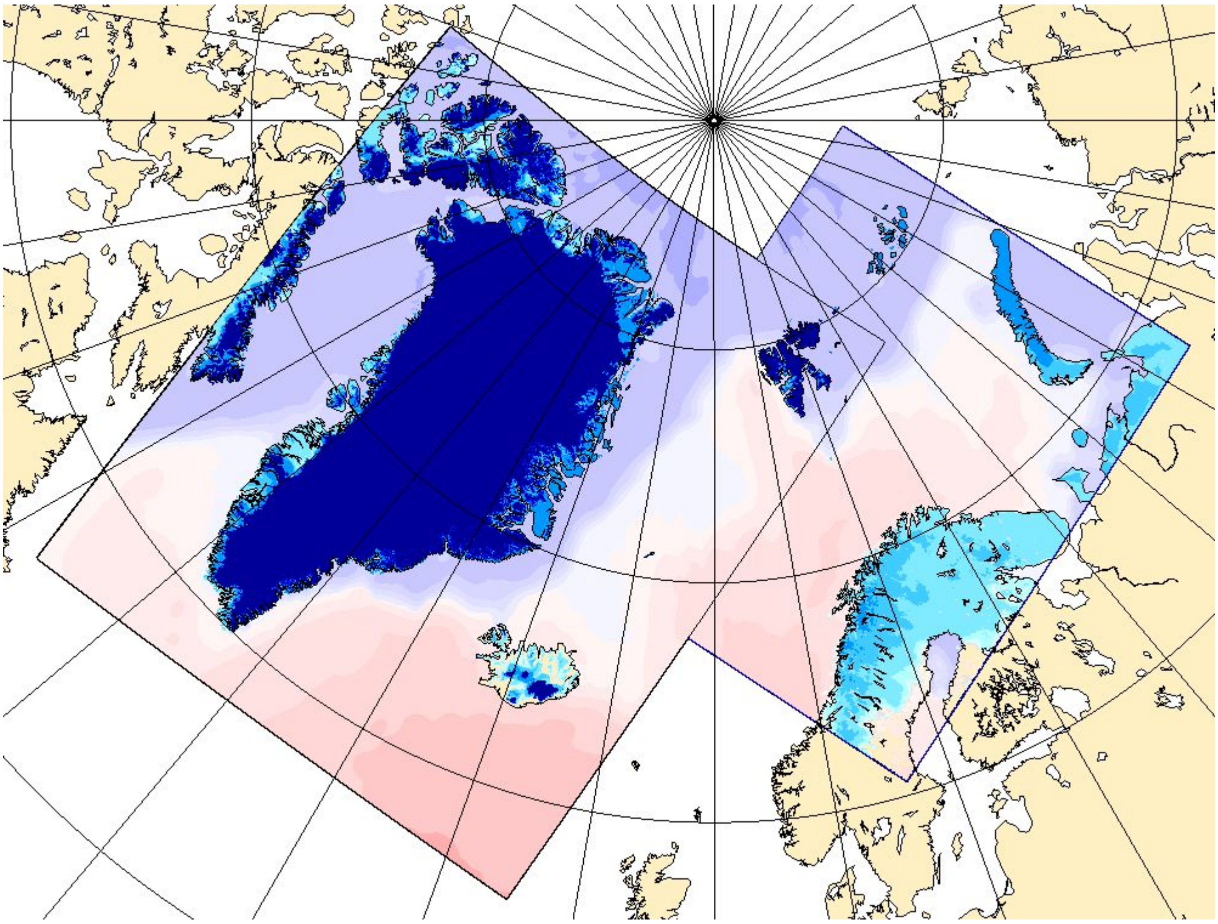

Figure 2: CARRA western and eastern domains.

Glaciers related improvements in CARRA

SURFEX glaciers are defined by a specific patch; PERMANENT SNOW. There is not yet any specific glacier model in SURFEX, so the performance over the glaciers is defined by the 1-layer snow scheme (D95). That is also the case in CARRA, but some improvements have been introduced:

- new glaciers masks
- improved snow albedo calculations, and use of an external glacier albedo data set
- Snow Water Equivalent on the glaciers is reinitialized to 10 ton/m^2 every year, 1 September
- the snow analysis do not change the SWE on the glaciers
- **snow free and hot glaciers** are avoided by introducing a lower limit of SWE on PERMANENT SNOW. The problematic performance is demonstrated in Fig. 3 by results for Svalbard 3 August 2017 from AROME-Arctic (left), and improved performance in CARRA (right).

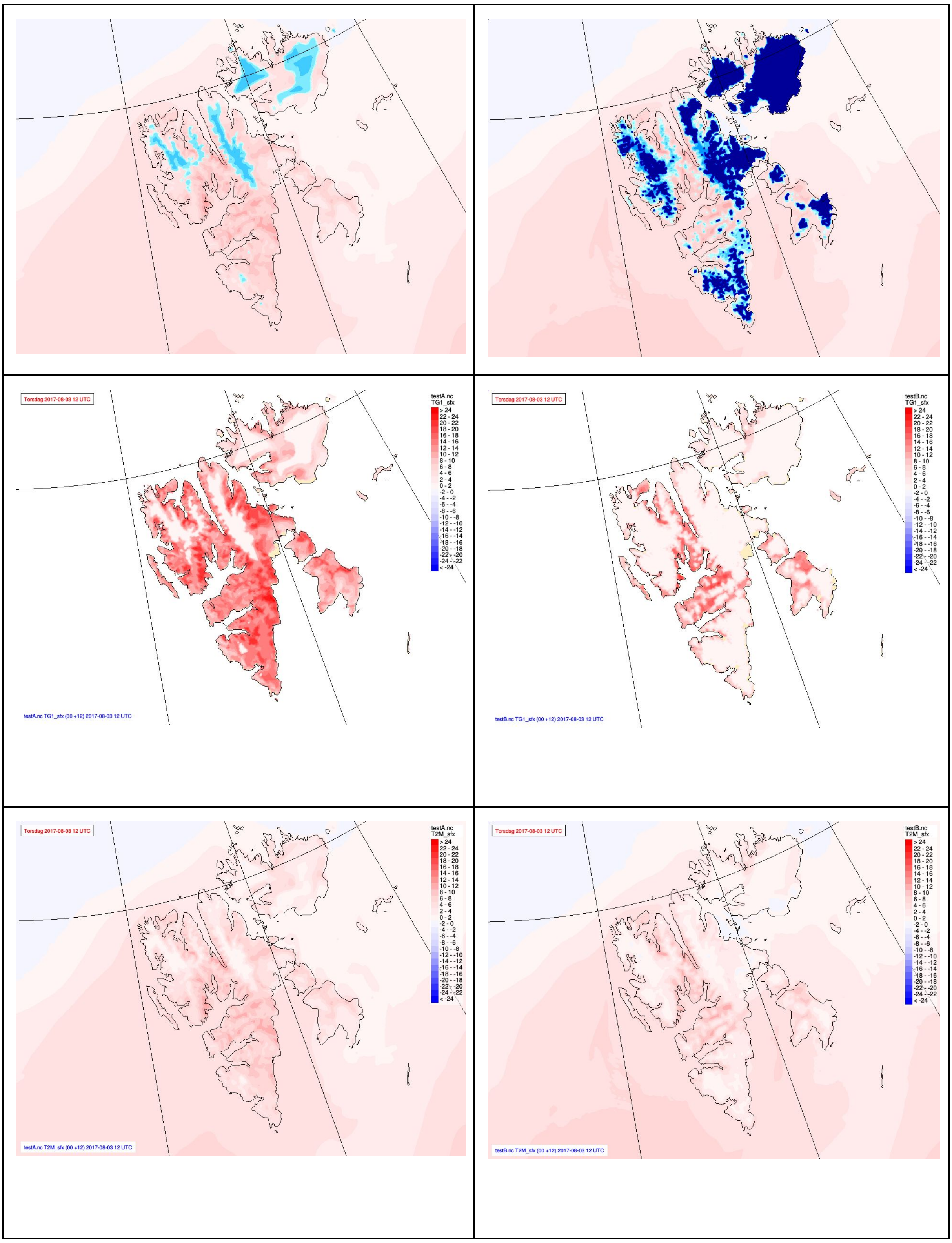

Figure 3: AROME-Arctic (left) and CARRA (right) Snow Water Equivalent (top), surface temperature (middle) and 2 meter temperature (bottom), Svalbard 3 August 2017.

Use of satellite snow extent in CARRA

The use of satellite snow extent in CARRA was motivated by the lack of conventional snow depth observations in parts of the domains, e.g. Greenland, Svalbard, Iceland.

Two different satellite products were considered for use

- HSAF snow extent produced operationally since autumn 2017 by N. Siljamo, FMI, documentation and data is available on https://landsaf.ipma.pt/en/
- CryoClim produced at MET Norway available 1982 – 2015, (Solberg et al. 2017, Killie et al. 2018)

HSAF and CryoClim are both based on AVHRR data and gives “probability of snow” or “snow extent” in cloud free regions. Comparisons of HSAF and CryoClim performed in the CARRA project by K. Kouki, FMI, show good agreement between the to data sets in most cases, but also some differences, and potential for improvements of the products. CryoClim was chosen for use in CARRA because the data were already available for most of the CARRA period.

The implementation in CARRA is based on an implementation in cycle 37, presented on ASM in Reykjavik in 2013, and documented in Homleid and Killie (2013). The satellite data is used in combination with conventional snow depth observations. The snow depth observations improve the snow amounts through the winter. The satellite data helps to discriminate between snow free and snow covered ground, which is of particular importance in the melting season. The satellite data is used with 5 km resolution on Iceland and Svalbard, but thinned to 10 km resolution else where to avoid significant increase in computation time in CANARI. The satellite data is assumed to have uncorrelated errors. «No snow» values are used as 0 and «snow» are used only when 1. guess < 28 kg/m^2, and set equal to the first guess. The satellite data is given less weight than conventional snow depth observations. The standard deviation of the background error and the observation error for conventional snow depths observations (converted to SWE) are 5 kg/m^2. The standard deviation of the observation error for satellite data is set to 8 kg/m^2.

CARRA experiments have shown that the satellite data has a small positive impact, both on the snow cover and on surface temperatures, particularly in the melting season.

5 Next steps

The Sami have more than 200 words for "snow" underlining the complexity of the phenomenon. In operational NWP we are still at a quite simple 1 layer snow scheme, **D95**, describing snow amount, density and albedo. The 25 years with **D95** might tell us that sometimes the simple is the best, or at least good enough. But we still aim at the ISBA Explicit Snow scheme (Boone et al. 2001) which has shown good performance in offline mode, in climate simulations and in the first NWP experiments with SURFEX version 8.1 in HARMONIE-AROME cycle 43.

6 References

Bengtsson, L. and Coauthors, 2017: The HARMONIE–AROME Model Configuration in the ALADIN–HIRLAM NWP System. *J. Atmos. Sci.*, 14**5**, 1919–1935, https://doi.org/10.1175/MWR-D-16-0417.1

Boone, A. and P. Etchevers, 2001: An intercomparison of three snow schemes of varying complexity coupled to the same land-surface model: Local scale evaluation at an Alpine site, J. Hydrometeorol., 2, 374–394.

Douville, H., J.-F. Royer and J.-F. Mahfouf, 1995: A new snow parameterization for the Météo-France climate model. Part I: Validation in stand-alone experiments. *Climate Dyn*., **12**, 21-35.

Homleid, M. and M. A. Killie: HARMONIE snow analysis experiments with additional observations, MET report 06/2013 available on https://www.met.no/publikasjoner/met-report/met-report-2013

Killie, M. A., S. Eastwood and A. M. Sørensen, 2018: Improvement and Validation of the Optical Component Used for Snow Mapping in CryoClim, Sentinel4CryoClim Phase 2 Project Report. METreport no 12/2018. Available on https://www.met.no/publikasjoner/met-report/met-report-2018.

Masson, V. and Coauthors, 2013: The SURFEX v7.2 land and ocean surface platform for coupled or offline simulation of earth surface variables and fluxes. Geosci. Model Dev., 6, 929–960, doi:10.5194/gmd-6-929-2013.

Solberg, R., Ø. Rudjord, A. B. Salberg, M. A. Killie, S. Eastwood and L.-A. Breivik, 2017: Advancement of global snow mapping in CryoClim, Sentinel4CryoClim Phase 1, Deliverables 1-6. Norsk Regnesentral, Oslo. NR-notat SAMBA/10/17. pp 80.

Taillefer, F.: CANARI - Technical Documentation - Based on ARPEGE cycle CY25T1 (AL25T1 for ALADIN). Available at http://www.cnrm.meteo.fr/aladin/, 2002.

Porting AROME on AMD

Ryad El Khatib

1 Introduction

Méteo-France is installing a new HPC system, based on AMD processors while the current system is working with Intel processors. Though both chips are designed from the same architecture (x86_64) it is worth analysing the differences and the needed effort to port NWP softwares to this new machine.

2 Configuration of tests

AMD is not ready to provide a competitive compiler suite ; therefore the Intel compiler, as well as the Intel MPI library are used. Intel also provides now a bitwise-reproducible mathematic library (MKL, in a pre-version 19) provided the proper environement variables are set.

The model should be evaluated on both platforms with the same configuration. Therefore 25 nodes of 128 cores AMD are allocated, against 80 nodes of 40 cores Intel. Furthermore I/Os are disabled, especially the I/O server, in order to get exactly the same computational profile in terms of cpu cores and distribution (MPI tasks, open-mp threads) on both platforms.

Though the namelists used are the quasi-operational ones, the tested AMD machine is small (this is a porting machine) therefore the time to solution is bigger than for operations. This should give more weight on compute parts than communications.

The cycles used are : 46T1 because it is the next candidate for operations ; and 47T1 because it contains various optimizations.

3 Raw comparison

Following the vendors' recommendations for AMD, three options should be adjusted :

1. A light depopulation : instead of using all available cores, a few of them are left aside, giving more memory bandwidth to the others. In this particular case, with 4 open-mp threads per task, 31 MPI tasks per core are used instead of 32 (in other words : 3,12 % of depopulation).
2. Use of the FFTW algorithm instead of the traditional FFT992 algorithm for the Fourier trasnforms.
3. NPROMA retuned to 16 (or more precisiely : -16 to force the program to use exactly this value without attempting to optimize it).

As shown in the figure 1, each of these recommendations improves the performance against a reference run with the traditional value NPROMA=-50.
Applied to Intel, these recommendations give the following results :

1. Depopulation is detrimental (but with less cores per node the minimal depopulation is relatively bigger)
2. FFTW is faster than FFT992, which is unexpected because early tests with FFTW on Intel platform said the contrary. Note that beside the question of performance, we had also to

consider the question of bit-wise reproducibility (possible with MIT FFTW package but not Intel MKL at that time) and the question of licensing policy of MIT for FFTW.

3. NPROMA=-16 is marginally faster.

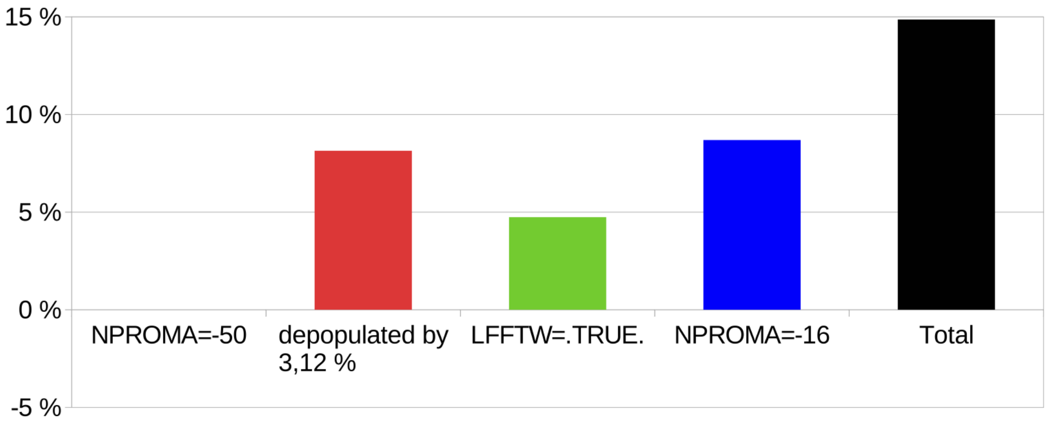

Figure 1 : Performance improvement of each recommendation against NPROMA=-50 on AMD

Globally, with the best tuning the new AMD core “Rome” should be 8% to 12% faster than the older Intel “Broadwell” core.

4 Sensitivity to NPROMA and depopulation

NPROMA

Fine tuning of NPROMA reveals that the best value should be a mutiple of 4, between 8 and 36. This is not very surprising because the AMD processor has AVX2 instruction for vectorization, which means 256 bits registers, while the model uses 64 bits real : the ratio of these numbers is 4.
The best value for NPROMA also depends of the software itself, which can be illustrated be the different source code cycles. As shown in figure 2, on AMD the best value 16 for cycle 46T1 is shifted to 24 for cycle 47T1 (which looks like good news because a bigger NPROMA means longer vectorization length and potentially more data kept inside the memory cache). On Intel the best values sem bigger, in the range 24 to 36.

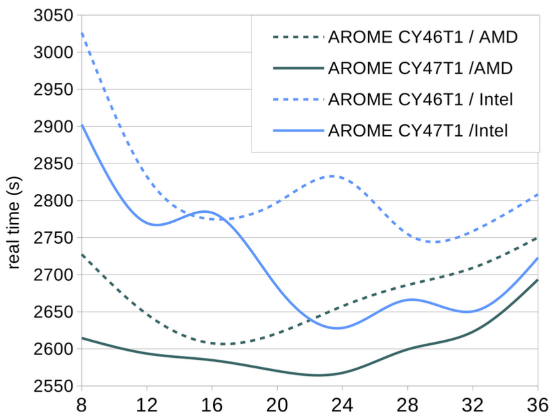

Figure 2: impact of NPROMA for different cycles and processors

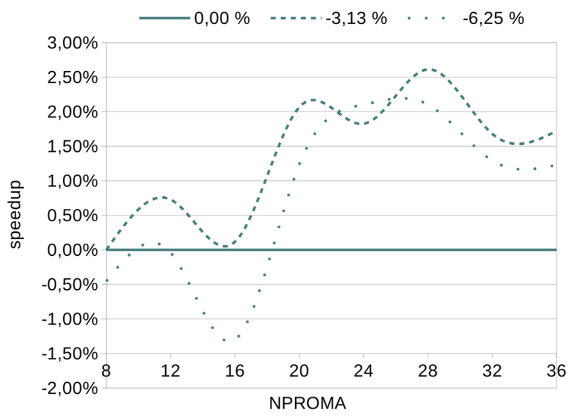

Figure 3 : impact of different depopulation rates for different NPROMAs (cy47T1)

Depopulation

Various rate of depopulation have been tested with different values of NPROMA. It confirms the benefit of a light depopulation (figure 3). However the rate of depopulation should also be confirmed with a bigger number of nodes involved, like in operations.

5 Best of both cycles 46T1 and 47T1 on computational parts

Cycle 47T1 comes with a few optimizations, concerning mostly the memory bandwidth and the vectorization. Though these optimizations makes Arome about 6% faster on Intel machine, the speedup on AMD machine is only about 2% to 3%.

Looking more in details on the most expensive and exclusively computing subroutines, we can see that on AMD with cycle 47T1 the optimal value of NPROMA (24) is paradoxically slowing down a few non-modified subroutine (figure 4). This phenomenon is neither observed when NPROMA is kept to 16 with both cycles, nor on Intel machine where the code seems to be less sensitive to the change of NPROMA from one cycle to another.

Besides, the subroutines running faster correspond exactly to the ones that have been optimized on the Intel machine.

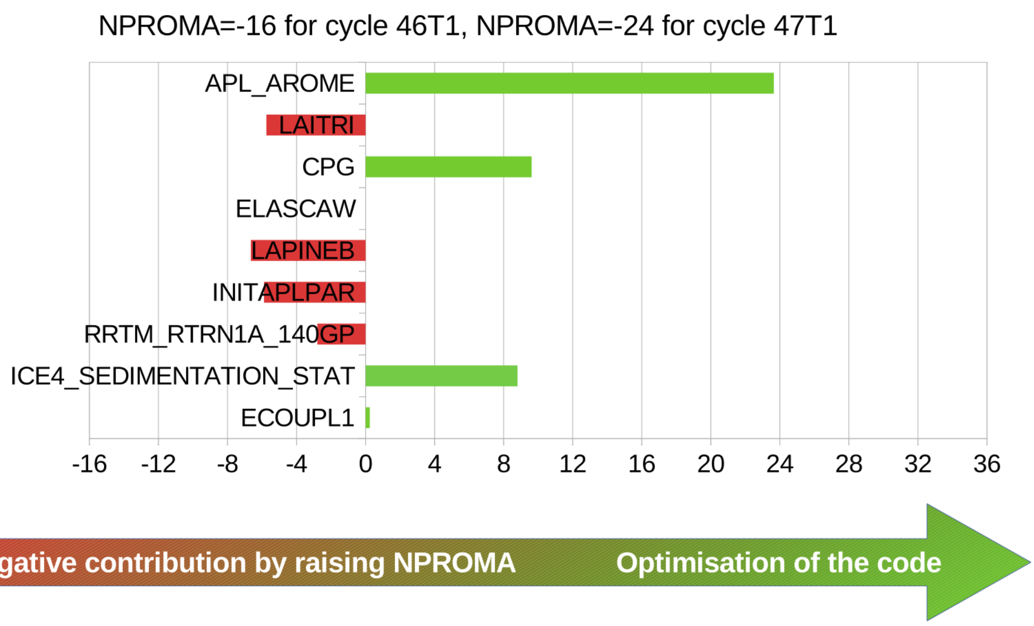

Figure 4 : subroutines going faster (green) and slower (red) on cycle 47T1 than on cycle 46T1 when the best value of NPROMA is used for each cycle (abscissa is in seconds)

6 Code sensitivity to NPROMA

The sensitivity to of the source code to NPROMA needs to be investigated further. In the figure 5 the cpu time cost of several subroutine are evaluated as a function of NPROMA on Intel (left) and AMD (right). The time cost is relative to each of the subroutines themselves in order to emphasize and possibly characterise the reasons of a dependency to NPROMA.

The low and flat curves on the left side show that the code does not depend very much of NPROMA on Intel machines (only ECOUPL1 dislikes very small values). On the contrary on the right for AMD, several subroutines are clearly penalized by big values of NPROMA. The curves poping up tell more about this dependency : INITAPLPAR does only initializations of arrays ; APL_AROME, and to a less extend LAPINEB are driven by copies of arrays ; and RRTM* uses indirect addressing quite a lot.

So we can conclude that AMD is very sensitive to memory-bound code. We can also suspect that the vectorization is less efficient on AMD than on Intel (remember the compiler used is Intel), and perhaps the efficiency of the vectorization on Intel compensates partly the need for more memory bandwidth.

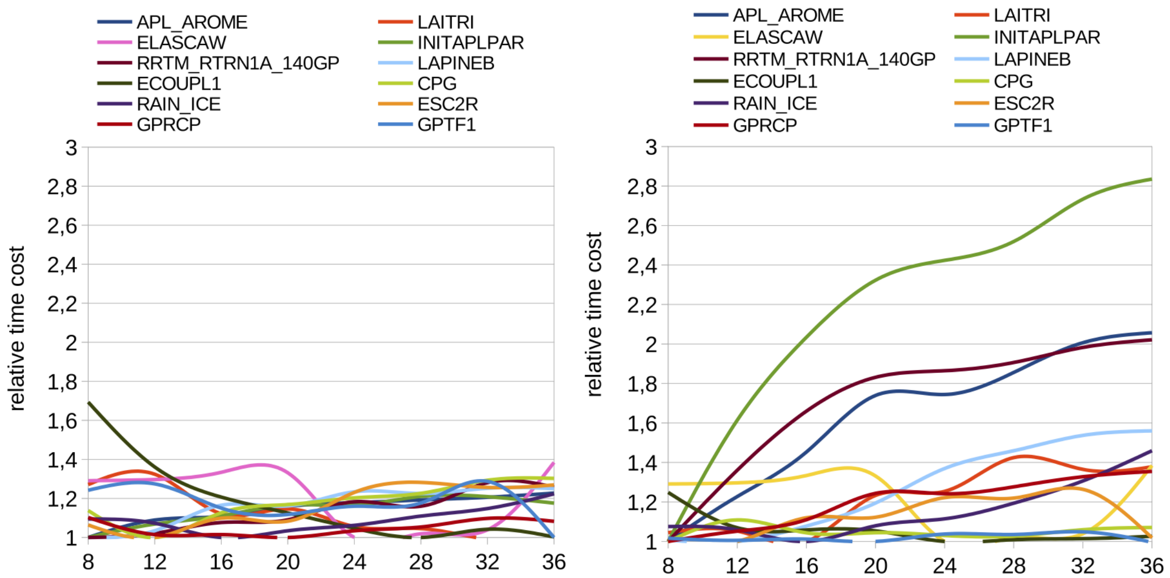

Figure 5 : Relative cost of certain subroutines as a function of NPROMA on Intel (left) and AMD (right)

7 Conclusion

- The usage of FFTW as a replacement of FFT992 is now recommended. However one should keep in mind the question of licensing if the package of MIT is used, or the question of reproducibility if an old version of Intel MKL is used.
- A light depopulation of nodes is beneficial. This is to be confirmed when a larger number of nodes is used, and then which rate of depopulation should be used.
- The optimizations made for Intel fit AMD.
  Optimal values for NPROMA on AMD are -16 or -24.
- Certain subroutines seem to be excessively sensitive to the value of NPROMA. They looked memory-bound (mostly driven by initializations of arrays or copies of arrays).

Application of convection-permitting ensemble C-LAEF at ZAMG

Clemens Wastl, Christoph Wittmann, Yong Wang

1 Introduction and Facts of C-LAEF

The C-LAEF system has been developed at the Austrian weather service ZAMG and is based on the convection-permitting AROME model (cy40t1). The ensemble comprises 16 (+1 unperturbed control) members using the first 16 out of a total of 51 members of ECMWF-ENS for the boundary conditions with a coupling frequency of 3 hours. Uncertainties in the initial conditions are represented by a combination of EDA (ensemble data assimilation), sEDA (surface ensemble data assimilation) and Ensemble-Jk. In Ensemble-Jk small-scale perturbations coming from 3D-Var EDA and large-scale perturbations coming from the driving model are blended. Model error in C-LAEF is represented by an innovative method in stochastic physics called HSPP - hybrid stochastically perturbed parametrization scheme (Wastl et al., 2019). In HSPP the individual parametrization tendencies of the physical processes radiation, shallow convection and microphysics are perturbed stochastically by a spatially and temporally varying pattern. Uncertainties in the turbulence scheme are considered by perturbing key parameters on the process level.
C-LAEF is running on the ECMWF HPC with 2.5 km resolution in the horizontal and 90 levels in the vertical direction. A 6-hourly assimilation cycle is operated with two long (00: +60h; 12 UTC: +48h) and two short runs (06 and 18 UTC: +6h). C-LAEF has been running in full operational mode since November 2019.

Domain		Model characteristics		LBC	
Grid points:	600x432	Code version:	CY40T1	Coupl. model:	IFS Ensemble
Horizon. resolution:	2.5km	Time step:	60s	Coupl. frequency:	3h
Levels:	90	Integration time:	60h (00 UTC), 48h (12 UTC),	Retrieval:	Internet/
Grid:	linear		6h (06, 18 UTC)		RMDCN
Orography:	mean	Physics:	AROME/Meso-NH incl. stophy	Archive:	local + MARS (08/2019)
		Dynamics:	non-hydrostatic		
		Initialization:	CANARI/OIMAIN, 3DVAR		
			EDA + surface EDA + Ensemble JK		

Table 1: Fact-sheet of C-LAEF.

2 Application of C-LAEF at ZAMG

To increase the applicability of the C-LAEF ensemble system at the forecasting offices and for customers, several probabilistic products and maps have been developed in a close cooperation between model developers and users. Figure 1 shows a C-LAEF 6-panel tailored to warning applications in summertime convective situations. The upper left panel shows the probbility of lightning for different thresholds (low - yellow, medium - orange, high – red), the upper center panel the diagnostic probability of hail and the upper right panel the predicted maxium 3h gusts. In the lower row the C-LAEF median of 3h accumulated precipitation (left), 3h sunshine duration (center) and cloudiness (right) are shown.

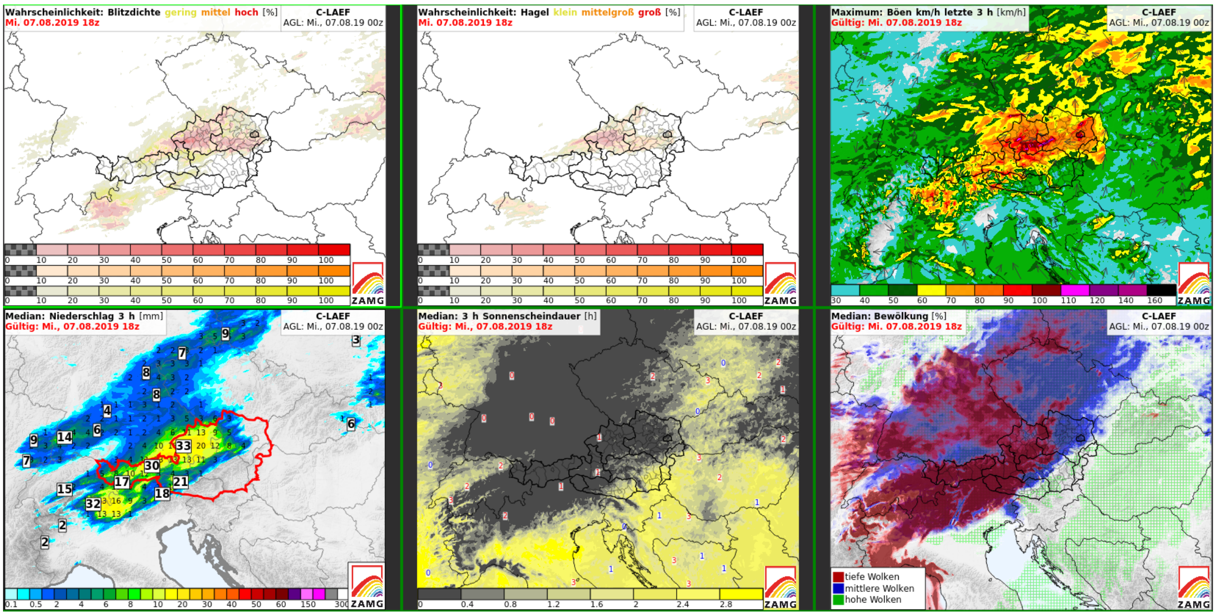

Fig. 1: C-LAEF panel used by the operational forecasters at ZAMG for a thunderstorm warning situation in August 2019.

Also for wintertime forecast purposes (road traffic safety, ski areas, avalanche warnings, etc.) an apropriate panel has been developed (Fig. 2). It contains information on precipitation (upper left panel), snow line (upper center), frost level temperature (upper right), low stratus (lower left), low stratus height (lower center) and temperature (lower right).

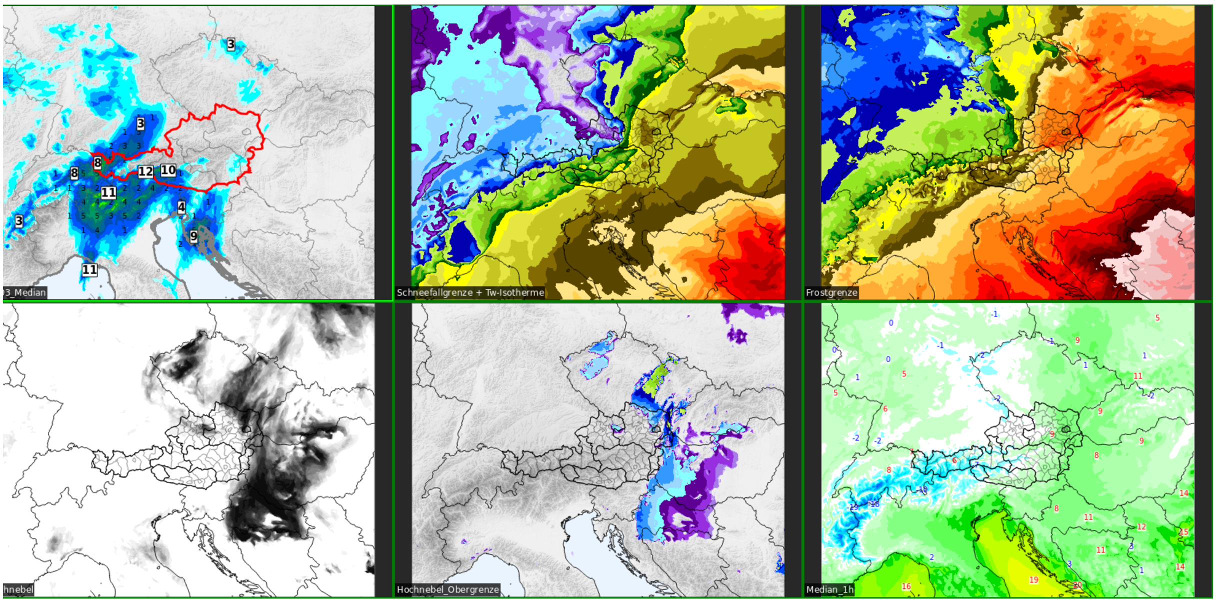

Fig. 2: C-LAEF panel used by the operational forecasters at ZAMG for a cold front in December 2019.

The main application of the C-LAEF ensemble is for warning purposes as several severe weather situations in 2019 have shown. The additional probabilistic information on exceeding warning thresholds or the plots of ensemble spread and extreme members are very helpful to better assess regional/temporal unceratinties as well as uncertainties in the intensity of severe weather. The overall feedback of C-LAEF after several months in daily operational use is very positive as a survey among the ZAMG forecasters has shown.

3 Verification of C-LAEF

Continuous verification of C-LAEF versus ALADIN-LAEF and ECMWF-ENS has clearly shown the benefit of a convection permitting EPS (Fig. 3 and Fig. 4).

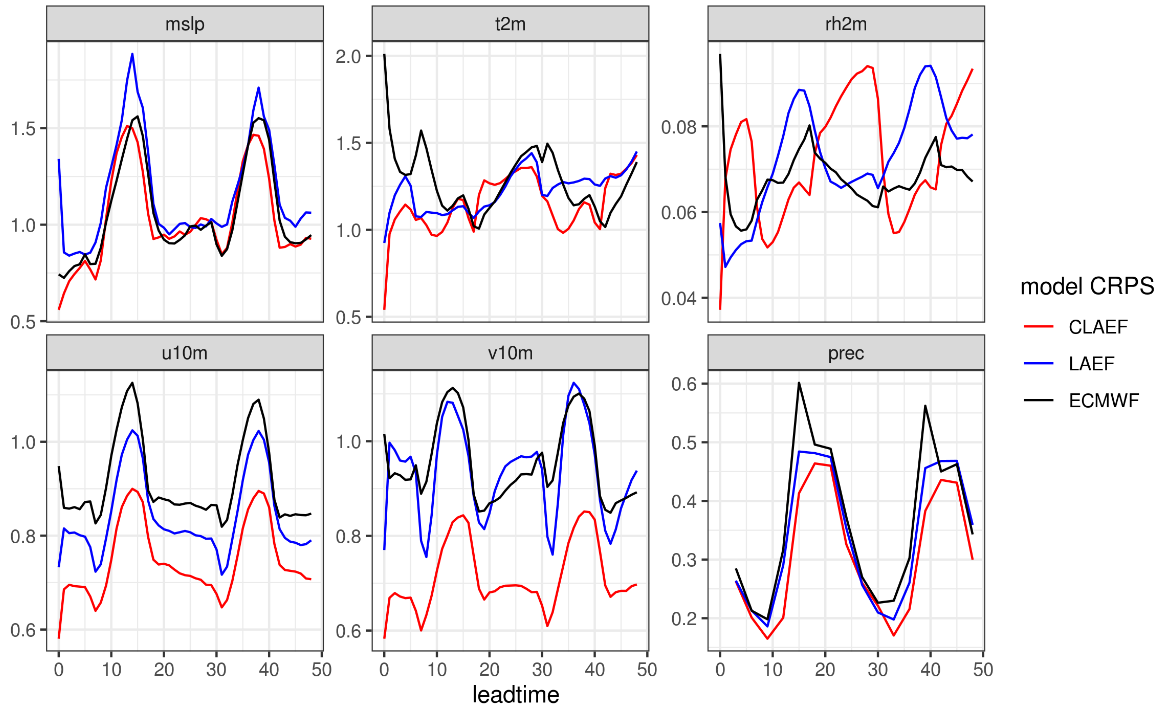

Fig. 3: Continuous Ranked Probability Score (CRPS) for different surface parameters of C-LAEF (red), ALADIN-LAEF (blue) and ECMWF-ENS (black) at all Austrian stations for August 2019.

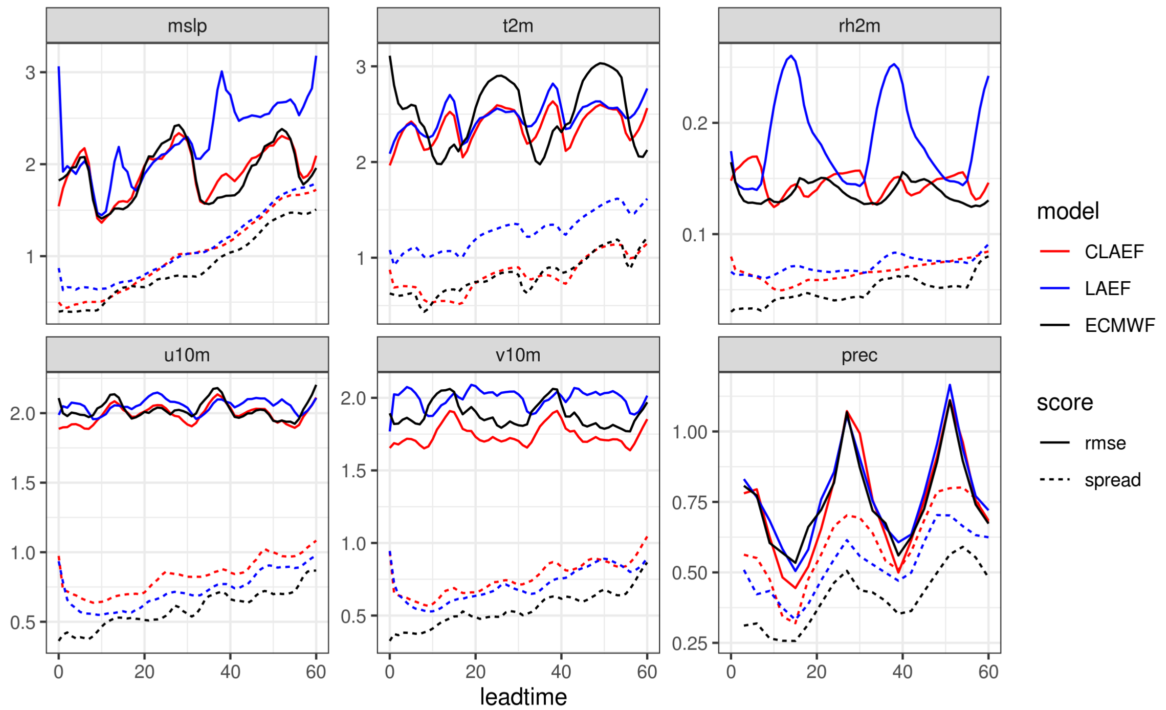

Fig. 4: Spread (dashed) and RMSE (solid) for different surface parameters of C-LAEF (red), ALADIN-LAEF (blue) and ECMWF-ENS (black) at all Austrian stations for February 2020.

About rainfall bias in AROME-France

Yann Seity, Pierre Brousseau

1 Introduction

As all convection-permitting non-hydrostatic models, AROME is supposed to improve rainfalls forecasts compared to models with parametrized deep-convection. Even if it is generally true, there are some cases reported by forecasters, mostly in the South-Eastern part of France, over the Alps, with clear under estimation of convective activity. It concerns cases of weakly forced diurnal convection, which were particularly numerous during 2018 summer. In April 2016, AROME-France configuration changed with among others, improved horizontal and vertical resolution. This new configuration as been shown to improve convection realism, with more realistic convective cells (Brousseau et al., 2016). However, forecasters had the feeling that previous AROME configuration was better for those weakly forced diurnal convection cases. We will present in this paper results from our investigations of this problem.

2 Case of July 25th 2018

Figure 1 shows an example of a problematic case. AROME operational forecast (Figure 1 b) clearly underestimates convection activity in the Eastern part of France and in Corsica compared to radar observations (Figure 1 a). AROME has been rerun in spin-up mode (surface and atmospheric fields initialized by ARPEGE) with pre (Figure 1c) and post (Figure 1d) April 2016 dynamics, resolution and diffusion settings . It shows that the problem, still present in spin-up mode using operational configuration, does not seem to be related to data assimilation, and that indeed, pre April 2016 configuration is better, even if it probably locally over-estimates convective activity.

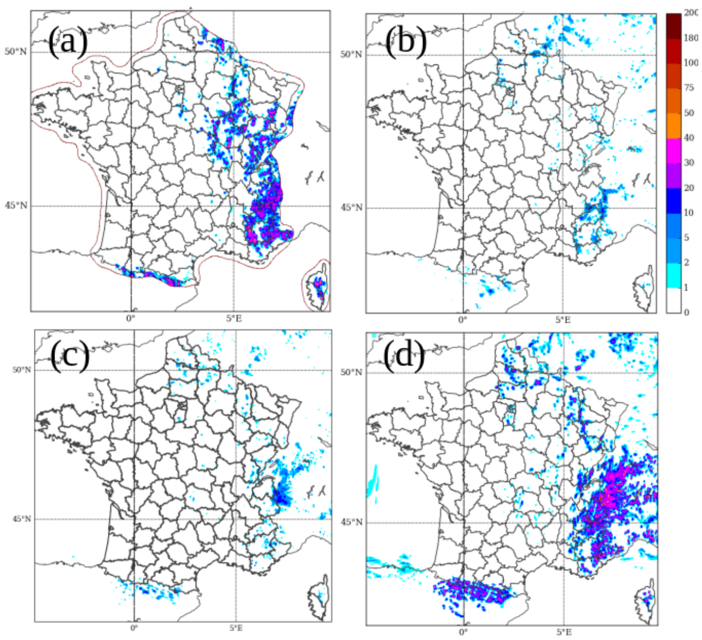

Figure 1: 24h cumlated rainfalls for July 25th 2018. (a) radar observations (b) AROME-oper (c) AROME-oper spinup mode (d) AROME 2,5km spinup mode.

A first investigation showed that the main impact on these convection cases are provided by changes in SLHD settings on hydrometeors. On the other hand, trials to find SLHD tunings allowing to improve these convective cases and to also keep correct precipitation scores in average did not succeed.

3 Semi academic case study

In order to investigate more deeply model's behaviour, we setup two small AROME domains and perform some semi academic tests. The first domain contains real orography whereas the second one has no orography (zs=0). Model domains contain 48x48 points, with 90 vertical levels. Horizontal resolution is 1250m. Initial conditions are provided by AROME-oper. All hydrometeors are set to 0 in the initial state except at one particular point, for rain, located in the center of the domain, at 2000m height, for which q_r=1g/kg. All the physical parametrisations are switched off, except the rain sedimentation and we only perform 40 model time steps integration. We calculate every time step the total mass of rain in the atmosphere, and reaching the ground, and we normalize it by the initial mass of rain put at the central point. We would expect in that particular case a mass conservation of the rain. Indeed, during 40 time steps, it should stay inside the domain and no physical process can create or destroy it. The only processed acting on it are the advection and the sedimentation. First results are illustrated in Figure 2 on December 21st 2019, a case with strong winds on this small domain covering the Eastern part of the French Rhône valley, with the first foothills of the Alps .

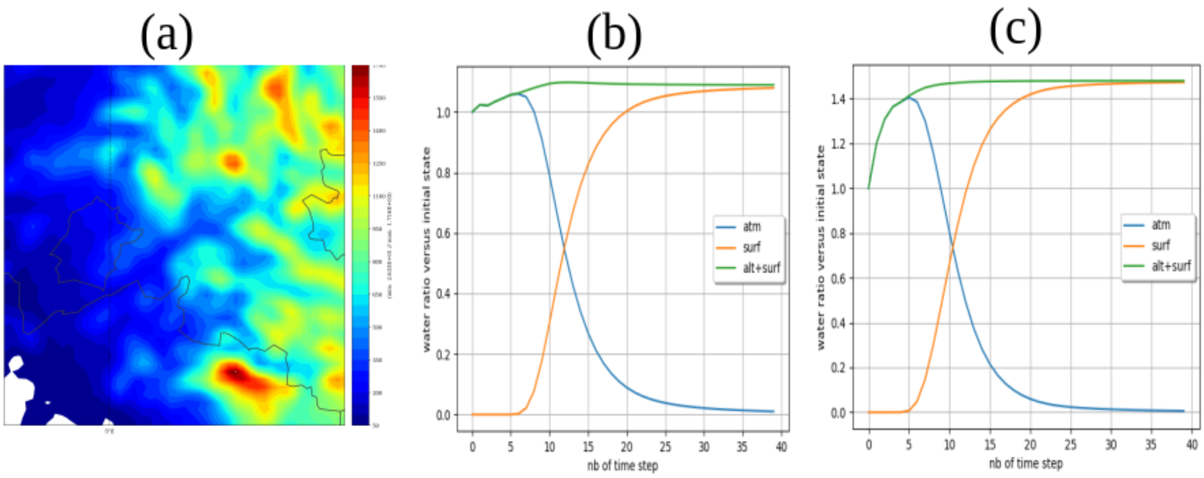

Figure 2: (a) AROME Small domain orography (b) total rain water time evolution with 'oper' settings (c) as b, without semi-Lagrangian horizontal diffusion

Figure 2b shows that total mass of rain (the one contained in the atmosphere in the blue curve + the one reaching the ground in the orange curve) is not conserved. About 7% of rain is created. Without semi Lagrangian horizontal diffusion (SLHD), it is even worst, as 45% of rain is created. SLHD diffusion (Vana et al., 2008) was a way to apply numerical diffusion on non spectral variables. It as been applied in hydrometeors since the first operational AROME version in 2008 (Seity et al., 2011) and, as shown in Figure 2, it may partly compensate a problem of positive bias due to mass creation by the model.

We now switch to a more academic case on the second small domain, without orography. The model is initialized as in Figure2, except that the wind and temperature fields are constant (u=v=2m/s, T=280K). The model is run in hydrostatic mode. In these conditions, the equivalent of Figure 2a is Figure 3c which exhibit a mass creation of 50%. By switching off rain advection (Figure 3a), we verify that rain sedimentation is mass conservative. Thus, mass creation is due to semi-Lagrangian advection (SL), as shown in Figure 3b. Replacing the quasi-monotonous interpolators by linear ones, we can reach perfect mass conservation in this case (Figure 3d). Red curves in Figures 3c and 3d corresponding to the total volume of the atmosphere with rain mixing ratio greater than 1% of its initial value shows that this interpolator does not seem to be much more diffusive that the one used in operational.

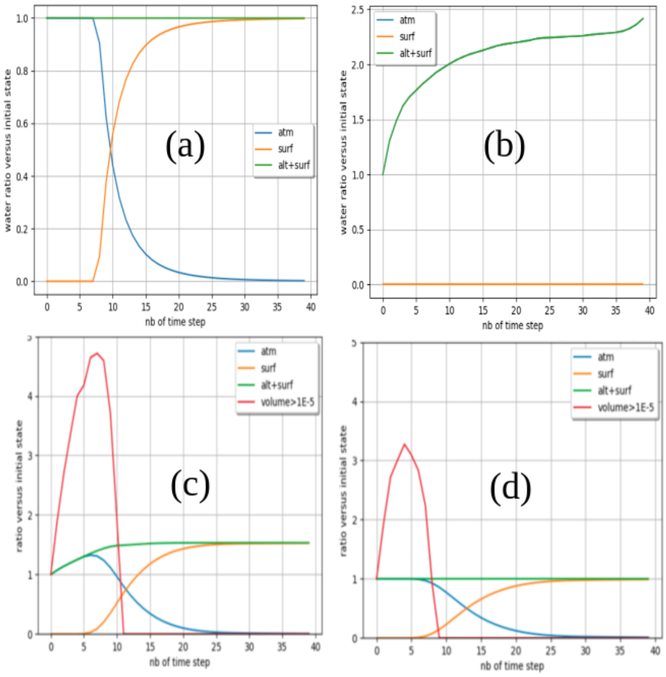

Figure 3: Same as Figure 2, more academic tests (constant wind and temperature, no orography) (a) without semi Lagrangian advection (b) without rain sedimentation (c) oper settings (d) c with linear semi-Lagrangian interpolators. In (c) and (d), the red curve corresponds to the total volume of atmosphere containing q_r > 1% of initial q_r.

Sensitivity tests performed on that case (not shown here) provided the following additional results : as smaller fall speed increases the remaining time in the atmosphere, replacing rain by snow increases mass creation. It is also the case if we increase the constant initial wind speed (not shown). On the other hand, by initializing rain on two (or more) contiguous points, we can reduce the mass creation.

4 Back to real cases

As shown in Figure 2, SLHD diffusion add compensating errors to the model. Using conservative SL interpolators will allow to switch off SLHD diffusion on hydrometeors. Figure 4 shows the impact on the case presented on Figure 1c. We can observe much more active convection, which is more realistic compared to radar observations (Figure 1a).
This modification has also been evaluated on other cases, over different seasons, with and without data assimilation. In average, scores are rather neutral compared to the operational configuration, but individual case studies such as the one presented in section 2 clearly show benefits of this modification. We also computed object oriented evaluation with statistics on convective cells size for instance as in Brousseau et al. (2016). Energy spectra are also correct.
Consequently, this modification is on the way to be included in our next CY46T1 e-suite next autumn.

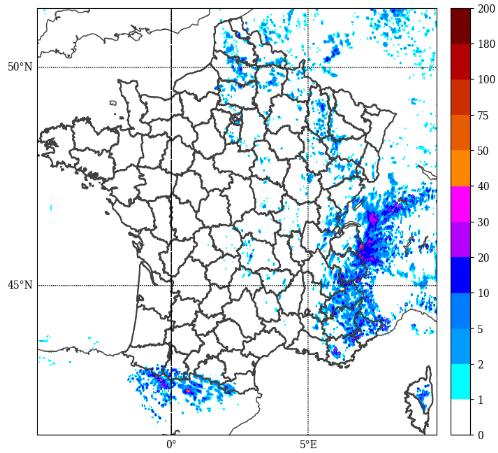

Figure 4: 24h cumulated rainfalls for July 25th 2018 with linear SL interpolators for hydrometeors and no SLHD (to be compared with Figure 1c).

5 Conclusions

Looking at some model drawbacks reported by forecasters on convective cases, we built semi-academic AROME configuration which allowed us to work on mass conservation in the model. It appeared that problems related with convection under estimation in AROME are connected to SLDH diffusion tunings on hydrometeors, activated to compensate the non mass conservative properties of the operational SL interpolators. It allowed us to propose new settings for next e-suite : Conservative SL interpolators for hydrometeors (Linear ones), and switch off SLHD on hydrometeors.
For longer terms, we may think about non-linear conservative SL interpolators, look at methods implemented in other models such as Zerroukat and Shipway (2017) in the UKV model, or implement an alternative advection scheme for grid-point prognostic variables (WENO scheme for instance).

6 References

Brousseau et al. (2016). Improvement of the forecast of convective activity from the AROME-France system. *Quarterly Journal of the Royal Meteorological Society*, *142*(699), 2231-2243.

Seity et al. (2011). The AROME-France convective-scale operational model. *Monthly Weather Review*, *139*(3), 976-991.

Vana et al., (2008). Semi- Lagrangian advection scheme with controlled damping : An alternative to nonlinear horizontal diffusion in a numerical weather prediction model. *Quarterly Journal of the Royal Meteorological Society*. 134., 523 – 537.doi :10.1002/qj.220.

Zerroukat, M. and Shipway, B.J. (2017), ZLF (Zero Lateral Flux): a simple mass conservation method for semi-Lagrangian-based limited-area models. *Quarterly Journal of the Royal Meteorological Society,* 143: 2578-2584. doi:10.1002/qj.3108

Improved parametrization of the boundary layer in Harmonie-Arome (focusing on low clouds)

Wim de Rooy, Peter Baas, Pier Siebesma, Erik van Meijgaard, Henk Klein Baltink, Jan Fokke Meirink, Hylke de Vries, Stephan de Roode, Geert Lenderink, Sander Tijm, Bram van ‘t Veen

1 Introduction

With the introduction of the HARATU turbulence scheme (Lenderink & Holtslag 2004, de Rooy 2014, Bengtsson 2017) in cycle 38, Harmonie-Arome improved on several output parameters, especially 10m wind speed. From the moment HARATU is included at KNMI (in 2015), Harmonie-Arome clearly and consistently outperforms wind speed forecasts of Hirlam, ECMWF and Harmonie-Arome with CBR turbulence. However, from cy38 onwards, the model underestimates low clouds and overestimates the cloud base height of low clouds, both crucial for e.g. aviation purposes. Within the Hirlam consortium this problem is considered as the most important deficiency of Harmonie-Arome.

Parameterization schemes most relevant for low cloud predictions are the cloud, turbulence and convection scheme. Together with increased physical realism of these boundary layer parameterizations, coupling between them becomes stronger. For example, turbulent and convective activity is used as input in the cloud scheme to determine sub-grid variance in humidity and temperature, key parameters in a statistical cloud scheme. Another example of such a direct, i.e. fortran coded, coupling is convective activity being used as a source term in the TKE budget equation of the turbulence scheme (so-called energy cascade term). Apart from these direct couplings, there are well-known indirect feedbacks, e.g.: more clouds lead to less radiation at the surface which will in turn influence turbulent and convective activity. Due to strong connectedness, the boundary layer parameterizations need to be developed and optimized together. Using such an integral approach, substantial modifications have been made to the Harmonie-Arome cloud, turbulence and convection scheme leading to clear improvements, especially in low cloud forecasts.
While this paper focuses on the impact of these modifications, a detailed description and motivation of the adjustments will be described in a separate paper (in preparation). The modifications are based on a wide variety of arguments. Some are founded on theoretical considerations, like a correction in the thermodynamic derivation of the statistical cloud scheme. Another example is the modification of the turbulence scheme based on similarity theory. In addition, we use process studies in which LES and 1D model results are compared in detail for a wide variety of cases. Finally, Harmonie-Arome 3D sensitivity runs as well as long-term simulations are used to optimize uncertain parameters.

2 Results

Results of Harmonie-Arome cycle 40 including all modifications in turbulence, convection and cloud scheme will be referred to as cy40NEW whereas the reference is denoted as cy40REF (as described in Bengtsson et al. 2017)

Clouds

We start with a clear example of underestimation of low clouds and overestimation of low cloud base heights in cy40REF.

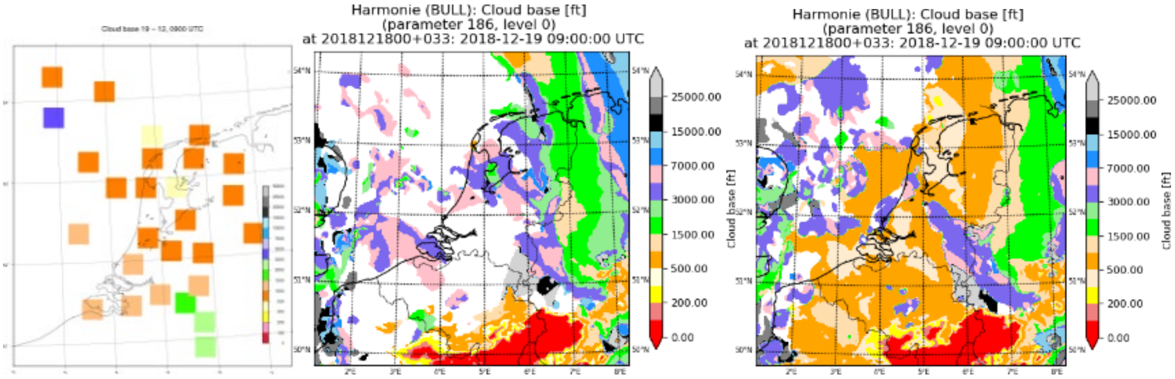

Figure 1:Cloud base height in feet on the 19th of December 2018 at 9:00 UTC. Left panel: observations at discrete locations. Middle and right panel show the results of cy40REF and cy40NEW resp. In the middle and right panel, white means no cloud base detected in the model.

Figure 1 shows a typical example of a poor low cloud forecast with cy40REF and the large impact and improvement with cy40NEW. The strong impact of the modifications is confirmed in long term verification. As an example we present the frequency bias in cloud base height for December 2018 in The Netherlands (Fig. 2). Note the large underestimations of cy40REF, where e.g. the +24h forecasts produce less than 20% of the observed number of cloud base heights around 176 ft. The negative biases are clearly smaller in cy40NEW. Also in other months there is substantial improvement in low cloud base height distributions with cy40NEW (not shown).

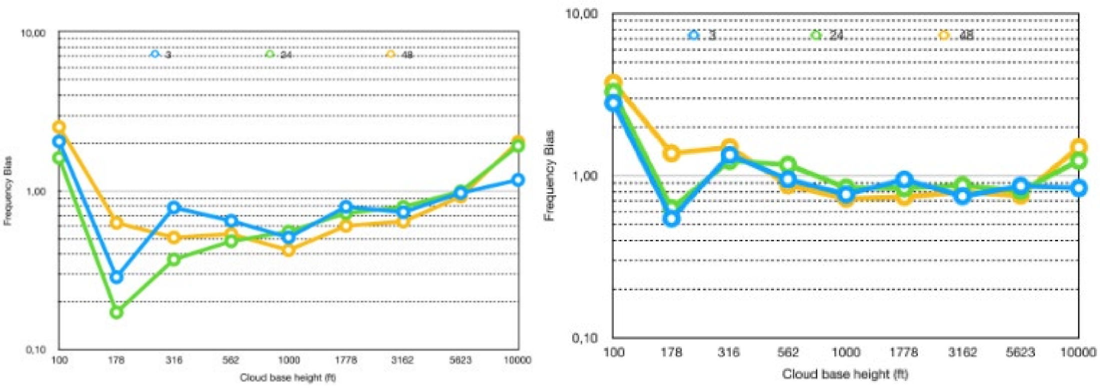

Figure 2:Frequency bias (1 is optimal) of cloud base height in feet for December 2018 above The Netherlands. Left panel, cy40REF and right panel cy40NEW.

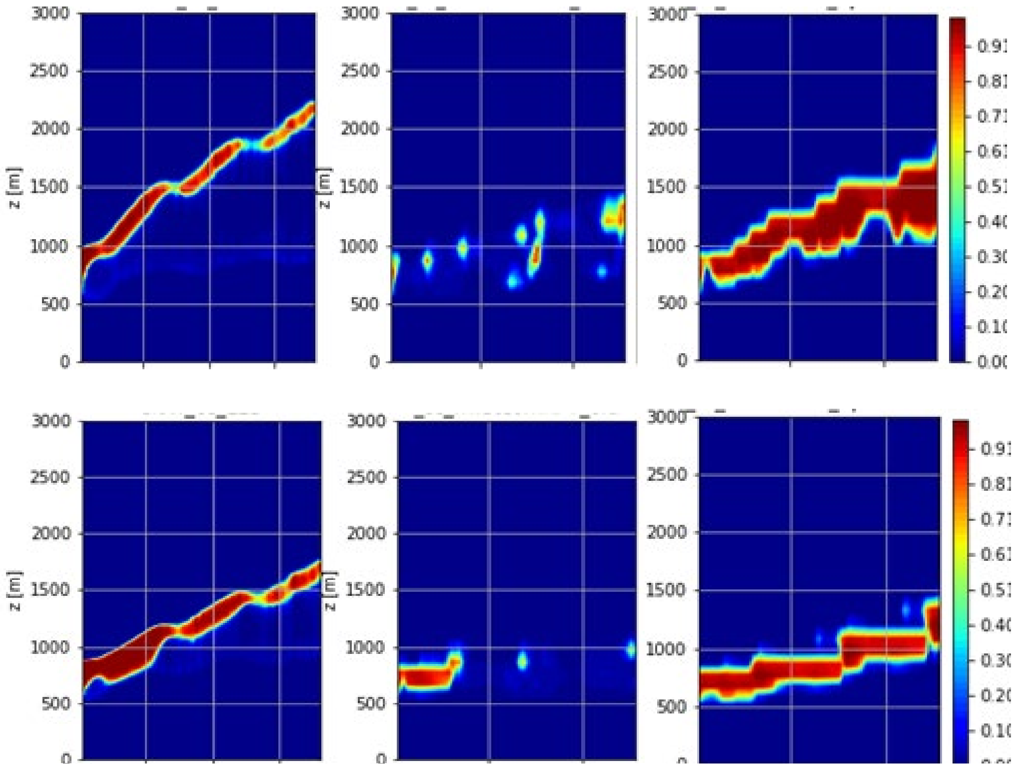

Figure 3:Cloud cover versus height and time (red is high, blue is low fraction) for inter-comparison case ASTEX fast (upper panels) and ASTEX slow (lower panels). Left, middle and right panels show LES, cy40REF, and cy40NEW results resp.

Precipitation

Apart from impact on low clouds, increased atmospheric inversion strengths influence triggering of resolved deep convection and the associated precipitation. This is illustrated in Fig. 4, where intense precipitation was observed but not triggered in cy40REF. By contrast, cy40NEW did produce resolved convection and rain. Fig. 4 reveals the stronger building up of humidity under the inversion in cy40NEW which enables upward motions and finally, deep resolved convection.

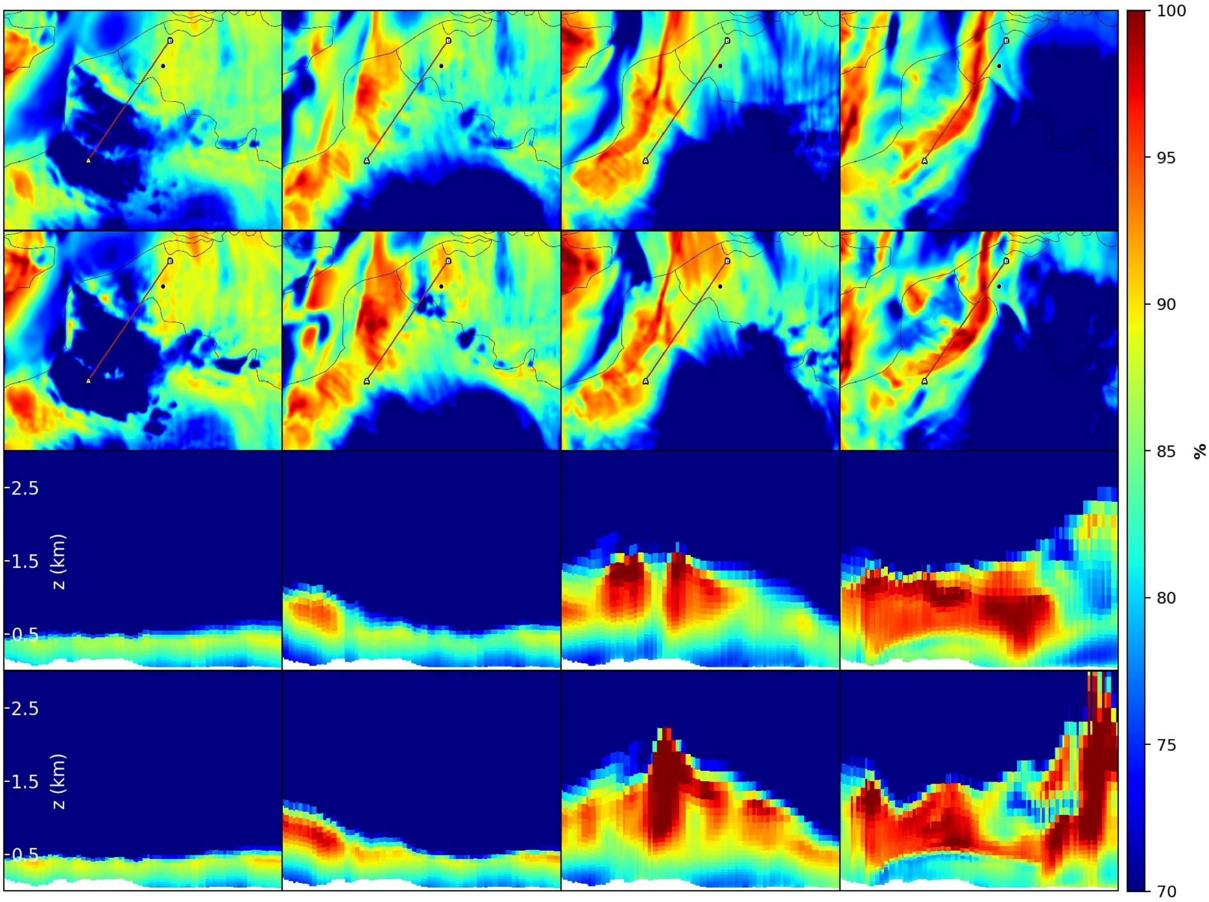

Figure 4: Relative humidity plots (red means high, blue low relative humidity) for the 10th of September 2011. The four columns refer to hours 12, 14, 16 and 18 UTC. The first row(cy40REF) and second row (cy40NEW) show a map of The Netherlands, Belgium and the North West of France as well as a black line. Along this line a vertical atmospheric cross-section is shown in the third (cy40REF) and fourth (cy40NEW) row. In the cross-sections, the boundary layer can be recognised by relatively high relative humidity values.

The improvement on precipitation forecasts is confirmed in long-term verification. Figure 5 shows the Fraction Skill Score (higher values means better) above The Netherlands for a 8month period in 2019. Cy40NEW performs significantly better than cy40REF (and cy36).

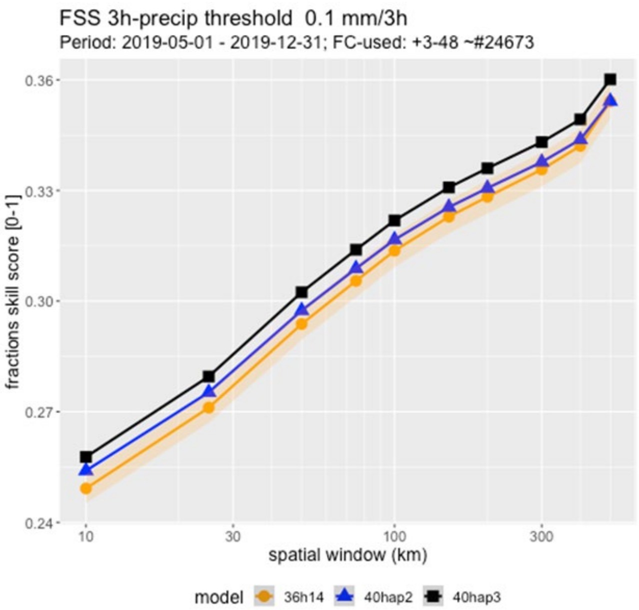

Figure 4:Fraction skill scores for precipitation amounts > 0.1mm in 3h over The Netherlands as a function of the spatial window. Calibrated radar data is used as observation. Shown are the results for cycle 36 (orange), cy40REF (blue) and cy40NEW (black).

Apart from the impact on clouds and precipitation, the modifications influence several aspects of the model. For example, results for GABLS1 reveal improved vertical profiles (less mixing) during moderately stable conditions (not shown). Good results for 10m wind speed with cy40REF are preserved in cy40NEW.

4 Conclusions

Strong feedback between boundary layer schemes demands an integral approach to develop and optimize the parameterizations involved. In such an approach, substantial changes have been made to the Harmonie-Arome turbulence, convection and cloud scheme based on theory, process studies (LES) and evaluation of 3D model runs. The modifications result in a clear improvement, especially on clouds and precipitation. At KNMI, Harmonie-Arome including all modifications (cy40NEW), already runs in parallel to cy40REF and cy36 since May 2019. Therefore, long term verification was possible, firmly substantiating the improvements and demonstrating the conservation of cy40REF's good performance on e.g. wind speed (de Rooy & de Vries, et al. 2017).
All modifications will be included in the tagged Harmonie-Arome cycle 43. In a later stage, the improvements will also become available for Harmonie Climate (Belušić, 2020) with undoubtedly impact on e.g. precipitation extremes in future weather experiments (Lenderink et al. 2019). All modifications and the corresponding argumentations will be described in a separate paper (in preparation).
Verification of model clouds is notoriously difficult. As part of the CRIME project we therefore developed a cloud validation system based on a combination of Cloudnet and satellite observations. First validation results will soon become available and be published.

Acknowledgements
This work has been done within the KNMI multi-annual strategic research (MSO) project CRIME (Cloud Representation IMprovement and Evaluation in harmonie) and the Norwegian Research Council project no. 280573, 'Advanced models and weather prediction in the Arctic: enhanced capacity from observations and polar process representations (ALERTNESS)'.

3 References

Lenderink, G., and A. A. Holtslag, 2004: An updated length-scale formulation for turbulent mixing in clear and cloudy boundary layers. Quart. J. Roy. Meteor. Soc., ***130****, 3405–3427, doi:https://doi.org/10.1256/qj.03.117.*

de Rooy, W. C., 2014: The fog above sea problem: Part 1 analysis. ALADIN-HIRLAM Newsletter, No. 2, Météo-France, Toulouse, France, 9–15. [Available online at http://hirlam.org/index.php/component/docman/doc_download/1490-aladin-hirlam-newsletter-no-2-april-2014?Itemid=218.]

Bengtsson et al., 2017: The HARMONIE–AROME Model Configuration in the ALADIN–HIRLAM NWP System. Monthly Weather Review, Vol. 145, https://doi.org/10.1175/MWR-D-16-0417.1

Neggers et al. 2017: Single-column model simulations of subtropical marine boundary-layer cloud transitions under weakening inversions. JAMES, Vol 9, pages 2385-2412

de Rooy W.C. & de Vries H., et al.: Harmonie verification and evaluation. Hirlam Technical report Nr. 70, 79 pp. [Available from HIRLAM-A Programme, c/o J. Onvlee, KNMI, P.O. Box 201, 3730 AE De Bilt, Netherlands.]

Belušić D., et al., 2020, HCLIM38: A flexible regional climate model applicable for different climate zones from coarse to convection-permitting scales. Geosci. Model Dev., 13, 1311–1333 https://doi.org/10.5194/gmd-13-1311-2020

Lenderink G., D. Belušić, *H. Fowler, E. Kjellström, P. Lind, E van Meijgaard, B. van Ulft, H. de Vries: Systematic thermodynamic responses of hourly precipitation extremes in a warming experiment with a convection-permitting climate model. ERL, 2019 https://iopscience.iop.org/article/10.1088/1748-9326/ab214a)*

Update of the Use of Cams Aerosols in Harmonie-Arome

Daniel Martin-Perez

1 Introduction

The HARMONIE-AROME model is being adapted to use the mass mixing ratio (MMR) aerosol fields from the Copernicus Atmosphere Monitoring Service (CAMS). The main purpose is to have a more realistic behavior of the model in cases when the aerosol concentration is far from the climatology. The use of aerosol fields have an impact in the radiation scheme and in the microphysics processes. The advances introduced during the last year will be detailed after giving a short summary of the previous stage.

2 Use of CAMS aerosol in HARMONIE-AROME

Apart from the radiation scheme, the use of CAMS aerosol in HARMONIE-AROME is described in Martin-Perez, 2018. The adaptation was done in experiments based on the cycle 40h1.1. Here a brief summary is presented.

CAMS aerosol fields.

Up to eleven different fields from CAMS are used in this experimental configuration of HARMONIE-AROME. There are three sea salt (SS) bins, three dust (DU) bins, hydrophilic and hydrophobic black carbon (BC) and organic matter (OM) and one sulfate (SU) field (for a description of CAMS aerosols see for example: Bozzo et al. 2020). While all of the aerosol fields are used in the radiation scheme of HARMONIE-AROME, only those that can behave as cloud condensation nuclei enter the microphysic scheme. All these fields enter the model through the first guess and the boundary conditions. The dynamic of the model advect the MMR fields. There are no sources of aerosols during the forecast, but the parametrization of the dry and wet sedimentation of aerosols has been introduced.

Mycrophysic scheme.

In the default configuration of the microphysic scheme in HARMONIE-AROME, the droplet number concentration is considered constant for every model level but depends whether the grid point is over sea (100 cm-3), over land (300 cm-3) or over urban terrain (500 cm-3). The MMR aerosol fields permit to estimate the cloud concentration nuclei (CCN) number concentration by considering a log-normal size distribution for every aerosol kind and applying the Kohler theory. Up to 6 fields are used, the three sea salt bins, the sulfate and the hydrophilic black carbon and organic matter. The cloud droplet number is considered equal to the CCN calculated. Autoconversion, cloud droplet sedimentation and the collision of cloud liquid are the parametrizations involved.

Radiation scheme.

The HARMONIE-AROME considers climatology values of the Aerosol Optical Depth (AOD) at the surface for every month while the values in the vertical are calculated by considering a prescribed vertical profile. The model consider separately the four Tegen species (LAND, SEA, DESERT and SOOT).

In this experimental configuration, the mass mixing ratios of the aerosol fields are used to calculate the 550 aerosol optical depth (AOD) at every point and for every aerosol specie. But, in order to check the impact without doing too many modifications in the code, the AOD obtained from the aerosol fields were distributed to keep the 4 tegen species in the following way:

LAND = Sulfate(11) + Hydrophobic Organic matter(7) + Hydrophilic Organic Matter(8)
SEA = Sea salt(1) + Sea salt(2) + Sea salt(3)
DESERT = Desert dust(4) + Desert Dust(5) + Desert dust(6)
SOOT = Hydrophobic Black Carbon(9) + Hydrophilic Black Carbon(10)

The impact of the inclusion of CAMS near real time aerosols in the model is high on the short wave radiation and the temperature in cases of dust intrusion as shown in Rontu et al. 2019.

3 Update

In this section, the modifications introduced during the last year are summarize.

CAMS upgrade

The 9th of July of 2019 the CAMS system was upgrade (for information about the upgrade: https://atmosphere.copernicus.eu/node/472). One of the major changes was in the number of vertical levels, passing from 60 to 137. Three new species of aerosol were introduced, two nitrate modes and one ammonium. It was found that with the new changes, the system produced a clear increase of mineral dust concentration. The HARMONIE-AROME CAMS experimental configuration was adapted to get the 137 levels, but not the three new aerosol species.

One month verification

A HARMONIE-AROME experiment with CAMS aerosols was run for one month (September 2019) in the domain covering the Iberian peninsula. The verification shows good results for the equitable threat score of the precipitation, although September 2019 wasn't a rainy month and degradation of the temperature with increasing forecast length (figure 1).

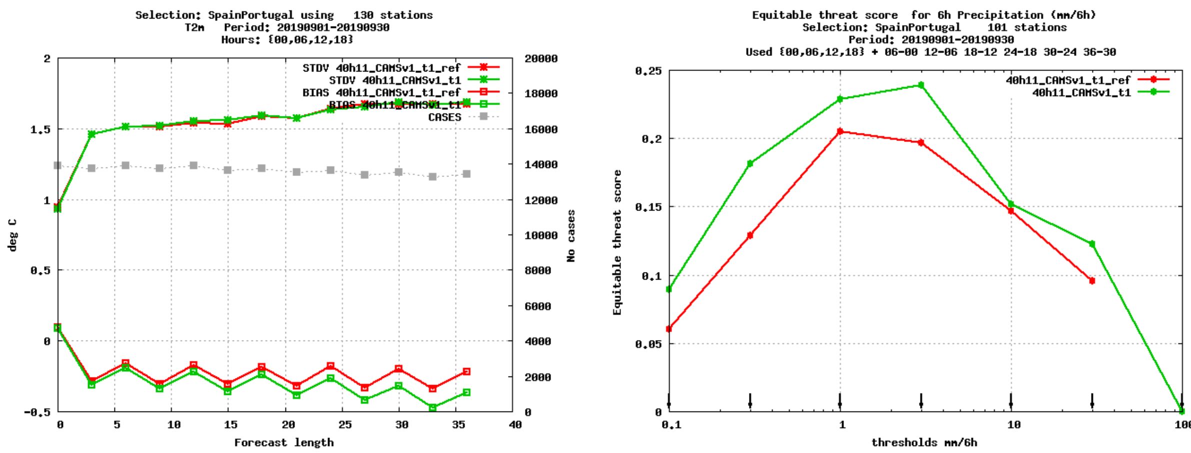

Figure 1: Bias and standard deviation of the 2 meter temperature as a function of the forecast length (left) and equitable threat score of the 6 hours precipitation (right). In red the control experiment and in green the HARM-nrt experiment.

The degradation in the temperature might be due to considering constant values of the extinction parameters.

Mass extinction dependence with the temperature.

As mention above, the experimental setup to include the CAMS aerosol considered constant values of the mass extinction for every kind of aerosol in the calculation of the AOD. The code was adapted to use this humidity dependence and a test case was run for 3 days. The result for Caceres station is shown in figure 2. With the mass extinction dependence, the short wave improves and have values closer to the observed data.

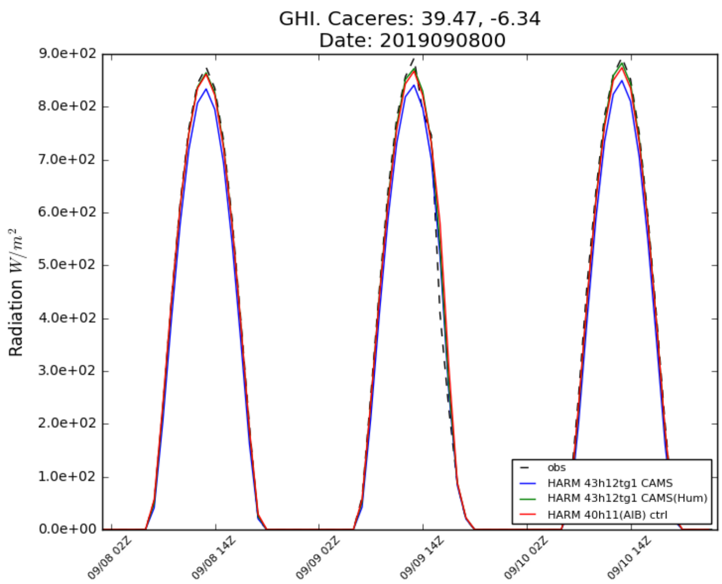

Figure 2: Short wave radiation at Caceres station for three days. With the introduction of mass extinction dependende of the humidity (green line) the forecast was closer to the observation (dashed black line) than before (blue line). Also the control experiment (red) shows a better agreement.

Update to cycle 43.

The code was also adapted to the cycle version 43. A test case was run for September 2019 (not shown) and it was found modifications in the 24 hours precipitation pattern showing a closer agreement with the radar observation.

Computational issues.

The use of 11 more 3D fields by the model means a reduction in the forecast runtime. For a 24 hours forecast there was an increase of 14% in the runtime of the Forecast (table 1).

Table 1: Time result of the execution of HARMONIE-AROME with CAMS aerosol vs. the Reference

	CAMS	REF.
Dispatched	Mon Nov 4 09:09:57 2019	Mon Nov 4 09:04:42 2019
Completed	Mon Nov 4 11:05:11 2019	Mon Nov 4 10:46:12 2019
Runtime	6914 seconds (+14%)	6065 seconds

It was also needed to increase the requested memory in the supercomputers for those tasks working with the boundary conditions fields as gl_db.

4 Conclusions

The experiment with CAMS aerosol based on cycle 40h1.1 gave good results in a one month verification for the precipitation, but not as good for 2m temperature with a degradation with increasing forecast length. It is expected some improvement when the mass extinction dependence of the humidity is introduced.

The scripts have been updated after the upgrade of CAMS to use the grib files of 137 levels from July 2019 instead of the ones of 60 levels as before. Still the ammonimu and nitrate aerosol fields are not included.

The mass extinction dependence with the humidity has been introduced (only introduce in the cy. 43h2.1tg1) showing closer agreement to observations for a test case.

A new experiment has been written based on cycle 43 with promising results in the precipitation pattern for a test case, but still a verification is needed.

With respect to the computational issues, it was found an increase of run time of 14% in a 24h forecast when using CAMS aerosols.

5 References

Bozzo, A., Benedetti, A., Flemming, J., Kipling, Z., and Rémy, S.: An aerosol climatology for global models based on the tropospheric aerosol scheme in the Integrated Forecasting System of ECMWF, Geosci. Model Dev., 13, 1007–1034, https://doi.org/10.5194/gmd-13-1007-2020, 2020.

Martin-Perez, D., 2018 : Use of CAMS Aerosol Fields to Modify the Cloud Condensation Nuclei in HARMONIE-AROME. 11th ALADIN-HIRLAM Newsletter.

Rontu, L., Pietikäinen, J.-P., and Martin Perez, D.: Renewal of aerosol data for ALADIN-HIRLAM radiation parametrizations, Adv. Sci. Res., 16, 129–136, https://doi.org/10.5194/asr-16-129-2019, 2019.

QA in HIRLAM-C 2019-2020

Bent Hansen Sass

SUMMARY

Many activities are part of meteorological Quality Assurance in HIRLAM-C: First the contents and outcome of a HARMONIE-AROME User Meeting are summarized. Next a short account is given of the training course in Harp verification system held in October 2019. Finally, in section 3 examples are shown of SAL precipitation diagnosis in DMI using harp. Also the status is mentioned of a new verification scheme diagnosing the spatial structure of local extremes.

1 HARMONIE User Meeting

The meeting was arranged by the HIRLAM-C Management in collaboration with Met Eireann. The meeting took place in Talent Garden, Dublin, 19-20 November 2020.

Fig.1 Participants at the HARMONIE-AROME User Meeting 2019

The Agenda of the meeting covered

- Progress report 2019 by HIRLAM-C management
- Forecast Centre Reports: Warnings for High Impact Weather: Practices and estimated needs for products based on NWP ensembles and special (post)-processing
- Presentation on probabilistic forecasting as input to subsequent group discussions (parallel groups A and B discussing Use of Ensembles for High impact Weather Warnings)

- Presentation on Postprocessing for High Impact Weather, e.g. new approaches and examples as input to parallel groups A and B discussing Postprocessing of NWP forecasts for warning conditions.

All presentations from the meeting are uploaded at
http://hirlam.org/trac/wiki/Meetings/Users/Users201911

Considerations from the meeting:

- Ensembles are useful for less predictable situations
- In some weather conditions it is useful to call developers to be with forecasters
- Fast production using suitable graphics presentation is important and critical for Nowcasting
- Suggestion: Make easy overview of observations and corresponding predictions from ensembles.
- Is it desirable to select a " best member" by e.g. following the evolution of observations compared with individual members ?
- Upscaled products for precipitation, wind gusts, hail etc are useful , and presentations of low, medium and high percentiles

Education, training and communication to the public:

- More education of forecasters to use EPS products and tools and a related time for training is needed
- Are new products well enough documented to forecasters, e.g. how they should be used ?
- Understanding probabilities: New initiatives to communicate how to work with probabilities should be continued, e.g. at which probability should warnings be issued to find balance between under- and overforecasting ? The needs of forecasters education is different from the needs of general public
- Communication to the Public: How communicate probabilities to different types of users ?
- The best possible communication of risks is still an open area. Should we give categorical forecasts because people WANT it ?

EPS not yet perfect:

- How reliable is the ensemble ?, too few members is problematic, often too small spread, with sometimes missing signals of important events.
- Calibration of EPS needs more focus to increase quality, also for treatment of extremes
- How to know systematic errors. Easily accessible list of common model issues on the consortium level + local ones reachable by all forecasters (reports on hirlam.org and other means ?)
- Challenge to know the properties of new cycle compared with old one regarding extreme weather , Possible options for improved procedures: parallel model versions, improved release notes of new cycles ?

Exchange of forecasters' experiences:

- Sharing information between forecasters locally or in the future by Web-meetings between forecasters ?
- Is the concept of a HIRLAM-forum useful, e.g. to communicate experiences with new postprocessing (increasingly relevant for UWC when forecasts and postprocessing are better shared). The continuation of `physical´ User meetings is another option.

New products:

Many proposals for new products to be realized : severe convection products, tornadoes, forest fire, hail size product, extreme forecast index (scaled with e.g. model climatology) , access to combined probabilities, - for military and aviation: Better decription of near surface inversions, forecasting of icing, indices for high- and low level of turbulence, visibility on other wavelengths than visible light ….

Conclusion:

- It seems important to consider new ideas to best realize improved future communication between model developers and forecasters.
- A next User Meeting will be held in 2021 and the special topic will be: Setups for NWP Nowcasting

2 Harp training

Around 30 participants from 15 Institutes in ALADIN-HIRLAM countries participated in this event. Slides from the meeting are provided at https://speakerdeck.com/harp

RSTUDIO cloud was used during the course. The meeting covered the following topics:

- An introduction to R programming (e.g. R basics)
- R packages
- Writing R scripts and R functions
- Inroduction to Harp
- Harp for point data (reading and interpolating forecasts and observations)
- Deterministic and EPS
- SQLITE-files
- Plotting data and scores (detailed training on this)
- Harp spatial
- Installing Harp.
- Discussion on future evolution steps, e.g. Documentation and Communication of Harp

3. Spatial precipitation diagnostics

One of the popular verification schemes in the Limited Area model community, for verifying precipitation spatially, is the SAL scheme**:** **S**tructure –**A**mplitude and **L**ocation (Wernli et al., 2009). This scheme has been developed for diagnosing the quality of precipitation forecasts in a limited area and requires that a precipitation analysis field is available for comparison with comparable forecast precipitation accumulations. Producing a high quality precipitation analysis is challenging, but since 2019 DMI has produced routine quality controlled precipitation analyses for this purpose. The harp verification system has been used for SAL diagnosis. The current emphasis is on 3h accumulations of precipitation. Often results of SAL are shown as scatter diagrams. Here we choose to display results as a function of month and forecast length respectively which may reveal some features of SAL performance more easily. The results are shown in Figs. 2 – 5. It is planned to maintain the monthly statistics to become annual statistics which will strengthen the monitoring of model performance characteristics.

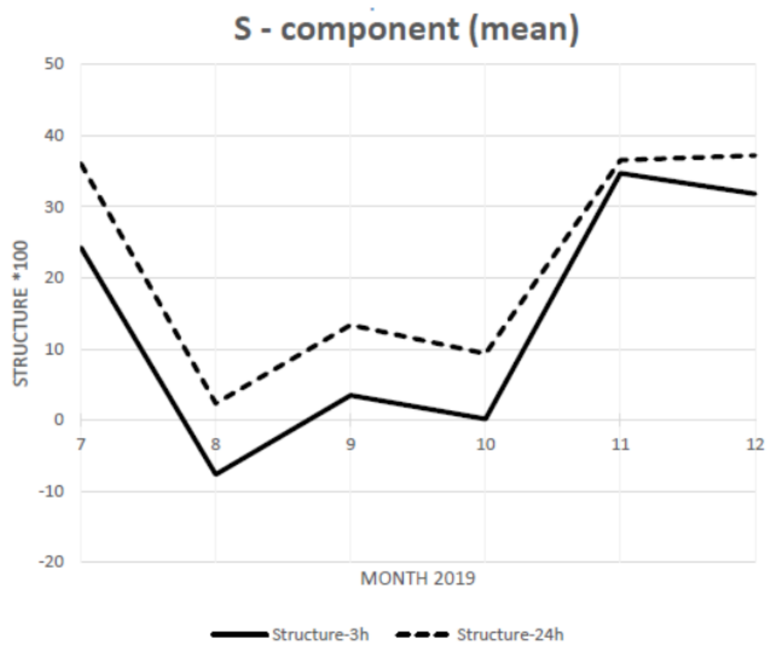

Fig2: Structure component of SAL (model area covering Denmark). Model = NEA (2.5km grid) . Data covering periods from July to December 2019. Solid line shows 3h accumulated precipitation at +3h , dashed line shows 3 hour accumulation valid at 24h. Drift towards more positive values from 3h to 24 h indicates that the forecast has more large scale characteristics as the forecast length increases.

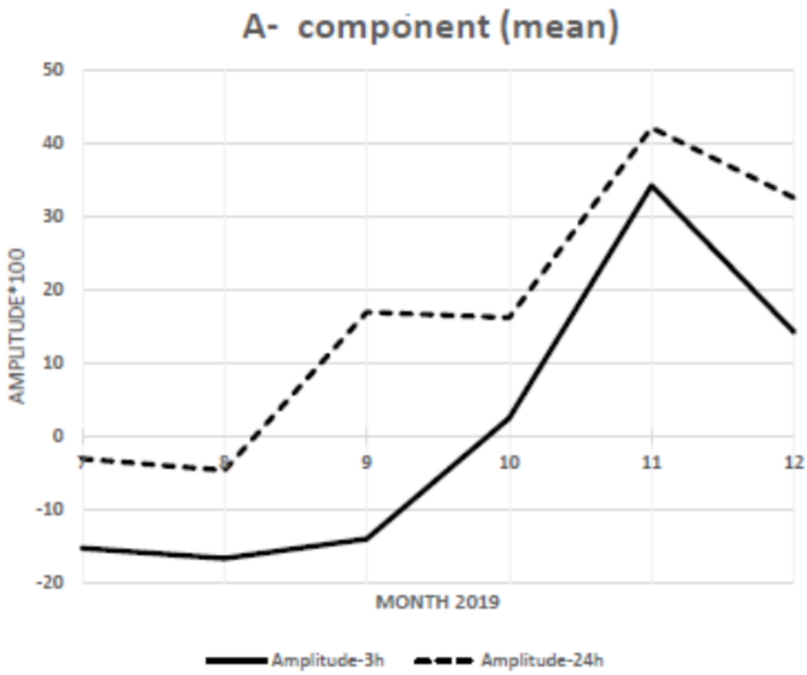

Fig.3: Same model and resolution as shown in Fig.2, but for the A-component of SAL. More positive values evolve during the forecast. Negative values in Summer months indicative of some spinup issues.

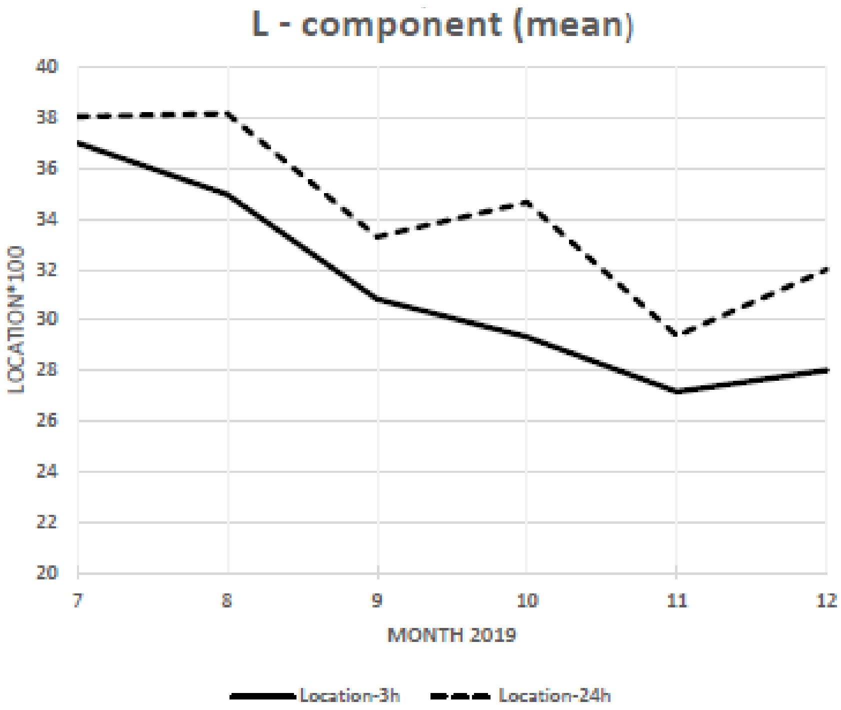

Fig.4 Similar display concept as in Fig.2 and Fig.3. Negative slopes of curves indicate increased location accuracy of precipitation in winter months.

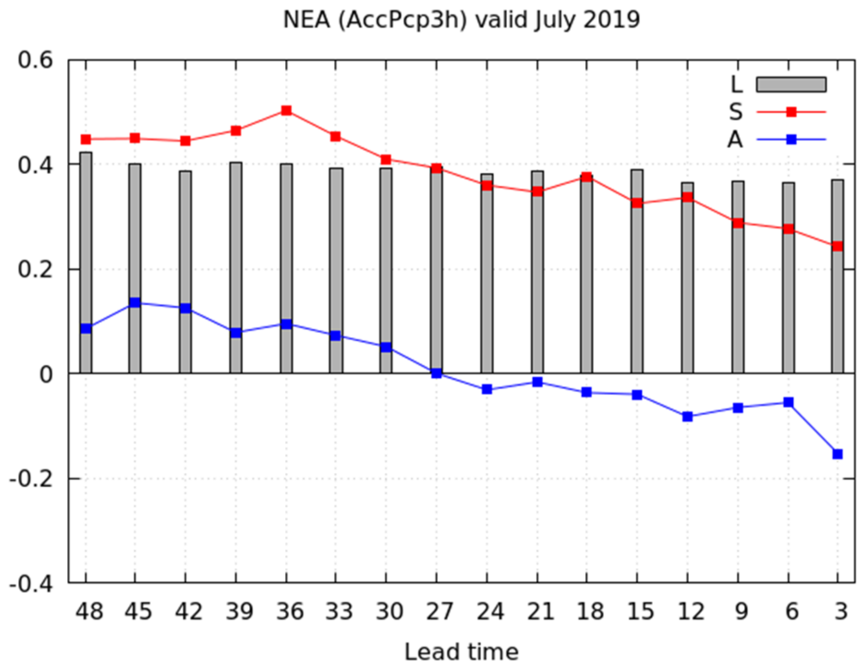

Fig.5 Time evolution (3h -48h) of SAL components in DMI HARMONIE-AROME operational runs (NEA) over Denmark, verified using DMI precipitation analyses, valid for July 2019. (from Henrik Feddersen , DMI)

Spatial structure of local extremes

Also a new spatial scheme developed to verify the ability of a NWP model to forecast local extremes (Sass, 2019) has been developed further towards operational use. It has been interfaced to harp used in DMI. The input fields are similar to those used for the SAL scheme. The score SLX consists of 4 sub-scores related with, respectively, fit of forecast to observed maxima, fit of forecast to observed minima, fit of analysis to forecasted maxima and fit of analysis to forecasted minima. A report has been prepared for a journal. The report investigates the properties of the verification looking at large scale fields, \`noisy´ fields, precipitation band displaced, a real case of summer convection and simulations of operational conditions. The scheme has desirable properties when considering the risk of \`hedging´.

4 References

Sass, B. Hansen, 2019: SLX Verification Scheme, *ALADIN-HIRLAM Newsletter, NL13,* Aug. 2019, 37-40.

Wernli, H., Hofmann,C. and M. Zimmer: Spatial Forecast Verification Methods Intercomparison Project: Application of the SAL Technique, *Wea. and Forecasting, 24,* 2009: 1472-1484.

SAPP (Scalable Acquisition and Pre-processing System) at TSMS

Yelis Cengiz, Hüseyin Gökhan Akdağ, Mustafa Sert, Meral Sezer

1 Introduction

TSMS (Turkish State Meteorological Service) has been using observation pre-processing tools which were basically developed by ECMWF since 2007. The main purpose of this pre-processing step is to collect observations in GTS (Global Telecommunication System) that have the WMO standards and to convert them in BUFR format and finally to archive these observations.
SAPP was developed by ECMWF to process the observation data and in 2014, ECMWF started to use SAPP (Fucile at al., 2014). In 2018, ECMWF Council approved the Optional Programme to share SAPP with the member, and the Co-operating States and TSMS stated to participate in this programme the same year.
Implementation of SAPP at TSMS and observation pre-processing will also be playing a crucial role and become more important for the NWP system since the observations obtained from the SAPP will be utilized by the AROME-Turkey data assimilation system as a next step.

2 Pre-processing Steps in SAPP and Data Processed by SAPP at TSMS

The main steps of the SAPP system are shown in Figure 1 (Fucile et al., 2014) and these steps include acquisition step where the incoming data is controlled, processing step where the process dispatcher prepares the data which will be processed by SAPP and the output of the step is evaluated as successful or as unsuccessful and specified on the database and extraction step where the data is sent for the assimilation.

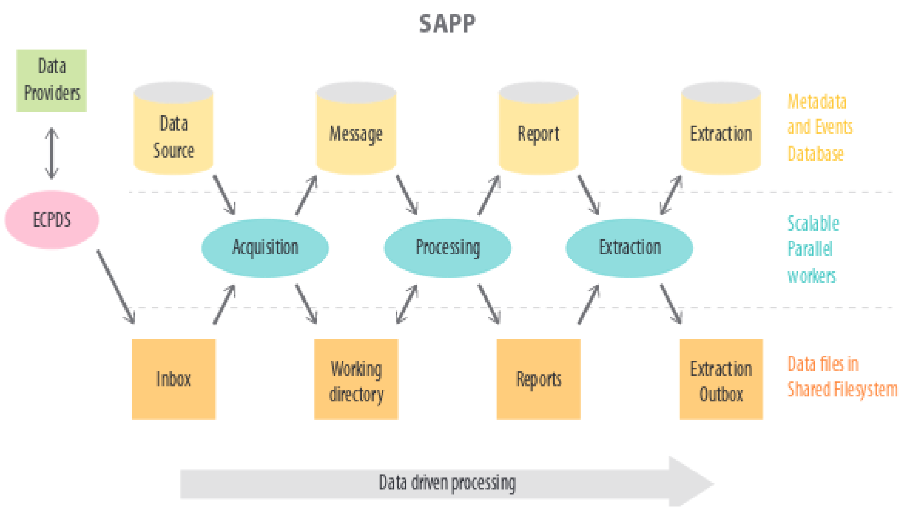

Figure 1: Data flow of SAPP (Fucile et al., 2014).

At TSMS, synop, temp, airep, metar, and ship observations that are available on GTS are collected by SAPP servers in ASCII-Text format and then converted to BUFR format by corresponding decoders. Also the data coming from automatic stations located in Turkey are gathered, converted to synoptic code format, and then used as input data for SAPP synoptic decoder. And finally this data is converted to BUFR format and archived on servers. In Table 1, the archived data of 19 May 2020 which is the output of the SAPP system, is demonstrated. Depending on the needs, the new observation types will be included in the SAPP system and these data will be processed, archived and delivered to the corresponding divisons.

Table 1:19 May 2020 Observations obtained from SAPP system at TSMS

Observation Type	Total Daily Observations	Total Daily Stations/Observation Point
Synoptic	64484	5937
Local Awos	12062	1497
Temp	983	487
Ship	130	63
Airep	11606	704
Metar	53324	2775
Metar Auto	106947	2906

The practical usage and the quality control of the observations encouraged the NWP division to test the SAPP observations in the assimilatin system. Therefore firstly the synop data obtained from the SAPP system was tested by BATOR step of the AROME-Turkey surface assimilation system (Cengiz and Sezer, 2019). In this context, the necessary changes were made to be able to read the observations by BATOR (cy43t2-bf10) with the support of Eoin Whelan who provided the modified param.cfg and odb/pandor/module/bator_decodbufr_mod.F90 files and BATOR was able be to read the data successfully. In Figure 2, the locations of the stations which provide synoptic observations for the SAPP are illustrated on AROME-Turkey fullpos domain. These observations created the ECMA ODB for 20191023 06 network time in the assimilation system. The assimilation studies in AROME-Turkey will continue with the observations obtained from the SAPP system.

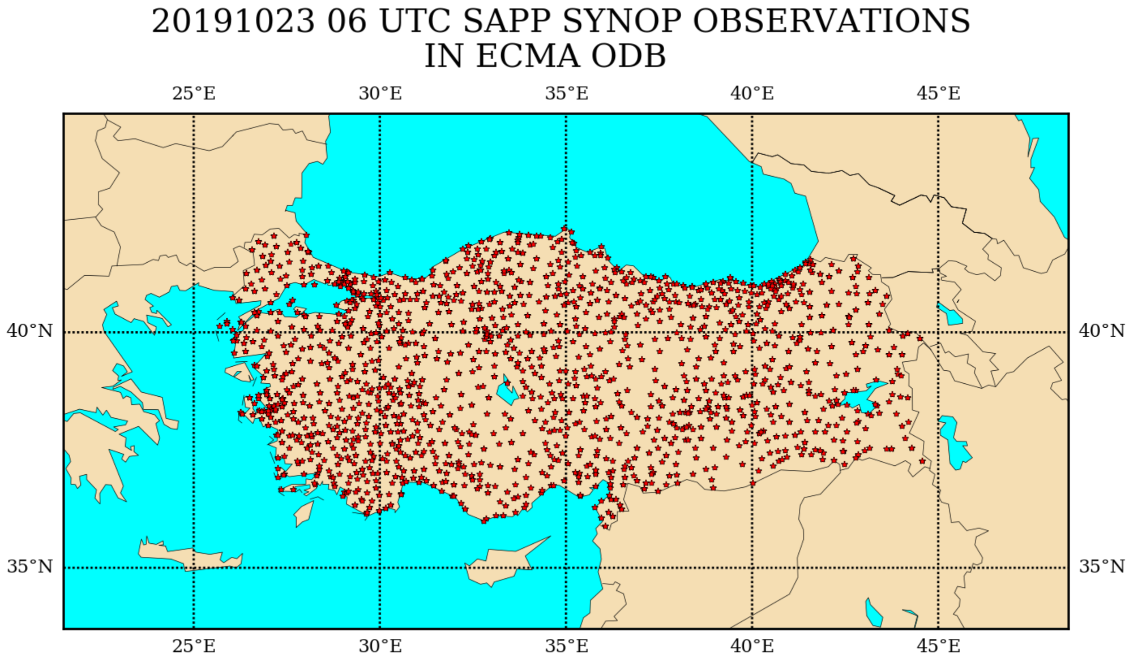

Figure 2: Locations of synoptic observations which are obtained from SAPP and read by BATOR.

3 Acknowledgements

The authors would like to thank Eoin Whelan for his support of using SAPP observations in the data assimilation system and for sharing the necessary files.

4 References

Cengiz, Y. and Sezer, M. (2020). Implementation of CANARI in AROME TURKEY. ALADIN-HIRLAM Newsletter 14: 151-153. https://www.umr-cnrm.fr/aladin/IMG/pdf/nl14.pdf

Fucile, E. et al., 2014:SAPP: a new scalable acquisition and pre-processing system at ECMWF. ECMWF Newsletter No. 140 – Summer 2014, pp. 37–41. doi: 10.21957/3ylomoa6. https://www.ecmwf.int/sites/default/files/elibrary/2014/17341-sapp-new-scalable-acquisition-and-pre-processing-system-ecmwf.pdf

Inter-comparison of integrated water vapor (IWV) derived from numerical weather prediction (NWP) AROME by IWV issue from global positioning system over Morocco

Mustapha Elouardi, Fatima Zahra Hdidou, Karim Benhachemi, Salma Elyabani

1 Introduction:

Atmospheric water vapor is a very important variable for short-term numerical weather forecasts. A good knowledge of the water vapor content in the air is necessary for the prediction of phase changes, especially for precipitation (Boniface et al, 2009). In recent years, numerous studies have shown that GPS is an effective tool for measuring the integrated water vapor in meteorology. Morocco has had several extreme phenomena especially in the southern regions. Thus, a good forecast of the integrated water vapor will be a decision support tool. This work aimed to make an inter-comparison between the integrated water vapor resulting from the Model AROME (IWV-AROME) by the integrated water vapor (IWV-GPS) deduced from the 9 permanent GPS stations. This inter-comparison was made through a statistical study between 3 hours forecasts of IWV that we calculated from the AROME model and the IWV from GPS.

2 Methodology and Result

The integrated water vapor from zenith tropospheric delay (ZTD) which is provided from GPS observations by BERNESE processing software (Hdidou FZ et al, 2018)(IWV-GPS) has already been validated by integrated water vapor from radiosonde with correlation and (Root Mean Square Error) RMSE respectively 0.98 and 2.51 mm.
The model data used for this inter comparison are the data from the AROME-Morocco model (Sbii et all, 2019. Hdidou et al., 2020). To calculate the water vapor from the model humidity field, we used the formula of Bock et al., 2005. The comparison is made in Root Mean Square Error (RMSE), bias and correlation for all stations in the Moroccan GPS meteorology network.
The correlation between IWV-AROME and IWV-GPS for all stations throughout the study period (February 20 to March 20, 2016) varies between 0.74 and 0.91. By analysing the RMSE of the stations individually we notice that it varies respectively between 2.32 mm and 6.96 mm. The minimum is recorded for the city Dakhla (South of Morocco) with a value of 2.32. For the average of all GPS stations we found a correlation of 0.83 associated with a standard deviation of 4.81 mm and a bias of -0.41 mm.

Table 1: *Statistics of differences between IWV- GPS and IWV- AROME between February 20 and March 20, 2016*

Sites	Altitude (m)	Means(mm) IWV-GPS	Means(mm) IWV-AROME	RMSE	Biais	Correlation
Tanger	14	20.73	15.93	6.96	-4.8	0.83
Oujda	465	15.6	17.91	4.23	2.31	0.82
F`es	571	17.58	19.68	4.41	2.09	0.76
Rabat	74	21.02	18.39	5.24	-2.64	0.74
Casablanca	58	18.8	17.13	4.23	-1.67	0.82
Benimellal	512	18.11	20.88	4.59	2.75	0.82
Marrakech	464	16.98	19.32	4.07	2.34	0.91
Agadir	75	21.62	17.27	3.54	-2.35	0.91
Dakhla	12	14.72	13.06	2.64	-1.66	0.88
All sites		18.35	17.95	4.34	-0.40	0.83

3 References

Bock, O. (2005). Validation of precipitable water from ECMWF model analyses with GPS and radiosonde data during the MAP SOP. Q. J. R. Meteorol. Soc., p. 3013-3036

Boniface, K. (2009). Quantification de la vapeur d’eau atmosphérique par GPS et apport à la prévision des événements cévenols. PhD thesis, Université de Montpellier II.

Hdidou, F.Z., Mordane, S., Moll, P., Mahfouf, J.F., Erraji, H., and Dahmane, Z. (2020). Impact of the variational assimilation of ground-based GNSS zenith total delay into AROME-Morocco model, Tellus A: Dynamic Meteorology and Oceanography, 72:1, 1-13, DOI: 10.1080/16000870.2019.1707854

Sbii, S. (2019). Description succincte d’AROME-MAROC Cycle 41t1 et son évaluation par rapport aux données AMDAR. Cahier de Recherche. Vol. 2, 14-21. (Disponible sur le site intranet.marocmeteo.ma)

Roughness length determination and tests

Radmila Brožková, Ján Mašek

1 Introduction

In the framework of preparations to run the ALARO upper air physics with the SURFEX scheme we perform a progressive validation. One of the validation steps is to examine differences between the physiographic conditions provided by the traditional "e923" procedure calculated from the rather aging databases and those available via the SURFEX scheme, and of course also to assess the model answer to such alternated conditions.

Here we briefly present results of our work focused on the determination of sub-grid-scale orographic features and surface roughness length determination due to orography and vegetation.

2 Experimental framework and results

Model setup

The ALADIN model configuration is based on the CHMI operational one, i.e. non-hydrostatic dynamical core with the horizontal resolution of 2.325 km and linear grid, 87 vertical levels, 90 s time-step, ALARO-1 enhanced upper air physics and the ISBA surface scheme. The library cycle is the CY43T2_bf.10 basis with some local improvements. The operational version uses the orography and land-sea mask calculated from the recent GMTED2010 topographic database, with the so-called quadratic spectral fit. The sub-grid scale orographic fields are however still determined from the old GTOPO30 database.

On the way to move to the SURFEX surface scheme, the first intended step was to calculate sub-grid scale orographic fields from the GMTED2010 database as well to get both a better precision and consistency with the main model orography field. Since one of the sub-grid scale orography derived field is the roughness length, the second step was to complete this information by the vegetation roughness length from the database used by SURFEX.

Orography and sub-grid scale orographic fields

Note that the ALARO upper air physics may share rather easily the schemes of the global model ARPEGE. One of such, still used operationally at the CHMI configuration of ALADIN, is the parameterization of the unresolved orographic forcing known shortly as the "gravity wave drag" although it is wider than the wave part of the effects. This scheme needs three sub-grid scale fields: variance, orientation and anisotropy of orography. These fields we newly obtained by running the so-called PGD procedure and we inserted them into the e923 one similarly as it was done for the orography and land-sea mask.

Comparing the above mentioned fields with respect to the old GTOPO30 results, we have obtained much more details as expected thanks to the better quality and resolution of the new GMTED2010 database (we used the 7.5'' resolution version). Besides, there is much less of the orography variance now. Consequently, the gravity wave drag scheme gets much less active when using it and thus we could foresee not to use that scheme any more. Until now, we have kept its use because of a compromise regarding scores at the surface. However, the surface scores had a chance to improve by using more realistic orographic roughness length. Here the question was on how to prepare the final version of this field, since its amplitude was traditionally reduced by the factor of 0.53 and in addition, it was smoothed. In contrast to it, in the SURFEX, there is no reduction factor applied. We have taken a pragmatic approach and tested answer of the 10 m wind scores to the various setups of reductions and smoothing. We have not retained the smoothing operator available in the e923 configuration but we have replaced it by the rather standard Laplace-type one.

As a result, both the reduction and smoothing of the orographic roughness length contributed to a slight increase of 10 m wind velocity but more importantly to the reduction of its random error. The orographic roughness length reduction had a more important impact than smoothing alone. The final tuning confirms the validity of the old choices: reduction factor of 0.53 and triple application of the smoothing operator. Fig 1 shows the impact on 10 m wind scores.

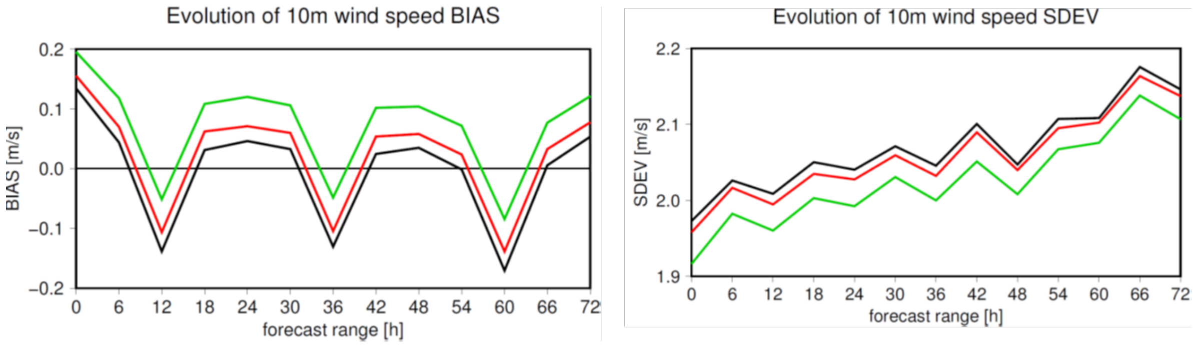

Figure 1: Bias (left) and standard deviation (right) scores for wind (m/s) at 10 m. Black: no reduction and no smoothing are applied; red: no reduction and triple smoothing; green: reduction by the factor of 0.53 and triple smoothing. Period: November 2019.

In the end, we could drop the use of the gravity wave drag schemes according to the expectations at such high horizontal resolution. Like that, we obtained improvements of the scores at 850 hPa namely by reducing positive temperature bias (not shown) while the surface results profited from the new orographic roughness length.

Vegetation roughness length.

Because of the orographic roughness length update, the following logical step was to complete it by importing more recent vegetation roughness data. The cycle CY43T2 implies the use of SURFEX version 8, and ECOCLIMAP I databases by default. We have thus taken the vegetation roughness length computed from the ECOCLIMAP I database. While there are desired details in the field, in Central Europe the values are in general much lower in comparison to the e923 reference. This has quite a detrimental impact on the surface wind scores. Fig 2 presents an important worsening of 10 m wind velocity bias. Standard deviation of this parameter got worse too (not shown).

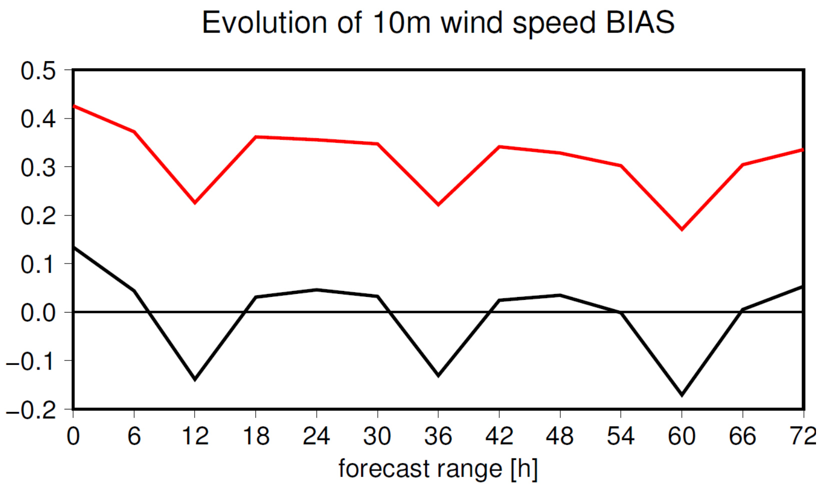

Figure 2: Bias score for wind (m/s) at 10 m. Black: reference e923 vegetation roughness length is used; red: vegetation roughness length is computed from the ECOCLIMAP I database.

As a possible alternative, we have examined the ECOCLIMAP II database regarding the vegetation roughness length. There are important differences in the fields structures and in their annual variation in comparison with the ECOCLIMAP I. In cold season the ECOCLIMAP II keep higher vegetation roughness, i.e. the decrease with respect to summer season is in this database remarkably lower than in the old e923 and the ECOCLIMAP I cases. Still, to reach the comparative amplitude during summer with the e923 result it was necessary to multiply the tree height by the factor of 1.5.

Fig 3 shows resulting Central European mean values of the vegetation roughness length during the year. We see that the ECOCLIMAP I curve roughly copies the e923 one but is considerably lower. As mentioned above, the ECOCLIMAP II manifests much lower annual variation. Finally the last curve represents the final choice of the ECOCLIMAP II database including the tree height multiplication by 1.5.

This final choice lead to the desired improvement of the scores of 10 m wind velocity. On Fig 4 we can see that better results were obtained for both winter and summer seasons. Although these results are valid for the complete proposal, which comprises the omission of the gravity wave drag parameterizations together with the new setup of both orographic and vegetation roughness lengths, the impact of the roughness length is dominant. As one could expect from the annual variation of the newly exploited vegetation roughness length, the winter season shows a more pronounced positive impact.

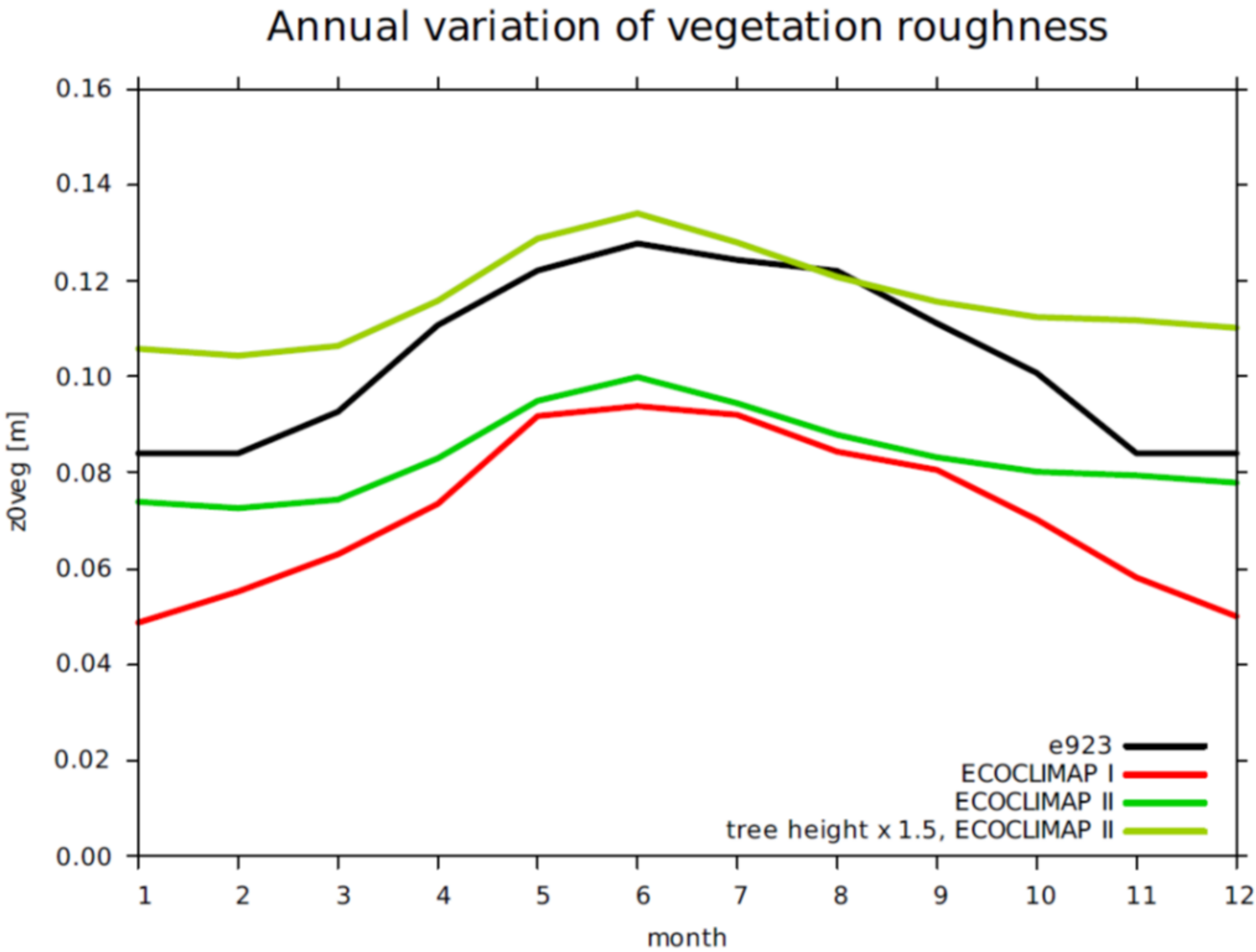

Figure 3: Annual variation of the mean vegetation roughness length over the Central European domain. Four cases are presented: 1) black – the original e923 result; 2) red – the ECOCLIMAP I database result; 3) dark green – the ECOCLIMAP II database result; 4) light green – the ECOCLIMAP II database result with the tree-height multiplied by the factor of 1.5.

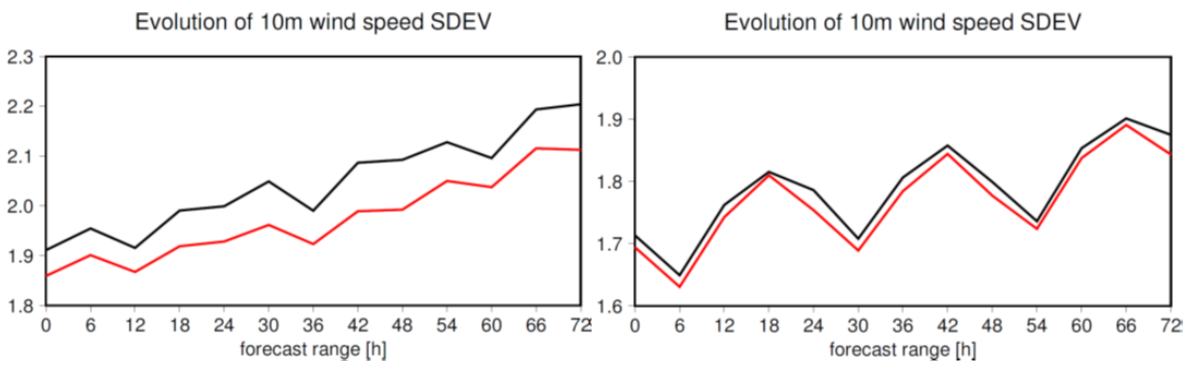

Figure 4: Standard deviation score for wind (m/s) at 10 m. Left: result for the winter period from 21 November to 10 December 2019; right: result for the summer period from 14 May to 21 May 2019. Black curve: operational reference; red curve: new proposal including the turning off the gravity wave drag parameterization family and new fields of orographic and vegetation roughness lengths.

3 Conclusions

As we have seen from the briefly presented strategy and results, the vegetation roughness length was determined in a very pragmatic way. Since we cannot really measure this quantity, while we measure the wind at 10 m, the approach of relaying on better wind scores can be justified after all. We ought to note that the impact of the roughness length on surface wind is local, i.e. the results presented here are valid for the Central Europe. We have not presented impacts of the roughness length choices on the other surface parameters, as temperature and humidity, since they are hardly touched, and this is to note as well. In addition, the upper-air fields also do not feel the roughness length modifications that much.

Finally, we would like to acknowledge advices on both technical and scientific aspects by François Bouyssel, Patrick Lemoigne, Marie Minvielle and Florian Suzat.

Preparation of ECMWF LBCs for RC LACE: spectral analysis

Nina Črnivec, Benedikt Strajnar, Neva Pristov, Jure Cedilnik

1 Introduction

The horizontal kinetic energy spectra represent a valuable tool for numerical weather prediction (NWP) model evaluation (e.g., Skamarock, 2004). In order to run a limited area weather forecast model, such as the mesoscale model ALADIN, the lateral boundary conditions (LBC) are required. The latter are regularly derived from global models, whereby the meteorological fields from a global domain need to be interpolated onto the finer grid of the target limited-area model (LAM).

Many countries involved in ALADIN consortium use Integrated Forecasting System (IFS) of European Centre for medium-range weather forecast (ECMWF) as LBCs for their operational systems. For members of Regional Cooperation for Limited Area modeling in Central Europe (RC LACE), whose national model domains largely overlap, the preparation of LBCs is a two-step procedure; in order to decrease the data transfer, the global ECMWF forecast is first interpolated to a common LBC-LACE domain, and then interpolated to the final grid at each national service.

In the present article we investigate how various approaches used for operational LBC preparation from IFS/ECMWF affect the information content in spectral space, in the case of Slovenian operational ALADIN model domain.

2 Methods

2.1 Various approaches to LBC preparation

In this investigation using currently operational domain SIS4 of the Slovenian Environment Agency (4.4 km horizontal resolution and 87 vertical levels), three approaches to prepare the LBCs are studied.

The old procedure which was in use for many years (denoted as "old") is designed as follows: firstly, the fields from a global ECMWF model are interpolated to the LBC-LACE domain (15.4 km resolution) via the twofold interpolation path, using the ALADIN/ARPEGE model configurations c901/e927. This implies interpolation from ECMWF to ARPEGE and another interpolation from ARPEGE to ALADIN model geometry. Subsequently, the fields from the LBC-LACE domain are interpolated onto the final SIS4 domain utilizing the ee927 configuration.

In the new version which became operational on 9 June 2020 (denoted as "new"), on the contrary, the fields from a global model are interpolated to the LBC-LACE domain using the onefold interpolation procedure as provided by the ALADIN configuration c903. As in the earlier approach, another ee927 step is needed to reach the final SIS4 domain.

To evaluate both aforementioned approaches, an experimental setup (denoted as "exp"), moreover, interpolates the fields from a global model directly to the target domain SIS4 through c903 pathway. The various interpolation possibilities for the LBC preparation from ECMWF are illustrated on Fig. 1.

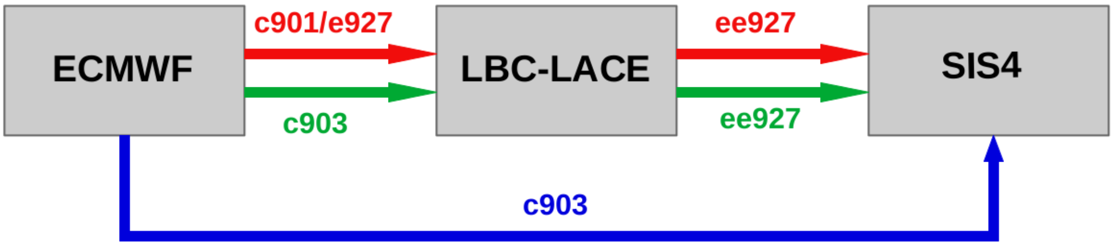

Figure 1: Various interpolation techniques during the course of LBC preparation: the "old" operational version is marked red, the "new" (current) operational version is marked green, whereas the "exp" setup is marked blue.

2.2 Horizontal kinetic energy spectra computation

We investigate how do various LBC preparation techniques affect the information content in spectral space. The horizontal kinetic energy spectra for various vertical model levels are thereby computed as a function of the total horizontal wave number $K = \sqrt{k^2 + l^2}$, where k and l represent the wave numbers in horizontal x in y direction. For a comprehensive explanation of the spectra computation the reader is referred to Blažica et al. (2013), who employed the same approach. The following graphs display the spectral kinetic energy in dependence of the total horizontal wavelength, whereby both axes exhibit logarithmic scale. In addition, the theoretical limits of $K^{-5/3}$ (three-dimensional turbulence; characteristic of mesoscale and smaller scales) and K^{-3} (two-dimensional turbulence; characteristic of larger scales) are shown for comparison. These theoretically derived slope limits have been advocated by several observational studies (e.g., Nastrom and Gage, 1985; Lindborg, 1999) as well as numerical modelling investigations (e.g., Skamarock, 2004; Blažica et al. 2013; Skamarock et al., 2014).

3 Results

The analysis is performed for a single meteorological situation, a 12-hour forecast initialized at 14 May 2020 0 UTC. Figure 2 (top row) shows the horizontal kinetic energy spectra of the LBC-LACE domain for both interpolation possibilities (old and new) for two selected vertical model levels. In the free atmosphere (model level closest to 500 hPa), the spectra follow the K^{-3} line, whereas somewhat more signal is preserved in the new (c903) approach for horizontal scales smaller than around 300 km. Near the ground, the spectra follow the theoretical slope of $K^{-5/3}$, and differences appear to be very small.

In the bottom row of Fig. 2, the spectra at SIS4 model domain are shown, here also including the direct (exp) approach. While the final spectra of old and new operational approaches are very comparable, there is more spectral energy at horizontal scales between 50 and 25 km in the exp approach (blue line). This is visible at 500 hPa and especially near the surface, and corresponds to the resolved scales of ECMWF which is cut off during interpolation to LBC-LACE, due to its resolution and quadratic spectral truncation. The blue line follows the theoretical curves of $K^{-5/3}$ and K^{-3} over these scales, supporting the assumption that they are meteorologically meaningful.

Figure 3 shows the wind speed in the SIS4 domain at the lowest model level in grid-point space, comparing the results of new and exp approaches. This illustrates that the additional spectral energy in the experimental approach results in a wind field exhibiting finer structures compared to those obtained from the new operational approach.

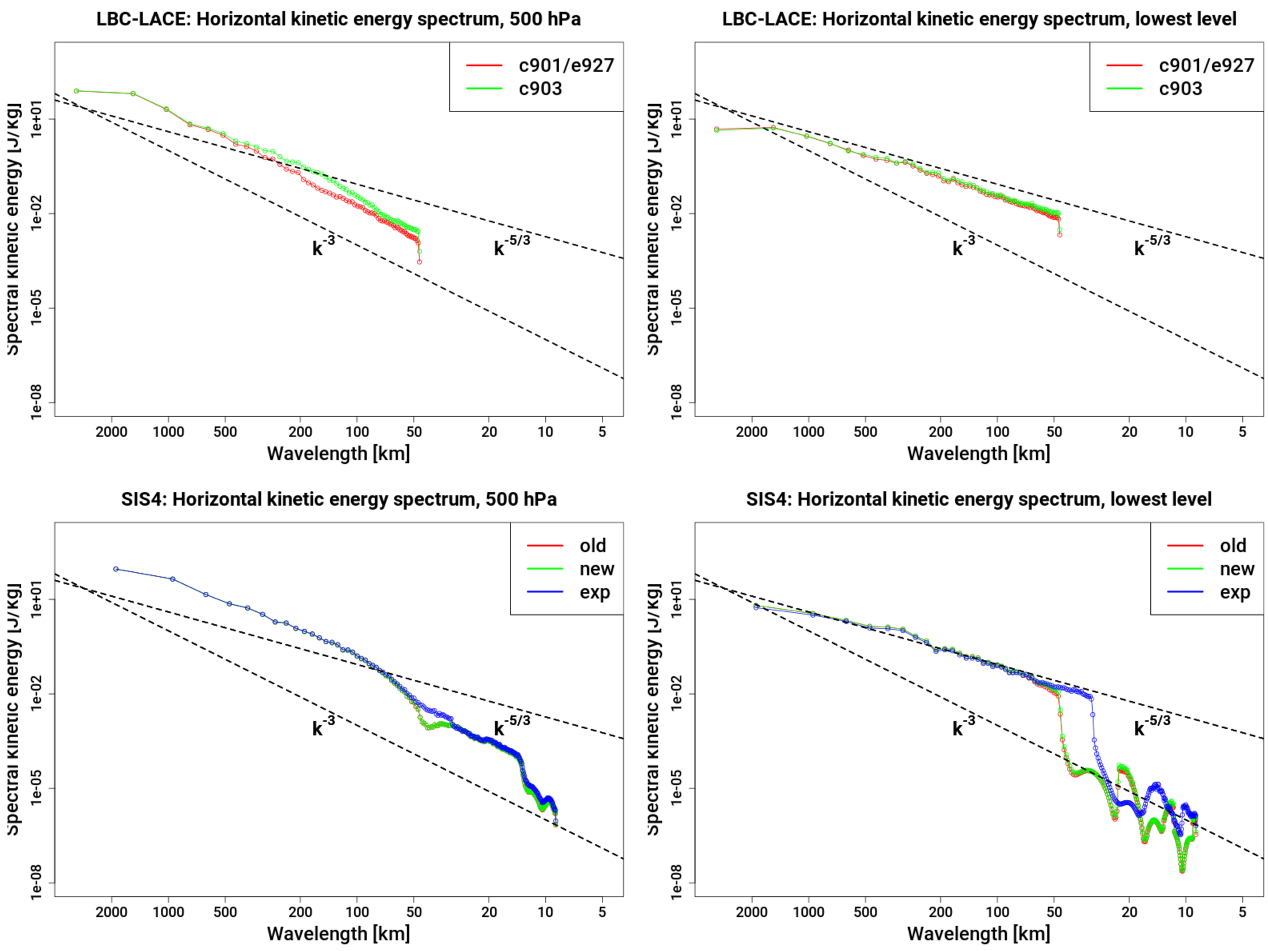

Figure 2: Top row: horizontal kinetic energy spectra for the LBC-LACE domain in conjunction with two different interpolation pathways: c901/e927 and c903. Bottom row: horizontal kinetic energy spectra for various coupling possibilities: old and new operational versions as well as the direct approach (exp). Shown are spectra for the model level closest to 500 hPa (left panels) and the lowest model level (right panels). The theoretical limits $K^{-5/3}$ and K^{-3} (black dotted lines) are displayed for comparison.

4 Discussion and conclusions

The present investigation compares the previous and current operational procedure to prepare LBCs from IFS/ECMWF model, in relation to direct interpolation to the target LAM grid which is meteorologically justified but operationally unfeasible. The resolution of the ALADIN grid used at Slovenian Environment Agency lies in the middle of model resolution range (1-10 km) applied by RC LACE countries.

The comparison of the old and new approach to obtain LBCs at the common LACE domain in terms of kinetic energy spectrum shows that more energy is preserved in the new, c903 approach at scales below around 200 km. From the analysis of spectra it is evident that wave components with wavelength between 25 and 50 km, present in the ECMWF predominantly near the surface, are cut out from the final spectrum of SIS4 at 4.4 km when interpolating through the LBC-LACE domain. This is caused by the relatively coarse resolution of the LACE-LBC domain (15.4 km) and use of quadratic truncation, which means that only wavelengths above 45 km are retained. This may present a deficiency for the quality of the final ALADIN forecast.

This analysis suggests reconsideration of the resolution of the common LBC-LACE domain, in order to better represent the current resolution of ECMWF, at the expense of increased computation cost and data transfer.

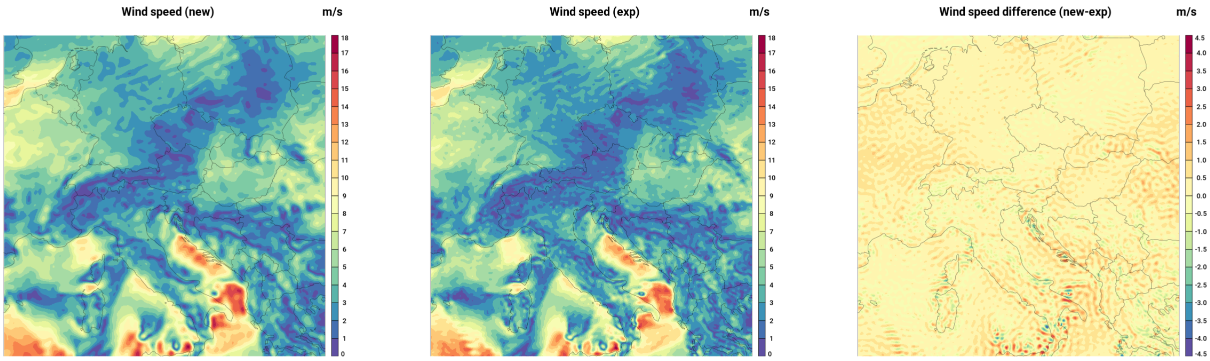

Figure 3: Wind speed at the lowest model level in the SIS4 domain in the new operational version (left panel), in the direct experimental approach (middle panel), and finally the corresponding difference between the two methodologies (right panel).

Otherwise, the presumably useful meteorological signal at part of mesoscales is lost during the two-step interpolation procedure.

5 References

Blažica, V., Žagar, N., Strajnar, B., and Cedilnik, J., 2013: Rotational and divergent kinetic energy in the mesoscale model ALADIN. Tellus A, 65, 18918.

Lindborg, E., 1999: Can the atmospheric kinetic energy spectrum be explained by two-dimensional turbulence? J. Fluid Mech., 388, 259-288, https://doi.org/10.1017/S0022112099004851.

Nastrom, G. and Gage, K., 1985: A climatology of atmospheric wavenumber spectra of wind and temperature observed by commercial aircraft. J. Atmos. Sci., 42, 950-960.

Skamarock, W. C., 2004: Evaluating Mesoscale NWP Models Using Kinetic Energy Spectra. Mon. Weather Rev., 132, 3019-3032, https://doi.org/10.1175/MWR2830.1.

Skamarock, W. C., Park, S., Klemp, J. B., and Snyder, C., 2014: Atmospheric Kinetic Energy Spectra from Global High-Resolution Nonhydrostatic Simulations. J. Atmos. Sci., 71, 4369-4381, https://doi.org/10.1175/JAS-D-14-0114.1.

Martin IMRIŠEK

Dept. of Theoretical Geodesy of the Slovak University of Technology
January 28, 2020, Bratislava, Slovakia

More information on the previous ALADIN PhDs on the aladin website :
http://www.cnrm-game-meteo.fr/aladin/spip.php?article88

Click on the picture for more information on the PhD

Monitoring of atmospheric water vapour variability in multi-GNSS constellation

Martin Imrišek, Slovak University of Technology, Faculty of Civil Engineering
Supervisor: prof. Ing. Juraj Janák, PhD.
Date of defence: 29.01.2020

Summary

The monitoring of atmospheric water vapour variability from estimation of tropospheric parameters from the Global Navigation Satellite System (GNSS) measurements is discussed in my thesis. The key parameter is the zenith total delay (ZTD), estimated from near real time processing of GNSS measurements at the Department of Theoretical Geodesy at the Faculty of Civil Engineering at the Slovak University of Technology in Bratislava.

Multiple GNSS networks are nowadays processed at the Department of Theoretical Geodesy. In general the networks can be distinguished according to the latency. The final solutions of the sub network of EUREF Permanent GNSS Network (EPN) and CEPER network are estimated with two weeks latency based on daily observation files with the Precise Network Positioning method. On the contrary, the networks processed in near–real time have latency in minutes after the hourly observation files are downloaded. The requirements for tropospheric parameters estimated in near–real time are following: the tropospheric parameters should representatively describe the state of the troposphere, and the latency should be small to satisfy the needs of numerical weather nowcasting systems. These two requirements are in contradiction. Therefore a balance between these two requirements and optimal processing strategy should be implemented to satisfy these requirements. The processed GNSS network consists of 59 permanent stations distributed in Slovakia and neighbouring countries. The data files includes GPS and GLONASS measurements only. The coordinates and tropospheric parameters are estimated by multi–GNSS data processing software developed at the Astronomical Institute of the University of Bern version 5.2. All mandatory files required for processing, the rapid Earth orientation parameters, ionospheric corrections and satellite clock corrections are downloaded from the Center for Orbit Determination in Europe data centre (CODE). The rapid satellite positions are primarily downloaded from IGS. In case this combined solution is not available the CODE solution is downloaded. The PNP method is using baselines to differentiate observations between permanent GNSS stations. The baselines are created with the OBS–MAX optimization criterion. This method creates baselines upon the amount of common time epochs of the same satellite measurements between two stations. The outputs from the Global Model of Pressure and Temperature and Global Mapping Function are used as a priori zenith hydrostatic delay and coefficients of mapping functions in parameter estimation. The model Chen & Herring is chosen for estimation of tropospheric gradients.

Multiple validations of zenith total delays estimated in near real–time at SUT were done: one year long error analysis of ZTD, the comparison ZTD of SUT, the E-GVAP and IGS solutions. The zenith total delay error analysis was carried out for the year 2018. This analysis was performed over several GNSS permanent stations chosen to represent various regions and to cover the whole network. The mean error of ZTD at GNSS permanent stations varies from 0.80 mm in the winter to 1.56 mm in the summer. The mean ZTD errors are 25% higher in the summer than in the winter. This difference is caused by increased content of water vapour in the atmosphere in the summer period.

The ZTD errors at 00 and 12 UTC were compared for the whole year. No significant increase due to diurnal cycle was detected. On a couple GNSS stations without GLONASS measurements were noted an increased ZTD error about 50% to stations receiving signals from multiple GNSS. However, the error of estimated zenith total delay is only 0.05% of its absolute value. Therefore we can consider estimated ZTD suitable for further usage.
Mean values of differences from the comparison of SUT and E–GVAP solutions are relatively small. They are only 0.05% of absolute value of ZTD and they are comparable to the estimated ZTD error from the previous comparison.
The IGS service provides a final solution with 21 days delay estimated with Precise Point Positioning method for permanent GNSS stations included in IGS network. The IGS solution is estimated with a different approach and the most precise corrections. This makes the IGS solution suitable for comparison. Comparison was done in one month period of February 2019. The mean absolute values of differences for stations are approximately twice bigger than in E–GVAP comparison, but it is only 0.2% of the ZTD. The differences are mainly caused by different processing approach. In the Precise Point Positioning method there are no baselines created, so the estimated parameters are independent from measurements of another station.
The SUT solution provides reliable ZTD comparable quality to the products from E-GVAP and IGS. Therefore, based on this conclusion, the SUT data are further processed, visualised and made available via public web page. Multiple products and additional information about the processing for chosen stations are online: 31 day long time series of ZTD, 31 day long time series of precipitable water vapour, 31 day long time series of tropospheric gradients, last 5 hours of ZTD maps, last 5 hours of precipitable water vapour maps, vertical and horizontal cross sections of GNSS tomography valid for last processing, time series of position differences between SUT and EPN solutions, station data availability statistic for last day, last 7 and 31 days, complete processing summary valid for last processing. The GNSS tomography is a technique to estimate three–dimensional information about a humidity distribution in the troposphere. This estimation is based on intersection of GNSS signals from different satellites and permanent stations. The tomographic reconstruction is carried out every hour. The slant total delays are computed from azimuth and elevation to satellites and Global Mapping Function with atmospheric parameters. Azimuth and elevation to satellite is derived from satellite position and station coordinates. The atmospheric parameters are derived from the operational ALADIN/SHMU NWP model.

In order to illustrate the potential of exploitation of the ZTD in the high resolution numerical weather forecasting the multiple experiments were conducted: comparison if the impact of assimilation of ZTD with respect to other types of observations, the long term assimilation impact study and assimilation of ZTD into the ALADIN-Limited Area Ensemble Forecasting (A-LAEF). All observations were assimilated using Three-Dimensional variational (3D-Var) data assimilation method. The impact analysis of ZTD assimilation on the AROME/SHMU NWP model with respect to other different observation types was carried out. The Degrees of Freedom for Signal (DFS) diagnostic was calculated for the SYNOP (~5000 obs.), AMDAR (~2000 obs.), TEMP (~4000 obs.), AMV (~250 obs.) and ZTD (~120 obs.). The DFS diagnostic is the derivative of the analysis increments in the observation space with respect to the observations used in the analysis system. The absolute impact of ZTD assimilation is low compared to other observation types. The ZTD are outnumbered by factor ~42 compared to SYNOP observations and by factor ~33 to TEMP observations. However, the relative DFS of one assimilated observation compared to other observation types is dominant. The decrease of relative impact of the SYNOP and TEMP observation could be related to space overlapping increments from different observations of the same type (e.g. over ascending of radiosonde). The two months impact study (July and November) of assimilation ZTD on analysis and six hour forecast was performed. Two parallel experiments with assimilation of the SYNOP, AMDAR, TEMP, AMV were performed. The ZTD were assimilated in addition in the second experiment, this experiment is denoted as +ZTD. These experiments were compared to ECMWF analyses. The assimilation of ZTD in addition to other observation types provided better AROME/SHMU NWP analysis of specific humidity at the 925 hPa (decrease of differences about 32%) and the 700 hPa (decrease of differences about 47%) in July 2018. The most significant improvement of the six hour specific humidity forecast was noticed at the 700 hPa (decrease of differences about 83%). On others pressure levels was the impact neutral or slightly negative. The increments of specific humidity of assimilation ZTD were one order of magnitude smaller in November 2018 than in summer. However, positive impact was noticed on specific humidity forecast at 925, 800 and 700 hPa about 2.3% (decrease of differences).

The 3D-Var data assimilation in upper air was successfully implemented in the existing LAEF 5km system. The 3D-Var was included into the LAEF system after Ensemble of Surface Data Assimilation and before upper air Blending. Also the perturbation of assimilated data was successfully implemented in data quality check. The forecast verification of temperature, relative humidity, geopotential and wind speed was performed. The impact was assessed on four pressure levels: 250, 500, 850 and 925 hPa. The bias, outliers, RMSE and spread was computed for the ensemble system with and without 3D-Var assimilation. The number of outliers of ensemble decreased and spread increased. However, slight degradation of the RMSE in geopotential was noticed.

In my dissertation thesis I presented the developed processing system of GNSS measurements in near real time focused on zenith total delays. Estimated zenith total delays at SUT were successfully compared to ZTD from E-GVAP and IGS. Afterwards, multiple assimilation experiments were performed to assess the impact of assimilation of ZTD to AROME/SHMU and A-LAEF NWP systems. More information can be found in the paper *Estimation of GNSS tropospheric products and their meteorological exploitation in Slovakia*.

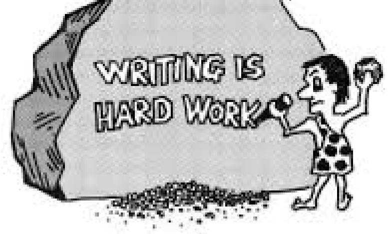

Just published ...

Contributions to Geophysics & Geodesy

Current | Archives | Announcements | About

Home / Archives / Vol 50 No 1 (2020) / original research papers

Estimation of GNSS tropospheric products and their meteorological exploitation in Slovakia

Martin Imrišek
Slovak University of Technology, Bratislava, Slovak Republic
Mária Derková
Slovak Hydrometeorological Institute, Bratislava, Slovak Republic
Juraj Janák
Slovak University of Technology, Bratislava, Slovak Republic

PDF

Published
2020-05-24

MDPI | Journals | Information | Author Services | Initiatives | About

Search for Articles: Title / Keyword | Author / Affiliation | Atmosphere | All Article

Journals / Atmosphere / Volume 10 / Issue 10 / 10.3390/atmos10100615

atmosphere
Submit to this Journal
Review for this Journal
Edit a Special Issue

Article Menu
Article Overview
- Abstract
- Supplementary Material

Open Access | Article

A Preliminary Impact Study of Wind on Assimilation and Forecast Systems into the One-Dimensional Fog Forecasting Model COBEL-ISBA over Morocco

by Driss Bari
Direction de la Météorologie Nationale, Casablanca 22000, Morocco

Atmosphere 2019, 10(10), 615; https://doi.org/10.3390/atmos10100615
Received: 18 August 2019 / Revised: 8 October 2019 / Accepted: 8 October 2019 / Published: 11 October 2019
(This article belongs to the Special Issue Observation, Simulation and Predictability of Fog)

Journal
Tellus A: Dynamic Meteorology and Oceanography ›
Volume 72, 2020 - Issue 1

Enter keywords, authors, DOI,

Listen

Research Articles

Impact of the variational assimilation of ground-based GNSS zenith total delay into AROME-Morocco model

Fatima Zahra Hdidou, Soumia Mordane, Patrick Moll, Jean-François Mahfouf, Hassnae Erraji & Zaineb Dahmane

Pages 1-13 | Received 27 May 2019, Accepted 16 Dec 2019, Published online: 03 Jan 2020
Download citation | https://doi.org/10.1080/16000870.2019.1707854 | Check for updates

SN

Research Article

Machine-learning regression applied to diagnose horizontal visibility from mesoscale NWP model forecasts

Driss Bari[1] · Abdelali Ouagabi[2]

Received: 17 January 2020 / Accepted: 25 February 2020 / Published online: 5 M... 2020

Meteorological Applications
Open Access
RMetS

RESEARCH ARTICLE | Open Access

Improving heavy rainfall forecasts by assimilating surface precipitation in the convective scale model AROME: A case study of the Mediterranean event of November 4, 2017

Zahra Sahlaoui, Soumia Mordane, Eric Wattrelot, Jean-François Mahfouf

First published: 09 December 2019 | https://doi.org/10.1002/met.1860 | Citations: 1

Estimation of GNSS tropospheric products and their meteorological exploitation in Slovakia

Martin Imrišek, Mária Derková, Juraj Janák

Summary

This paper discusses the in near–real time processing of Global Navigation Satellite System observations at the Department of Theoretical Geodesy at the Slovak University of Technology in Bratislava. Hourly observations from Central Europe are processed with 30 minutes delay to provide tropospheric products. The time series and maps of tropospheric products over Slovakia are published online. Zenith total delay is the most important tropospheric parameter. Its comparison with zenith total delays from IGS and E–GVAP solutions and the validation of estimated zenith total delay error over year 2018 have been made. Zenith total delays are used to improve initial conditions of numerical weather prediction model by the means of the three–dimensional variational analysis at Slovak Hydrometeorological Institute. The impact of assimilation of different observation types into the numerical weather prediction model is discussed. The case study was performed to illustrate the impact of zenith total delay assimilation on the precipitation forecast.

More detailed information can be found in Imrišek, M., Derková, M., & Janák, J. (2020). Estimation of GNSS tropospheric products and their meteorological exploitation in Slovakia. *Contributions to Geophysics and Geodesy*, *50*(1), 83-111. https://doi.org/10.31577/congeo.2020.50.1.5

A Preliminary Impact Study of Wind on Assimilation and Forecast Systems into the One-Dimensional Fog Forecasting Model COBEL-ISBA over Morocco

Driss BARI

CNRMSI/SMN, Direction de la Météorologie Nationale, 22000 Casablanca, Morocco.

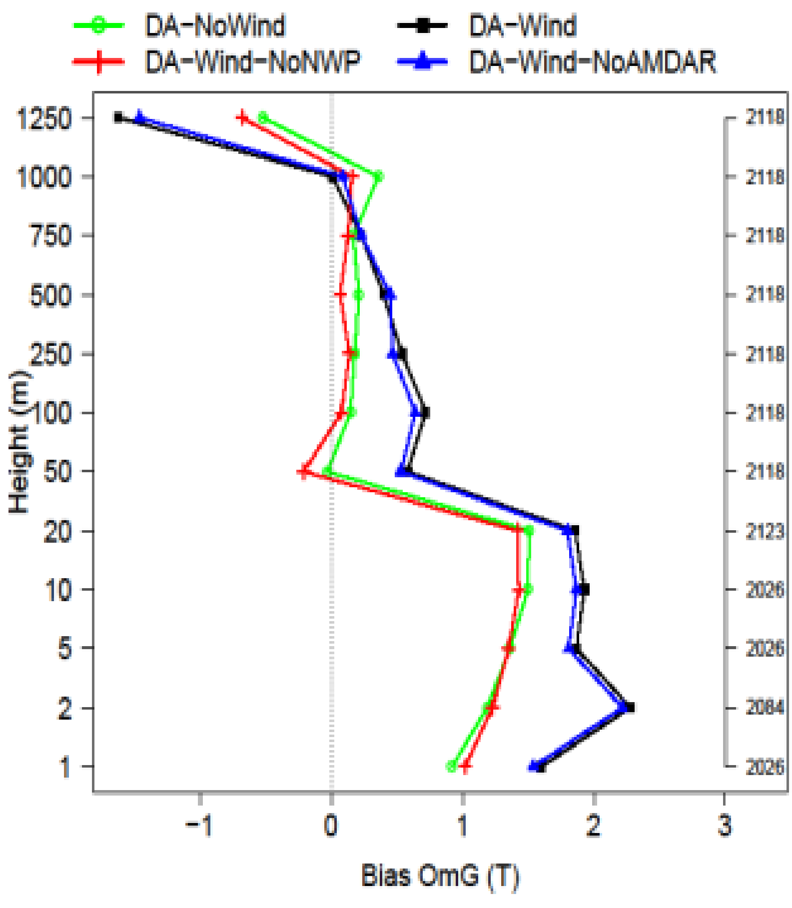

Summary

The assimilation impact of wind data from aircraft measurements (AMDAR), surface synoptic observations (SYNOP) and 3D numerical weather prediction (NWP) mesoscale model, on short-range numerical weather forecasting (up to 12 h) and on the assimilation system, using the one-dimensional fog forecasting model COBEL-ISBA (Code de Brouillard à l'Échelle Locale-Interactions Soil Biosphere Atmosphere), is studied in the present work. The wind data are extracted at Nouasseur airport, Casablanca, Morocco, over a winter period from the national meteorological database. It is the first time that wind profiles (up to 1300 m) are assimilated in the framework of a single-column model. The impact is assessed by performing NWP experiments with data denial tests, configured to be close to the operational settings. The assimilation system estimates the flow-dependent background covariances for each run of the model and takes the cross-correlations between temperature, humidity and wind components into account. When assimilated into COBEL-ISBA with an hourly update cycle, the wind field has a positive impact on temperature and specific humidity analysis and forecast accuracy. Thus, a superior fit of the analysis background fields to observations is found when assimilating AMDAR without NWP wind data. The latter has shown a detrimental impact in all experiments. Besides, wind assimilation gave a clear improvement to short-range forecasts of near-surface thermodynamical parameters. Although, assimilation of SYNOP and AMDAR wind measurements slightly improves the probability of detection of fog but also increases the false alarms ratio by a lower magnitude.

Keywords : Assimilation; Wind; COBEL-ISBA; Fog; AMDAR; 1D fog forecast; AROME

The article is available via the link :

Bari, D. A Preliminary Impact Study of Wind on Assimilation and Forecast Systems into the One-Dimensional Fog Forecasting Model COBEL-ISBA over Morocco. *Atmosphere* **2019**, *10*, 615. DOI:10.3390/atmos10100615.

Impact of the variational assimilation of ground-based GNSS zenith total delay into AROME-Morocco model

Fatima Zahra Hdidou, Soumia Mordane, Patrick Moll, Jean-François Mahfouf, Hassnae Erraji and Zaineb Dahmane

1 Introduction

The description of water vapour in initial conditions of Numerical Weather Prediction (NWP) systems is a key parameter for the forecast of many physical processes in the atmosphere, in particular precipitation (Ducrocq et al., 2002). The application of Global Navigation Satellite System "GNSS" ground-based networks to derive integrated water vapour (IWV) has widely been demonstrated in recent years (Bevis et al. 1992). Indeed, the zenith total delay (ZTD) derived from GNSS measurements of radio signal delays is related to the IWV content above the GNSS station. Many studies have shown the benefit of using GNSS observations in NWP either for model forecast validation or for improving their initial conditions (Guerova et al., 2016). Results from previous studies on the assimilation of GNSS ZTD observations showed overall neutral to positive impacts on NWP forecasts of humidity and precipitation (Poli et al., 2007; Mahfouf et al., 2015). The main objective of this current research is to investigate, for the first time, the assimilation of the Moroccan GNSS network (Hdidou et al., 2018) on the high-resolution convection-resolved AROME-Morocco (2.5km). The impact study undertaken in the present paper is expected to provide a new assessment of the impact of GNSS ZTD data over the North African region, which has a different climate and has received until now little attention in the literature.

2 Methodology and results

To evaluate the impact of the assimilation of ZTD observations in AROME-Morocco, two assimilation cycle experiments are run over 1-month during February – March 2018 using the 3D-VAR system. This period has experienced a succession of rainy events. The scores computed for the 3-hour forecasts against radiosonde measurements over the period of interest reveal a reduction in terms of standard deviation errors for specific humidity in the low and mid-troposphere when GNSS ZTD are assimilated. A reduction in bias errors over the 0–24 hour forecast range is also noticed on 2m relative humidity as verified against surface observations. Objective verification of precipitation accumulation forecasts with rain gauge data over 1-month period gives mixed results. Improvements are found for high precipitation amounts when the GNSS ZTD observations are assimilated, but, the impact is rather neutral to negative for small threshold accumulations.

The impact of the GNSS ZTD assimilation on the prediction of a heavy precipitation event that occurred on the 1 March 2018 on the South of the Atlas region is also examined. An improvement in both location and intensity of the rain cells has been noticed when assimilating GNSS ZTD. This improvement has been explained by an increase in IWV and more advection of moist air in low levels.

More details can be found in the article published in "Tellus A: Dynamic Meteorology and Oceanography" journal:

- Hdidou, F. Z., Mordane, S., Moll, P., Mahfouf, J. F., Erraji, H. and Dahmane, Z. 2020. Impact of the variational assimilation of ground-based GNSS zenith total de- lay into AROME-Morocco model, Tellus A: Dynamic Meteorology and Oceanography, 72:1, 1-13.
https://doi.org/10.10W0/16000W70.201W.1707W54

3 References

- Bevis, M., Businger, S., Herring, T. A., Rocken, C., Anthes, R. A. and co-authors. 1992. GPS meteorology: remote sensing of atmospheric water vapor using the global positioning system. J. Geophys. Res. 97, 15787_15801.

- Ducrocq, V., Ricard, D., Lafore, J.-P. and Orain, F. 2002. Storm-scale numerical rainfall prediction for five precipitating events over France: on the importance of the initial humidity field. Wea. Forecasting 17, 1236_1256.

- Guerova, G., Jones, J., Dousa, J., Dick, G., de Haan, S. and coauthors. 2016. Review of the state of the art and future prospects of the ground-based GNSS meteorology in Europe. Atmos. Meas. Tech. 9, 5385_5406.

- Hdidou, F. Z., Mordane, S. and Sbii, S. 2018. Global positioning systems meteorology over Morocco: accuracy assessment and comparison of zenith tropospheric delay from global positioning systems and radiosondes. Met. Apps. 25, 606_613.

- .Mahfouf, J. F., Ahmed, F., Moll, P. and Teferle, N. F. 2015. Assimilation of zenith total delays in the AROME France convective scale model: a recent assessment. Tellus A 67, 26106.

- Poli, P., Moll, P., Rabier, F., Desroziers, G., Chapnik, B. and co-authors. 2007. Forecast impact studies of zenith total delay from European near-real-time GPS stations in Meteo-France 4D-Var. J. Geophys. Res. 112, D06114.

Machine-learning regression applied to diagnose horizontal visibility from mesoscale NWP model forecasts

Driss BARI[1], Abdelali OUAGABI[2]

[1] CNRMSI/SMN, Direction de la Météorologie Nationale, 22000 Casablanca, Morocco.
[2] Research Laboratory in Computer Science and Telecommunications (LaRIT), Department of Computer Science, Faculty of Science, Ibn-Tofail University, Kenitra, Morocco.

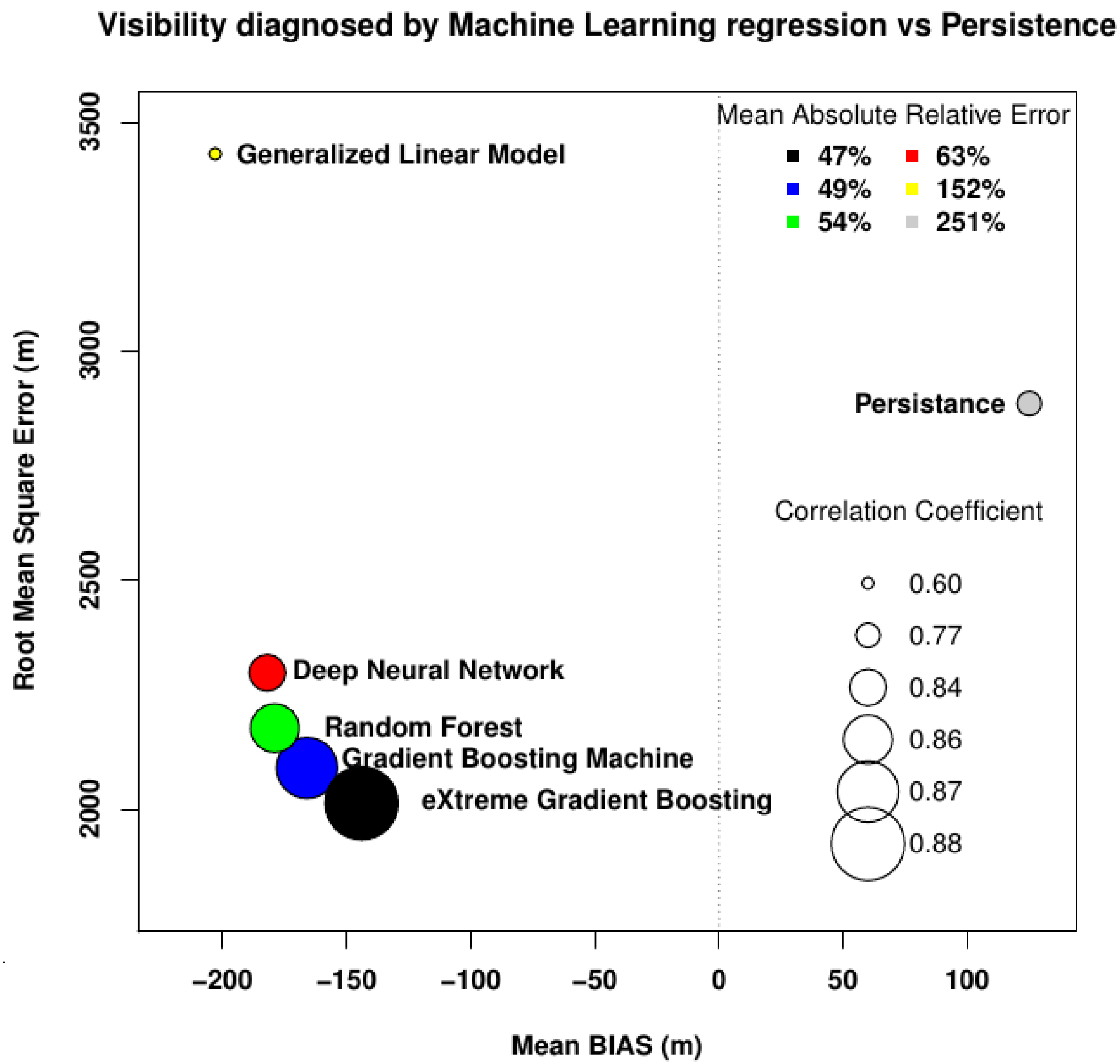

Summary

Low-visibility conditions are a weather hazard that affects all forms of transport, and accurate forecasting of their spatial coverage is still a challenge for meteorologists, particularly over a large domain. Current predictions of visibility are based on physical parametrizations in mesoscale models and are thus limited with respect to accuracy. This paper examines the use of supervised machine-learning regression techniques (tree-based ensemble, feed-forward neural network and generalized linear methods) to diagnose visibility from operational mesoscale model forecasts over a large domain. To achieve this, hourly forecasts of meteorological parameters in the lower levels of the atmosphere have been used. In the short-range forecasting framework, the machine-learning algorithms were developed to provide hourly forecasts up to 24 h. To assess the performance of the developed models, hourly observed data, collected at 36 synoptic land stations over the northern part of Morocco, have been used. This region is characterized by a heterogeneous topography. The tree-based ensemble methods have shown some improvement in visibility forecasting in comparison with the operational visibility diagnostic scheme based on Kunkel's formula and also with persistence. It is also found that this machine-learning technique performs better when the forecast depends on multiple predictors instead of only a few with very high importance. In addition, their performance is very sensitive to the disproportionality of data availability between daytime and night-time. Furthermore, it is found that the performance decreases when principal components are used instead of raw correlated data.

Keywords : Machine-learning · Visibility · Regression · Principal components · AROME

The article is available via the link :

Bari, D., Ouagabi, A. Machine-learning regression applied to diagnose horizontal visibility from mesoscale NWP model forecasts. *SN Appl. Sci.***2,** 556 (2020). https://doi.org/10.1007/s42452-020-2327-x

Improving heavy rainfall forecasts by assimilating surface precipitation in the convective scale model AROME: A case study of the Mediterranean event of November 4, 2017

Zahra Sahlaoui, Eric Wattrelot, Jean-François Mahfouf, Soumia Mordane
https://rmets.onlinelibrary.wiley.com/doi/full/10.1002/met.1860

1 Introduction

Improving precipitation forecast, at short and medium range, was deeply investigated by many research studies. In the frame work of ALADIN model, the role of initial conditions, especially those related to moisture field, was underlined by Ducrocq et al, 2002. However, issues related to accurate precipitation intensity and localisation forecast still rise when it comes to extreme events. During the last years, the use of convective scale models had allowed the assimilation of high density observations like radar data. Indeed, the 1D+3D-Var assimilation of radar reflectivity in AROME (Wattrelot et al. 2014) brought a substantial improvement in the precipitation forecast. Moreover, the assimilation of radar/gauge precipitation had shown a positive impact in both global and regional models (Stephan et al., 2008, Ban et al., 2017). It should be mentioned that in case of precipitation assimilation, the observation operator involves “non-linear” moisture-related processes like condensation and convection. Thanks to the linearized physical parametrization (Mahfouf, 1999; Lopez and Moreau, 2005), the 1D-Var assimilation allows to retrieve total column water vapour, temperature and humidity profiles from surface precipitation observation. This technique was used by Lopez and Bauer, 2007, in order to assimilate NCEP Stage-IV radar precipitation in the ECMWF global model.
In the current work, the retrieved temperature and humidity profiles are combined in relative humidity profiles and then assimilated in the AROME 3D-Var system. A case study was conducted to assess the impact of this method on the precipitation forecast during a Cévenol episode that occurred in November 4, 2017.

2 1D-Var+3D-Var precipitation assimilation in AROME

The present work aims to improve the forecast of heavy rainfall by assimilating surface precipitation in the AROME model. To achieve this goal, we propose a two steps method for precipitation assimilation. First, 1D-Var assimilation, based on linearized physical parametrization, is applied to hourly precipitation analysis (ANTILOPE) to retrieve relative humidity pseudo-profiles. In the second step, the pseudo-profiles are assimilated in the AROME 3D-Var system.
This method was applied to an extreme precipitation event (> 150 mm in 24 hours) that took place in November 4, 2017 over the Cevennes region.
Regarding SEVIRI and ATMS humidity sensitive channels, the assimilation of precipitation had improved the analysis of the humidity field. It had also modified other dynamical fields like pseudo adiabatic potential temperature, vertical velocity and potential vorticity, which became more suitable for convection occurrence. Thus, the localisation and intensity of the 24hrs-accumulated precipitation forecast matched better with the correspondent ANTILOPE precipitation. The comparison with the gauge data highlighted an enhancement of the statistical scores due to the additional information on the humidity field brought by precipitation assimilation, especially for precipitation amount exceeding 50 mm.

Exhaustive method explanation and detailed results can be found in the research article published in "Meteorological Applications" journal of the Royal Meteorological Society:
Sahlaoui, Z, Mordane, S, Wattrelot, E, Mahfouf, J-F. Improving heavy rainfall forecasts by assimilating surface precipitation in the convective scale model AROME: A case study of the Mediterranean event of November 4, 2017. Meteorol Appl. 2020; 27:e1860. https://doi.org/10.1002/met.1860

3 References

Ban, J., Z. Liu, X. Zhang, X.Y. Huang and H. Wang, Precipitation data assimilation in WRFDA 4D-Var: implementation and application to convection-permitting forecasts over United States, Tellus A, 69, 1–19, 2017. https://doi.org/10.1080/16000870.2017.1368310.

Ducrocq, V., D. Ricard, J.P. Lafore, and F. Orain, Storm-scale numerical rainfall prediction for five precipitating events over France: on the importance of the initial humidity field, Weather and Forecasting, 17(6), 1236–1256, 2002

Lopez, P. and E. Moreau, A convection scheme for data assimilation: description and initial tests, Quarterly Journal of the Royal Meteorological Society, 131, 409–436, 2005. https://doi. org/10.1256/qj.04.69

Lopez, P. and P. Bauer, '1D+4D-Var' assimilation of NCEP stage IV radar and gauge hourly precipitation data at ECMWF, Monthly Weather Review, 135, 2506–2524, 2007. https://journals.ametsoc.org/doi/full/10.1175/MWR3409.1

Mahfouf, J.F., Influence of physical processes on the tangent linear approximation, Tellus A, 51, 147–166, 1999. https://doi.org/10. 3402/tellusa.v51i2.12312

Stephan, K., S. Klink, and C. Schraff, Assimilation of radar derived rain rates into the convective-scale model COSMO-DE at DWD, Quarterly Journal of the Royal Meteorological Society, 134, 1315–1326, 2008. https://doi.org/10.1002/qj.269.

Wattrelot, E., O. Caumont and J.F. Mahfouf, Operational implementation of the 1D+3D-Var assimilation method of radar reflectivity data in the AROME model, Monthly Weather Review, 142, 1852–1873, 2014. https://doi.org/10.1175/MWR-D-13-00230.1.

Previous issues of the joint ALADIN-HIRLAM NL

No.14 January 2020

No.13 August 2019

No.12 January 2019

No.11 August 2018

No. 10. January 2018

No. 9. September 2017

No. 8. January 2017.

No. 7. September 2016

No. 6. February 2016.

No. 5. August 2016

No. 4. February 2015

No. 3. September 2015

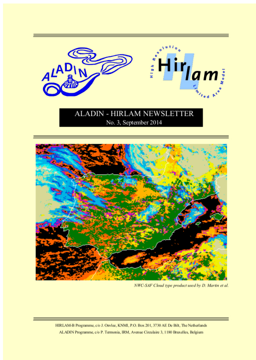

No. 2. April 2014

No. 1. September 2013